# *Process sensitivity of the Hybrid Sulphur thermochemical cycle*

Gerhard Venter
B.Eng (Chem. Eng) (North-West University)

Dissertation submitted in partial fulfilment of the requirements for the degree *Masters in Nuclear Engineering* at the Potchefstroom campus of the North-West University, South Africa.

Supervisor: Prof. Q.P. Campbell (North-West University)

May 2010

# ABSTRACT

A simple flowsheet of the hybrid sulphur cycle was devised and a steady state simulation thereof was built in Aspen. A sensitivity analysis was done and the snowball effect was identified as a significant process control issue. The flowsheet will become more complex as other process alternatives are investigated and optimisation and heat integration are done. This will probably result in further process control complications that need to be identified and dealt with.

A detailed literature study was done and future research needed was identified. This includes further research to be done into the electrolyser and the thermodynamics of the mixtures involved in the hybrid sulphur cycle.

The control related lessons learned were summarised in a very preliminary control strategy.

# CONTENTS

ABSTRACT ..... 1
CONTENTS ..... 2
ACKNOWLEDGEMENTS ..... 4
LIST OF FIGURES ..... 5
LIST OF TABLES ..... 7
NOMENCLATURE ..... 8
1. INTRODUCTION ..... 10
1.1 Background ..... 10
1.2 Aim ..... 11
1.3 Objectives ..... 12
1.4 Scope and Limitations ..... 12
2. LITERATURE STUDY ..... 13
2.1 Nuclear Hydrogen Processes ..... 13
2.1.1 The Sulphur-Iodine Cycle ..... 13
2.1.2 The Ispra Mark 13 cycle ..... 16
2.1.3 The Hybrid-Sulphur Cycle ..... 18
2.1.4 The UT-3 Cycle ..... 19
2.2 The HyS Process in detail ..... 22
2.2.1 Background ..... 22
2.2.2 The Process ..... 22
2.3 Previous Simulations ..... 39
2.3.1 Introduction ..... 39
2.3.2 Simulation Package ..... 39
2.3.3 Fluid Package ..... 39
2.3.4 Process units ..... 45
2.4 Process Control Issues Identified in Literature ..... 46
2.4.1 Cascaded Units ..... 46
2.4.2 Material Recycle Streams ..... 46
2.4.3 Heat Integration ..... 48
2.4.4 Chemical Component Inventories ..... 48
2.4.5 Process Units ..... 49
3. SIMULATIONS AND SENSITIVITY ANALYSES ..... 50
3.1 Introduction ..... 50
3.2 Sensitivity Analysis ..... 50
3.2.1 The Simplified Excel Simulation of the Process ..... 50
3.2.2 Aspen Simulation ..... 59
3.2.3 Aspen Simulation of Sulphur Trioxide Decomposition Section ..... 83
3.2.4 Aspen simulation of the cycle including detailed reactor ..... 95
4. PROPOSED PROCESS CONTROL ..... 101
4.1 Introduction ..... 101
4.2 Sulphuric acid decomposition section ..... 102
4.3 Oxygen/ sulphur dioxide separation section ..... 105
4.3 Electrolyser section ..... 108
4.5 Sulphuric acid concentration section ..... 112
5. CONCLUSIONS AND RECOMMENDATIONS ..... 115

REFERENCES ..... 117
APPENDICES ..... 123
A. THE NUCLEAR HEAT SOURCE ..... 123
A.1 Introduction ..... 123
A.2 Possible Reactor Types ..... 123
A.3 The High Temperature Gas Cooled Reactor ..... 127
A.4 Integration of the PBMR with the HyS ..... 132

## ACKNOWLEDGEMENTS

The author would like to thank Martin-David Coetzee, Angelique Venter and Dries Grundlingh for their help in better understanding the acid decomposition section, the electrolyser and the overall plant design, respectively. Also Professor Quentin Campbell for his patient guidance.

# LIST OF FIGURES

Figure 2.1: Block flow sheet of the SI cycle ..... 15
Figure 2.2: Block diagram of the Ispra mark 13 cycle ..... 17
Figure 2.3: Block diagram of the HyS cycle ..... 19
Figure 2. 4: Block diagram of the UT-3 cycle ..... 21
Figure 2.5 Block diagram of HyS cycle ..... 24
Figure 2.6 Equilibrium conversion of $SO_3$ to $SO_2$ at a pressure of 3bar ..... 28
Figure 2.7 Predicted $SO_3$ conversions over WX-1 catalyst at atmospheric pressure ..... 28
Figure 2.8: Simplified diagram of the original sulphur dioxide depolariser ..... 31
Figure 2.9: Simplified diagram of the new SRNL electrolyser design ..... 32
Figure 2.10 Tafel plot for SDE cell at 25°C and atmospheric pressure with different anolyte acid concentrations ..... 33
Figure 2.11 Tafel plot for SDE cell ..... 33
Figure 2.12 Tafel plot for SDE cell at 25°C with different pressures and anolyte flow rates ..... 34
Figure 2.13 Graph showing results of a study conducted using Aspen into the effect of cell conversion of thermal efficiency of the HyS ..... 34
Figure 2.14: Graph showing vapour pressure of sulphuric acid mixtures ..... 41
Figure 2.15: Graph showing heat of mixing for aqueous sulphuric acid mixtures ..... 42
Figure 2.16: Graph showing liquid heat capacity of sulphuric acid mixtures ..... 42
Figure 2.17: Graph showing vapour pressure of sulphuric acid solutions ..... 43
Figure 2.18: Graph showing the solubility of SO2 in sulfuric acid at 1.013-bar partial pressure ..... 44
Figure 2.19: Graph showing liquid-liquid phase equilibrium in the SO2-H2O system ..... 45

Figure 3.1: Block flow diagram of the simplified Excel simulation run ..... 53
Figure 3.2: Graph of the effect of changing the water feed flow rate ..... 55
Figure 3.3: Graph of the effect of decreasing sulphuric acid decomposition section conversion ..... 56
Figure 3.4: Graph of the effect of decreasing electrolyser section conversion per pass ..... 57
Figure 3.5: Process flow diagram of the process used for the Aspen simulation ..... 62
Figure 3.6: Graph of the effect of changing the conversion of REA-1 ..... 67
Figure 3.7: Graph of the effect of changing the conversion of ELC-1 ..... 68
Figure 3.8: Graph of the effect of changing the flow rate of stream S9 ..... 69
Figure 3.9: Graph of the effect of changing the sulphuric acid mol fraction in stream S1 ..... 70
Figure 3.10: Graph of the effect of changing the temperature of HX-1 ..... 71
Figure 3.11: Graph of the effect of changing the pressure of HX-1 ..... 72
Figure 3.12: Graph of the effect of changing the temperature of FLS-1 ..... 72
Figure 3.13: Graph of the effect of changing the pressure of FLS-1 ..... 73
Figure 3.14: Graph of the effect of changing the temperature of FLS-2 ..... 74

Figure 3.15: Graph of the effect of changing the temperature of FLS-2 ..... 75
Figure 3.16: Graph of the effect of changing the pressure of FLS-2 ..... 75
Figure 3.17: Graph of the effect of changing the temperature of FLS-3 ..... 76
Figure 3.18: Graph of the effect of changing the pressure of FLS-3 ..... 77
Figure 3.19: Graph of the effect of changing the temperature of FLS-4 ..... 77
Figure 3.20: Graph of the effect of changing the temperature of FLS-4 ..... 78
Figure 3.21: Graph of the effect of changing the pressure of FLS-4 ..... 79
Figure 3.22: Graph of the effect of changing the temperature of FLS-5 ..... 80
Figure 3.23: Graph of the effect of changing the pressure of FLS-5 ..... 81
Figure 3.24: Graph of the effect of changing the temperature of FLS-6 ..... 81
Figure 3.25: Graph of the effect of changing the pressure of FLS-6 ..... 82
Figure 3.26: PFD of the acid decomposition section simulation ..... 84
Figure 3.27: Graph of the effect of changing the feed temperature to all reactors ..... 90
Figure 3.28: Graph of the effect of changing the pressure in all reactors ..... 91
Figure 3.29: Graph of the effect of changing the molar feed flow rate ..... 92
Figure 3.30: Graph of the effect of changing the molar feed flow rate ..... 93
Figure 3.31: Graph of the effect of changing the mole fraction of sulphur trioxide in the feed ..... 93
Figure 3.32: Process flow diagram of the final Aspen simulation ..... 96
Figure 3.33: Graph of the effect of changing the $H_2SO_4$ mole fraction in stream S1 ..... 99
Figure 3.34: Graph of the effect of changing the temperature of HX-1 ..... 100

Figure 4.1: P&ID of the sulphuric acid decomposition section ..... 103
Figure 4.2: P&ID of the oxygen/ sulphur dioxide separation section ..... 106
Figure 4.3: P&ID of the electrolyzer section ..... 110
Figure 4.4: Sulphuric acid concentration section ..... 113

Figure A.1: Isometric view of the planned PBMR power plant with Brayton power conversion cycle ..... 130
Figure A.2: Diagram showing the structure of the PBMR fuel elements ..... 131
Figure A.3: Process flow diagram of a process heat plant (PHP) option for the HyS process ..... 133
Figure A.4: Diagram showing a PBMR configured to supply process heat .. 133

# LIST OF TABLES

Table 2.1 Electrolyser performance summary and comparison ..... 35
Table 2.2 List of components used by Mathias ..... 40
Table 2.3: Stream variable values ..... 98

Table 3.1: Base case flow values for simplified Excel simulation ..... 54
Table 3.2 Response variable values for base case of base case of simplified Excel simulation ..... 55
Table 3.3: Equipment list ..... 63
Table 3.4: Base case values for stream variables ..... 65
Table 3.5: Base case values for response variables (second simulation) ..... 66
Table 3.6: Equipment list ..... 84
Table 3.7: Base case flow values for the acid decomposition section ..... 88
Table 3.8: Base case values for response variables ..... 89
Table 3.9: Equipment list ..... 97

Table 4.1: Equipment list for sulphuric acid decomposition section ..... 104
Table 4.2: Equipment list for the oxygen/ sulphur dioxide separation section ..... 107
Table 4.3: Equipment diagram for the electrolyser section ..... 111
Table 4.4: Equipment list for the sulphuric acid concentration section ..... 114

Table A.1: Assessment of reactor concepts to provide heat for sulphuric acid decomposition ..... 126
Table A.2: Overview of HTR plants that have been built and operated ..... 127

# NOMENCLATURE

## Abbreviations

BWR: Boiling Water Reactor

DOE: Department of energy

HPST: High pressure steam turbine

HTR: High Temperature Reactor

HX: Heat exchanger

HyS: Hybrid Sulphur Cycle

IHX: Intermediate heat exchanger

IPST: Intermediate pressure steam turbine

LHHW: Langmuir-Hinselwood-Hougen-Watson kinetics

LPST: Low pressure steam turbine

MEA: Membrane electrode assembly

MSE: Mixed Solvent Electrolyte

NERI: Nuclear Energy Research Initiative

NWU: North-West University

PBMR: Pebble Bed Modular Reactor

PCU: Power conversion unit

PEM: Proton exchange membrane

PFD: Process flow diagram

P&ID: Process and instrumentation diagram

PWR: Pressurised Water Reactor

RPV: Reactor pressure vessel

SDE: Sulphur dioxide depolarised electrolyser

SRNL: Savannah River National Laboratory

SG: Steam generator

SI: Sulphur Iodine Cycle

SNL: Sandia National Laboratory

STP: Standard temperature and pressure

UT-3: University of Tokyo 3 cycle

## Symbols

$A$ : Pre-exponential factor

$C$ : Concentration

$C_P$ : Heat capacity

$\Delta H_{RX}$ : Heat of reaction

$E_A$ : Activation energy

$F$ : Molar flow rate

$R$ : Gas constant

$r$ : Reaction rate

$T$ : Temperature

$\theta_i$ : Ratio of flow rate of component i to the limiting reagent flow rate

$t$ : Time

$V$ : Volume

$X$ : Conversion

## Subscripts

A: $SO_3$

B: $SO_2$

C: $O_2$

# 1. INTRODUCTION

## *1.1 Background*

The demand for energy is growing to the extent that it seems as though the global energy consumption will increase by two thirds from 2005 to 2030 (Dorian *et al.*, 2005:1984). More than 90% of this increased energy demand is to be satisfied by the combustion of fossil fuels (Dorian *et al.*, 2005:1984). This is alarming, considering the problems associated with the use of fossil fuels. These problems include the release of gaseous oxides of carbon, sulphur and nitrogen which contribute to global warming and acid rain (Ni *et al.*, 2006:461). Possible oil availability issues (mainly political in nature), along with the inevitable depletion of fossil fuel deposits, is also cause for concern (Dorian *et al.*, 2005: 984).

It seems obvious that cleaner, more reliable forms of energy need to be investigated. Nuclear energy is regaining popularity in this respect following the problems experienced in the 1970s and 1980s (Dorian *et al.*, 2005:1986). The high cost associated with renewable energy generation (Dorian *et al.*, 2005:1987) naturally contributes toward the attractiveness of nuclear energy.

Hydrogen is an effective energy carrier that has been used as such for the last 200 years (Solomon & Banerjee, 2006:781). Hydrogen can be made from – among others – fossil fuels, bio-fuels, renewable energy and nuclear energy (Rostrup-Nielsen, 2005:293). Currently most hydrogen is produced by the steam reforming of natural gas as this is the cheapest route (Solomon & Banerjee, 2006:781).

Hydrogen can be used for heating, cooking, distributed power generation, backup power, power for portable devices, and fuel for aircraft, locomotives, road going vehicles and commercial boats (Solomon & Banerjee, 2006:781). The use of hydrogen for these purposes should help combat urban air pollution, reduce dependence on oil, help slow climate change (due to lower carbon dioxide emissions) and reduce acid rain (Solomon & Banerjee, 2006:781). There are some obstacles that need to be overcome before hydrogen can replace fossil fuels as energy carrier (and the much spoken of hydrogen economy can come into being). These are mainly related to the maturity of hydrogen related technologies and a lack of infrastructure (Romm, 2006:2610).

This project forms part of an investigation into the feasibility of utilising the heat from a pebble bed modular reactor to generate hydrogen via the Hybrid Sulphur (HyS) process. The HyS is a two step thermo-chemical cycle for decomposing water into hydrogen and oxygen. Energy is supplied to the system as electricity and high temperature heat.

## *1.2 Aim*

The aim of this study was to identify the obstacles standing in the way of the commercial implementation of the HyS cycle, as part of a hydrogen economy, but also the construction of a pilot plant.

## 1.3 Objectives

A detailed literature study, as well as steady state simulations, were employed to achieve the following objectives

- Develop a simple flowsheet for the hybrid sulphur cycle and build a steady state simulation for it
- Investigate possible operational difficulties, including possible severity of phenomenon like the snowball effect
- Investigate challenges faced when simulating the hybrid sulphur cycle
- Propose a control structure for the flowsheet developed in order to summarise the lessons learned

## 1.4 Scope and Limitations

- The source of energy (both thermal and electric) is a Pebble Bed Modular Reactor (PBMR)
- Only the Hybrid Sulphur process was considered as a process route to produce nuclear hydrogen

# 2. LITERATURE STUDY

## *2.1 Nuclear Hydrogen Processes*

There are two main ways of producing hydrogen from water using nuclear energy. They are electrolysis and the thermochemical cracking of water (Uhrig, 2005:3-7). Thermochemical decomposition of water is considered to be the most economical way of producing hydrogen via nuclear energy because a higher thermal efficiency is possible and the capital costs associated are expected to be lower (Forsberg *et al.*, 2003:2). More than a hundred of these cycles have been identified (Brown *et al.*, 2000:iv). The Hybrid Sulphur, Ispra Mark 13, University of Tokyo 3 (UT-3) and Sulphur Iodine (SI) cycles have been identified as the best candidates after the second stage of an elaborate screening process conducted by the American Nuclear Energy Research Initiative (NERI) (Brown *et al.*, 2002:2-10). This chapter fleetingly discusses these four thermochemical processes followed by a detailed study of the Hybrid-Sulphur process.

### 2.1.1 The Sulphur-Iodine Cycle

Also known as the general atomic cycle or the ISPRA mark 16 cycle (Brown *et al.*, 2000:51), the Sulphur-Iodine cycle employs three reaction steps. The first being the endothermic catalytic decomposition of sulphuric acid at roughly 850°C. (Forsberg *et al.*, 2002:4)

$$H_2SO_4 \rightarrow SO_2 + H_2O + \frac{1}{2}O_2$$

The other two thermochemical reactions take place at 120°C and 450°C respectively (Forsberg *et al.*, 2002:4).

$$I_2 + SO_2 + 2H_2O \rightarrow 2HI + H_2SO_4$$

$$2HI \rightarrow I_2 + H_2$$

The following aspects are important when considering the Sulphur-Iodine cycle (Brown *et al.*, 2000:51-52):

- All species involved are fluids
- The thermodynamic properties of all these fluids are well known
- Very few side reactions occur and to a small extent
- It has been demonstrated on bench scale
- Hydrogen is produced at about 50 atm which is advantageous when pipeline transport is being considered
- The acid dehydration process in the acid generation step is very capital intensive because of the phosphoric acid used

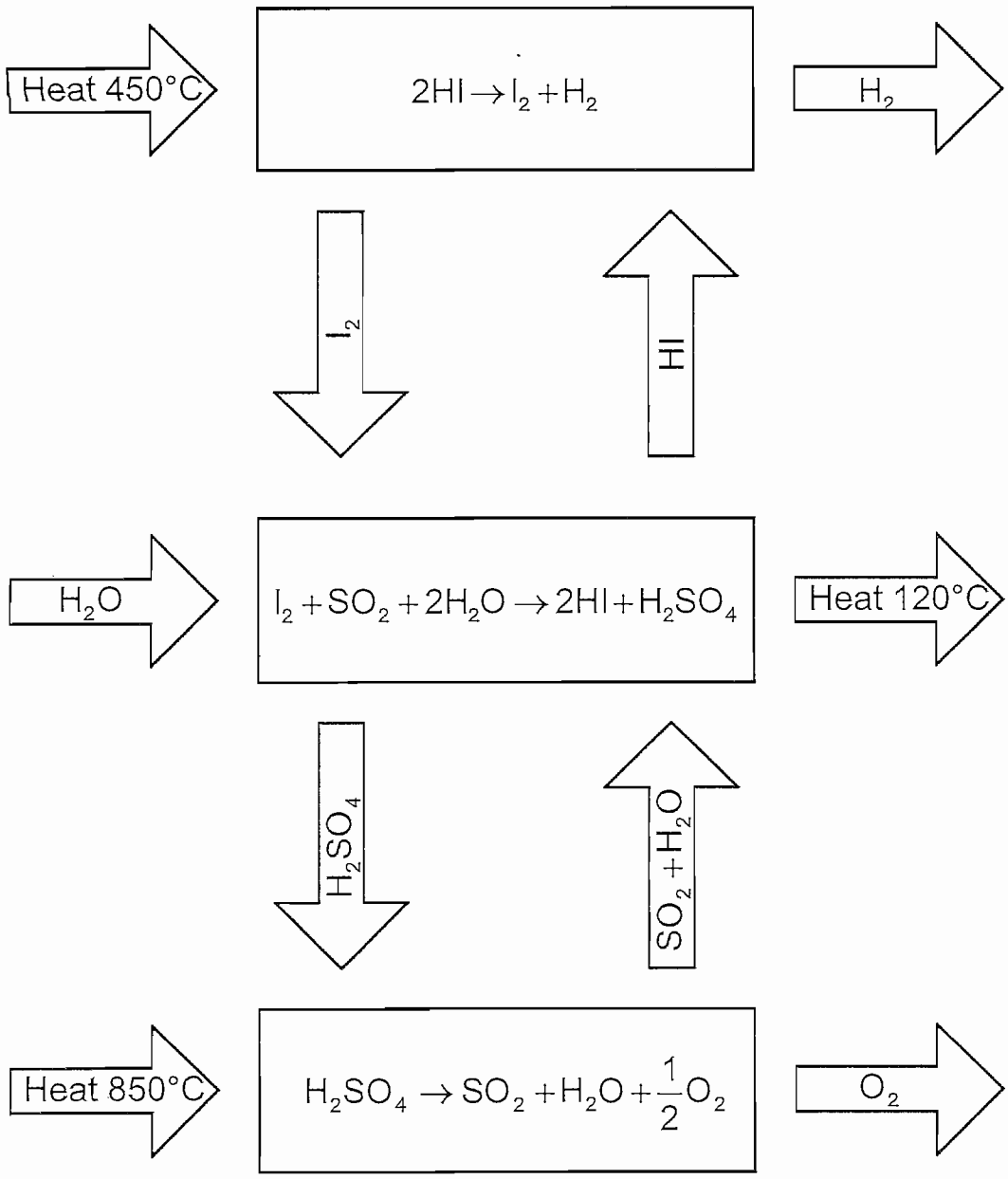


Figure 2.1: Block flow sheet of the SI cycle (Forsberg et. al., 2003:3)

### 2.1.2 The Ispra Mark 13 cycle

The Ispra Mark 13 also has three reactions as in the case of the Sulphur-Iodine cycle but the last reaction is an electrolytic one. The first reaction is identical to the first reaction of the Sulphur-Iodine cycle. (Forsberg et. al., 2003:3)

$$H_2SO_4 \rightarrow SO_2 + H_2O + \frac{1}{2}O_2$$

The second and third reactions both take place at 77°C.

$$Br_2 + SO_2 + 2H_2O \rightarrow 2HBr + H_2SO_4$$

$$2HBr \rightarrow 2Br_2 + H_2$$

The following aspects are important when considering the ISPRA mark 13 cycle (Brown et. al., 2000:50):

- All species involved are fluids
- Only three reactions take place
- All applicable thermodynamic properties are known
- Side reactions are negligible
- The process has been fully flow-sheeted
- The cycle has been demonstrated on pilot plant scale
- Some difficulty is experienced in scaling up the electrode systems

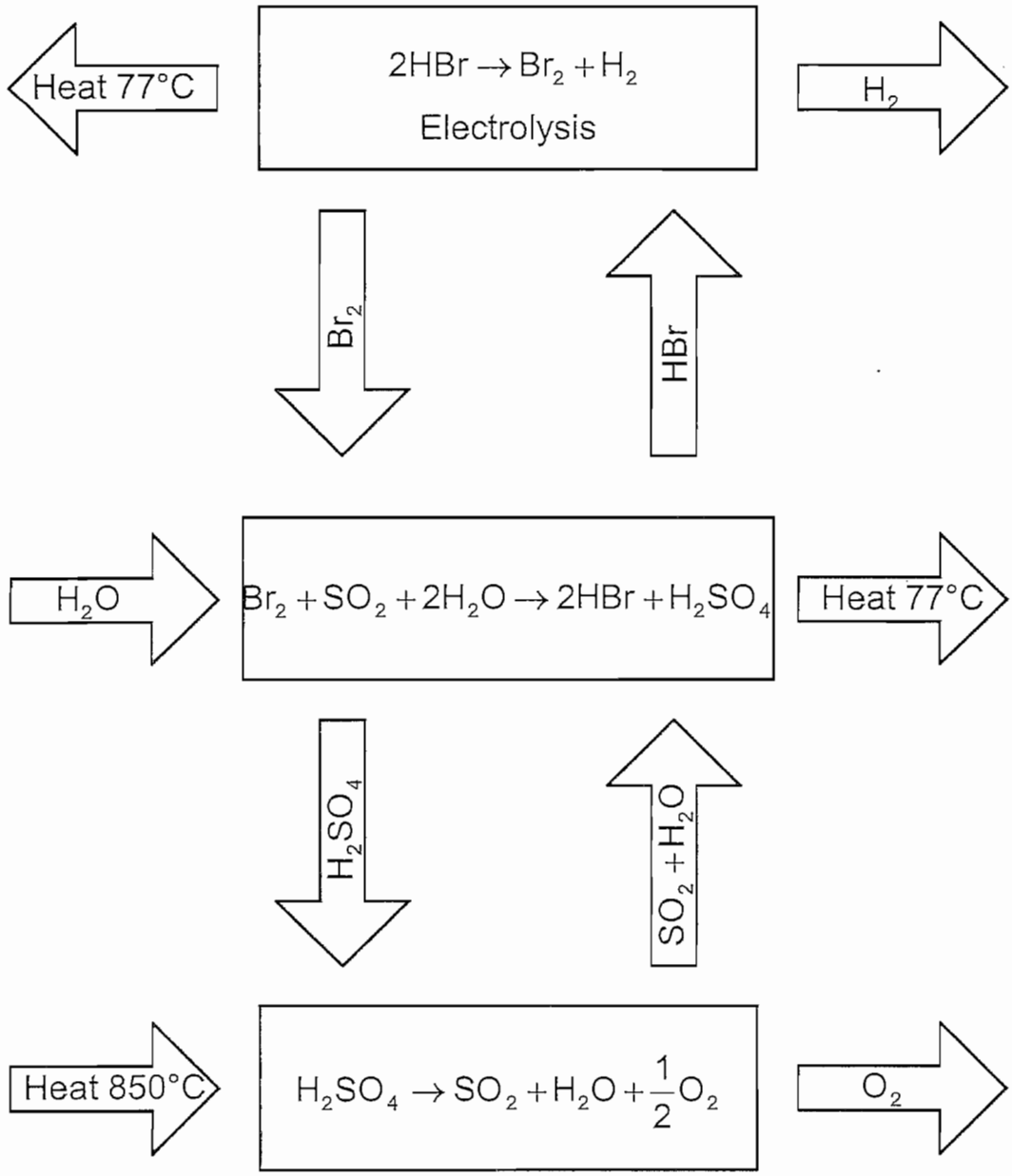


Figure 2.2: Block diagram of the Ispra mark 13 cycle (Forsberg et. al., 2003: 3)

### 2.1.3 The Hybrid-Sulphur Cycle

The Hybrid Sulphur cycle is also known as the Westinghouse, GA-22 and ISPRA mark 11 cycle (Brown et. al., 2000:49). The Hybrid Sulphur cycle has the same first reaction step as the other two cycles discussed, but only has one further reaction step. This electrochemical step takes place at 80°C. (Forsberg et. al., 2003:3)

$$H_2SO_4 \rightarrow SO_2 + H_2O + \frac{1}{2}O_2$$

$$SO_2 + 2H_2O \rightarrow H_2SO_4 + H_2$$

The following aspects are important when considering the hybrid sulphur cycle (Brown et. al., 2000:49):

- All species are fluids
- The cycle has only two reaction steps
- The thermodynamic properties of the species are well known
- Minimal side reactions take place
- Fully flow sheeted
- Has been demonstrated on bench scale
- Some difficulty is experienced in scaling up the electrochemical equipment

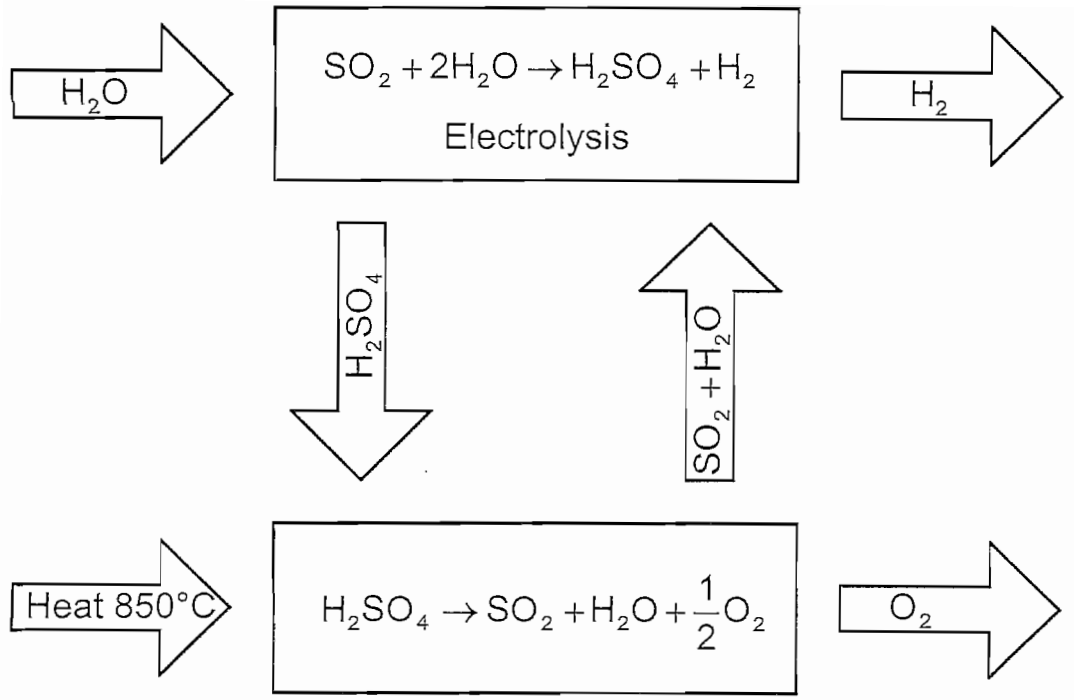


**Figure 2.3: Block diagram of the HyS cycle (Forsberg et. al., 2003: 3)**

### 2.1.4 The UT-3 Cycle

The University of Tokyo 3 cycle employs four reaction steps and involves the use of solids. It has been extensively studied in Japan and it is speculated that this cycle has some selling points that are not known to anybody but the Japanese (Brown et. al., 2000:50). The reactions are shown below along with the temperatures at which they occur in the cycle. Note that the hydrogen liberating reaction is electrolytic (Brown et. al., 2000:50).

| | |
|---|---|
| $2Br_2 + 2CaO \rightarrow 2CaBr_2 + \frac{1}{2}O_2$ | 672 °C |
| $3FeBr_2 + 4H_2O \rightarrow Fe_3O_4 + 6HBr + H_2$ | 560 °C |
| $CaBr_2 + H_2O \rightarrow CaO + 2HBr$ | 760 °C |
| $Fe_3O_4 + 8HBr \rightarrow Br_2 + 3FeBr_2 + 4H_2O$ | 210 °C |

The following aspects are important when considering the UT-3 cycle (Brown et. al., 2000:51):

- Some of the reacting species are solids
- The solid reactants are immobilized in fixed beds
- This cycle has been demonstrated on pilot plant scale
- Solid reactants need to be moved in order to make steady state operation possible

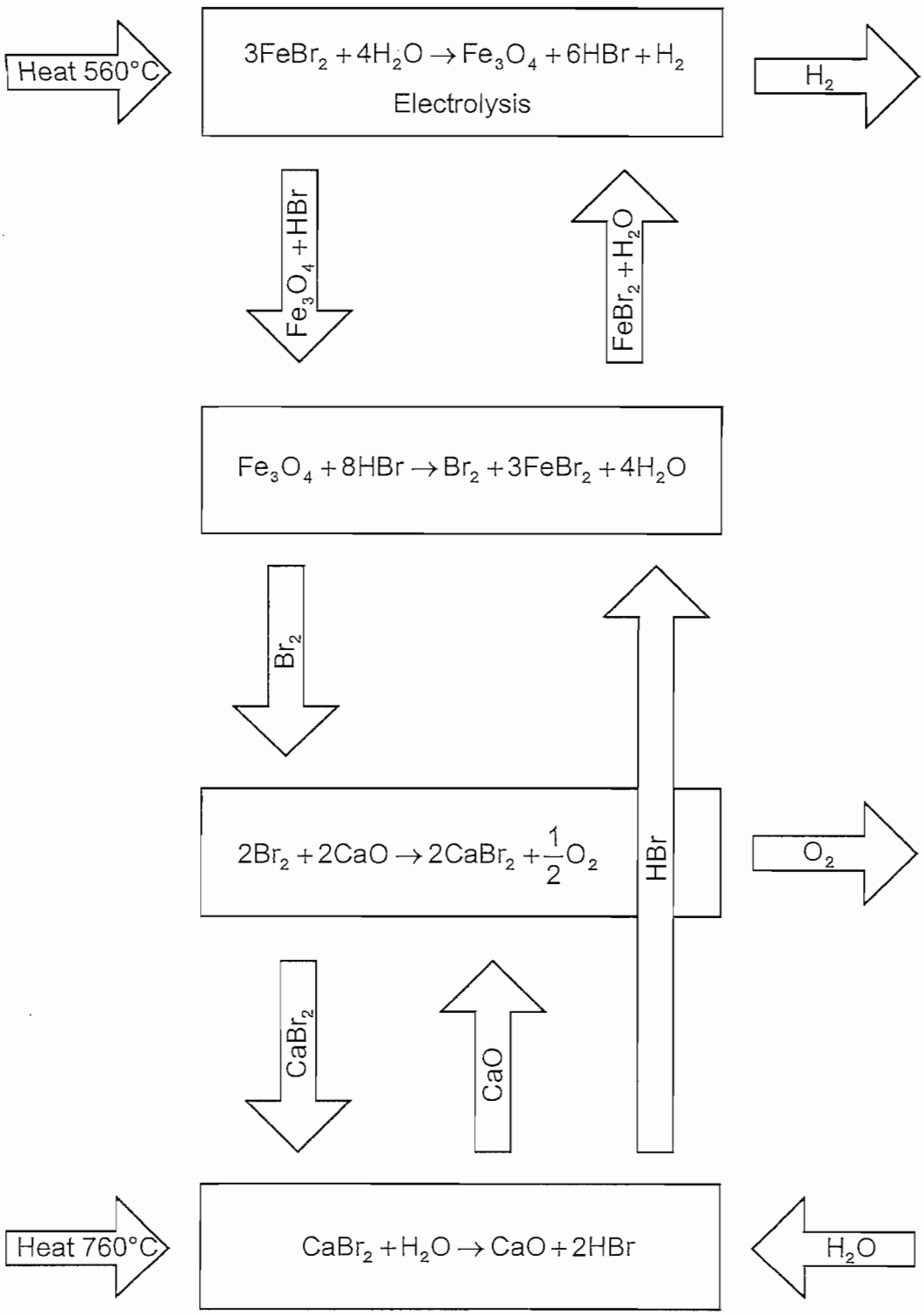


**Figure 2. 4: Block diagram of the UT-3 cycle (Doctor, 2006: 4)**

## *2.2 The HyS Process in detail*

### 2.2.1 Background

The HyS cycle was first developed in 1975 by the Westinghouse Electrical Corporation (Bilge & Petri, 2005:49). By 1978 they had built a 120 litre an hour (hydrogen at STP) closed-loop, bench-scale model of the process. They continued work on the HyS process until the readily availability of hydrogen from the steam reforming of natural gas and the reduced interest in high-temperature nuclear reactors and solar receivers forced them to stop in 1983. This work included equipment design and optimisation, work on materials of construction, integration with both solar and nuclear heat sources, process optimisation and economic evaluations (Summers et. al., 2005:2).

In 2002 the United States' Department of Energy (DOE) had a study done to compare all the thermochemical water splitting cycles they could find in literature. They found more than a hundred different cycles and after a first screening the HyS cycle was ranked first only to be discarded during a second screening because of the perceived capital cost issues associated with electrolysis (Summers et. al., 2005:2; Brown et. al., 2000:32).

### 2.2.2 The Process

*2.2.2.1 Overview*

Figure 2.5 shows a simplified schematic of the HyS process. Note that all the sulphur compounds are recycled and that there are only two reaction steps involved; making it the simplest of all the thermochemical water splitting cycles (Summers et. al., 2005:1). The two reactions follow (Forsberg et. al., 2003:4).

$$H_2SO_4(g) \rightarrow SO_2(g) + H_2O(g) + \frac{1}{2}O_2(g) \quad \text{(Reaction 1)}$$

$$SO_2(aq) + 2H_2O(l) \rightarrow H_2SO_4(aq) + H_2(g) \quad \text{(Reaction 2)}$$

Reaction 1 is the decomposition of sulphuric acid. This reaction is usually carried out at about 1150K over a catalyst in a reactor that can withstand the high temperature heat from a nuclear reactor. Reaction 1 takes place as two reactions in series (Barbarossa et. al., 2006:2):

$$H_2SO_4(g) \rightarrow H_2O(g) + SO_3(g)$$

$$SO_3(g) \rightarrow SO_2(g) + \frac{1}{2}O_2(g)$$

Reaction 2 is an electrochemical reaction. Sulphur dioxide, dissolved in 50 to 70wt% sulphuric acid, depolarises the anode of the electrolytic cell to produce sulphuric acid. Hydrogen gas is formed at the cathode. Initially micro porous rubber was used to separate the cell compartments but currently proton-exchange membranes are being investigated for this use (Summers et. al., 2005:2). Figure 2.5 Shows a block diagram of the HyS cycle. Note the three main parts of the process, namely: sulphuric acid concentration and decomposition, sulphur dioxide and oxygen separation and electrolyser and auxiliaries. Each of these will be discussed in turn.

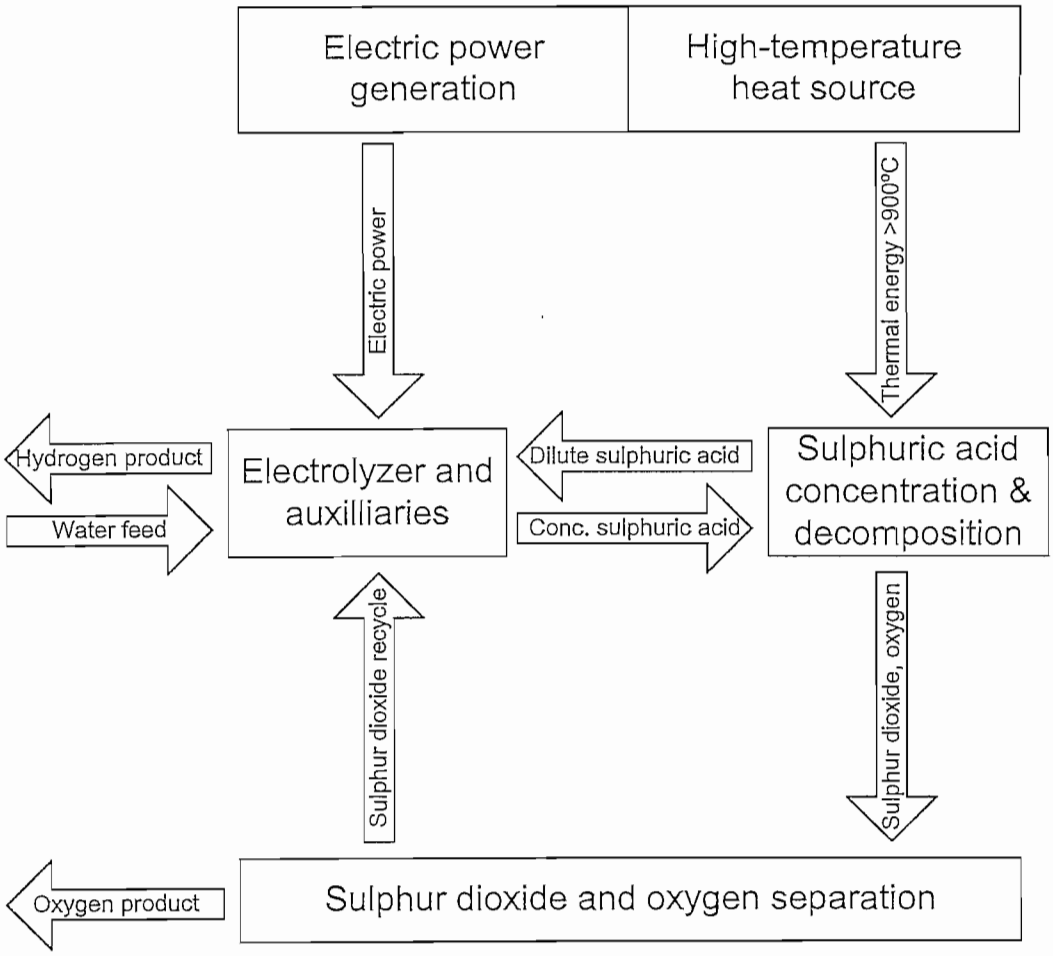


**Figure 2.5 Block diagram of HyS cycle (Summers et. al., 2005: 3)**

*2.2.2.2 Sulphuric Acid Concentration and Decomposition*

Sulphuric acid is concentrated (usually by a series of flash evaporators) from about 55wt% (this value depends on the specific flow sheet) to about 80wt% before being sent to the decomposition reactor. The low feed acid concentration (55wt%) is the highest acid concentration at which the electrolytic process can operate efficiently in practice (Cox, 1978:11). The use of distillation has also been suggested for the concentration of sulphuric acid in this cycle and could possibly increase efficiency (Huang & T-Raissi, 2005:638-643).

The liquid sulphuric acid is vaporised before being sent to the acid decomposition reactor. Sandia National Laboratories (SNL) in the United States carried out a series of pressurised sulphuric acid decomposition tests. The apparatus they used for this is very interesting insofar as steps to reduce corrosion are concerned. In their experience sulphuric acid is at its most corrosive when undergoing a phase change from liquid to vapour and consequently their acid boiler was designed in such a way that the sulphuric acid does not come into contact with the hastelloy C276 vessel. A bed of silicon carbide beads is used for this, it disperses and vaporises the sulphuric acid. The acid injector used was made of alumina ceramic after their previous experience with hastelloy injectors resulted in unacceptable corrosion (Gelbard et. al., 2005:16).

The apparatus used in the SNL study consisted of an acid boiler, acid decomposer and a condenser to remove sulphur dioxide and water from the product gas. All of these units were arranged linearly so there would be no place for acid to collect and corrode the pipes (Gelbard et. al., 2005:12). Liquid acid at ambient temperatures does not pose these problems and can be ducted in viton, neoprene, stainless steel, or hastelloy without significant corrosion (Gelbard et. al., 2005:16). The acid partially dissociates into sulphur trioxide and water while it is being vaporised. At temperatures exceeding 700°C the equilibrium conversion for this reaction becomes close to 100% (Huang & T-Raissi, 2005:643).

The acid decomposition reaction takes place at high temperature over a catalyst. A number of catalysts have been investigated, including Ag/Pd (Barbarossa et. al., 2006:883), $Fe_2O_3$ (Barbarossa et. al., 2006:883), Fe/Al (Kim et. al., 2006:39), Fe/Ti (Kim et. al., 2006:39), Cr/Fe oxide (Banerjee et. al., 2007:1) and Pt (Ginosar et. al., 2007:482).

A number of different reactor types were encountered in literature. A porous absorber reactor that directly absorbs concentrated sunlight from a reflector array is under investigation by HYTEC (Le Duigou et. al., 2006:1). Isothermal (electrically heated) experimental reactors have been operated (Barbarossa et. al., 2006:883). Convectively heated reactors (with helium as thermal fluid) seem to be the industry favourite (Cox, 1978:11). Even a reactor concept proposing to use inorganic membranes to separate out oxygen in order to shift the reaction equilibrium nearer to completion at lower temperatures was found (Forsberg *et al.*, 2003:8). The latest concept involves the use of annular, silicon carbide bayonets (usually used as thermowells). The catalyst is packed in the annular space and multiple bayonets are used as heat exchange barriers between the working fluid and the decomposing acid (Gorensek and Summers, 2007:8).

The current favourite material for reactor vessel construction seems to be hastelloy C276 (with gold o-rings used for seals) (Gelbard et. al., 2005:3) although duriron and durichlor have been previously suggested (Cox, 1978:12).

Two reactions take place in the reactor; sulphuric acid decomposes into sulphur trioxide and water and the sulphur trioxide decomposes into sulphur dioxide and oxygen. If high temperature process heat is used as heat source for the reaction, the sulphuric acid decomposition reactor should be as close as possible to the heat source in order to minimise temperature drops resulting from heat loss (Yildiz & Petri, 2005:62).

At low temperatures (1000K to 1100K) the efficiency drops sharply with an increase in pressure. This loss in efficiency is much lower at higher temperatures (1200K). Higher temperatures and pressures, of course, would allow the equipment to be smaller reducing capital costs but will also increase the operating cost of the plant (Yildiz & Petri, 2005:62).

The reactor effluent is cooled to condense the undecomposed acid and some of the water. The remaining gas is sent to the sulphur dioxide-oxygen separation system (Cox, 1978:12). The condensed acid/water solution is sent to the electrolyser section of the plant (Le Doigou *et al.*, 2007:1523).

The overall impression the literature leaves is that this section should pose no problems to the industrialisation of the HyS. The concentration of sulphuric acid can be accomplished in a number of manners including multi-stage flash (Cox, 1978:11), distillation (Huang & T-Raissi, 2005:640) and absorption (cox, 1978:50). These technologies are all mature.

As is the technology for the reactor itself, there is still ongoing research regarding possible catalysts to be used but Coetzee (2008:1,4) – in a related study at the NWU – identified a specific catalyst that could be used on a large scale and designed a reactor section around it. He proposed a five stage adiabatic reactor section design that could convert up to 72% of the feed $SO_3$ to $SO_2$ given a 90mol% H2SO4 feed. Figure 2.6 shows how the equilibrium conversion of $SO_3$ to $SO_2$ is affected by temperature and pressure and the maximum conversion of between 70% and 80% possible with five reactor stages in series. Inter-stage heating ensures that each reactor receives its feed at 870°C.

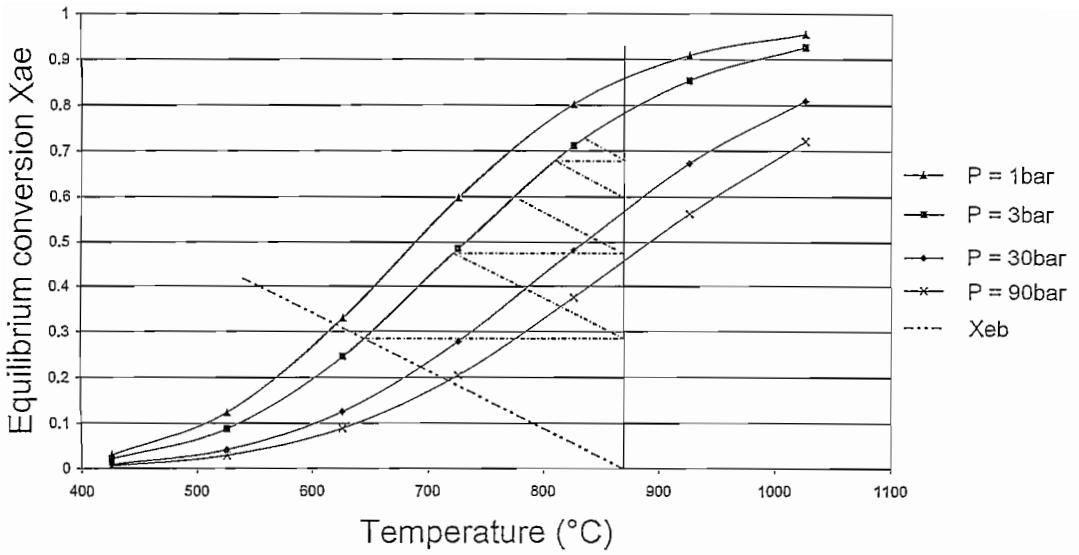


**Figure 2.6 Equilibrium conversion of $SO_3$ to $SO_2$ at a pressure of 3bar (Coetzee, 2008:4)**

Coetzee (2008:7,8) identified the space velocity and heat transfer as controlling factors of the conversion. Figure 2.7 shows how reactor conversion decreases with increasing space velocity.

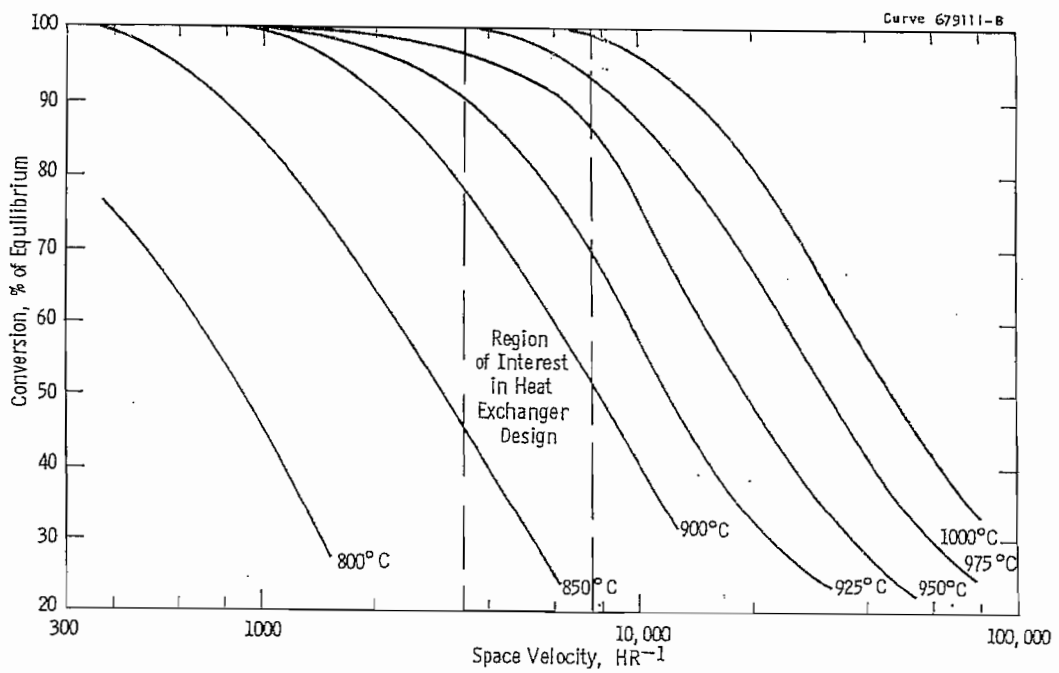


**Figure 2.7 Predicted $SO_3$ conversions over WX-1 catalyst at atmospheric pressure (Spewock *et al.*, 1976:53)**

Coetzee (2008:8) does recommend that further research be conducted into the use of the heat exchangers as reactors. According to his calculations there should be enough space inside the heat exchangers for the catalyst. This should also make the reactor more difficult to model and control.

#### *2.2.2.3 Sulphur Dioxide and Oxygen Separation*

The water and sulphur dioxide can be removed from the acid decomposition section's gaseous product stream by a number of methods. Westinghouse initially used compression and cooling while Ispra were testing an activated charcoal adsorption method (Cox, 1978:12). The sulphur dioxide and water is sent to the electrolysis section while the purified oxygen can be vented to the atmosphere or used for a different process (Cox, 1978:12).

#### *2.2.2.4 Electrolysis*

The reversible potential difference for water electrolysis is 1.23V at 25 °C while the reversible potential difference for sulphur dioxide electrolysis is only 0.17V. This potential difference increases to 0.29V if the sulphur dioxide is dissolved in 50wt% sulphuric acid but an actual industrial-scale performance of 0.6V is expected (Summers & Steimke, 2006:4). Naturally a lower potential difference results in a smaller energy requirement explaining the higher energy efficiency of the HyS cycle when compared to direct water electrolysis.

The half-cell reactions for the electrolysis step of the HyS cycle is given below (Summers, 2006:13). Hydrogen product is formed at the cathode (99.9% pure) while sulphuric acid is formed at the anode. The sulphur dioxide is removed from the sulphuric acid stream leaving the electrolyser and the sulphuric acid is sent to the acid concentration section of the plant (Cox, 1978:11).

$$SO_2(aq) + 2H_2O(l) \rightarrow H_2SO_4(aq) + 2H^+ + 2e^- \quad \text{(Oxidation at anode)}$$

$$2H^+ + 2e^- \rightarrow H_2(g) \quad \text{(Reduction at cathode)}$$

Precious metals are usually used as catalyst with platinum or palladium being common choices, with providing better catalytic activity. The metal is supported on carbon. The oxidation of sulphur dioxide at the anode is the rate-limiting step as its rate is much slower than the cathodic reaction (Colón-Mercado & Hobbs, 2007:2649,2650).

The electrochemical step in the HyS process is carried out in a sulphur dioxide-depolarised electrolyser (SDE). In the original Westinghouse designs these were parallel plate electrolysers with a porous rubber separator or membrane to keep the catholyte and anolyte from mixing (Cox, 1978:11). The catholyte was at a slightly higher pressure than the anolyte in order to prevent the diffusion of sulphurous acid to the cathode which would result in the formation of solid sulphur which could build up in the cell decreasing faradic efficiency. The overpressure at the cathode side causes a flow of sulphuric acid from the cathode to the anode and an increase in the internal resistance of the cell (Cox, 1978:11). The electrodes were made of briquetted carbon with $17\,mg/cm^2$ of platinum catalyst (Summers, 2006:11). Figure 2.8 shows a simplified diagram of the old type of electrolyser proposed for use in the HyS cycle.

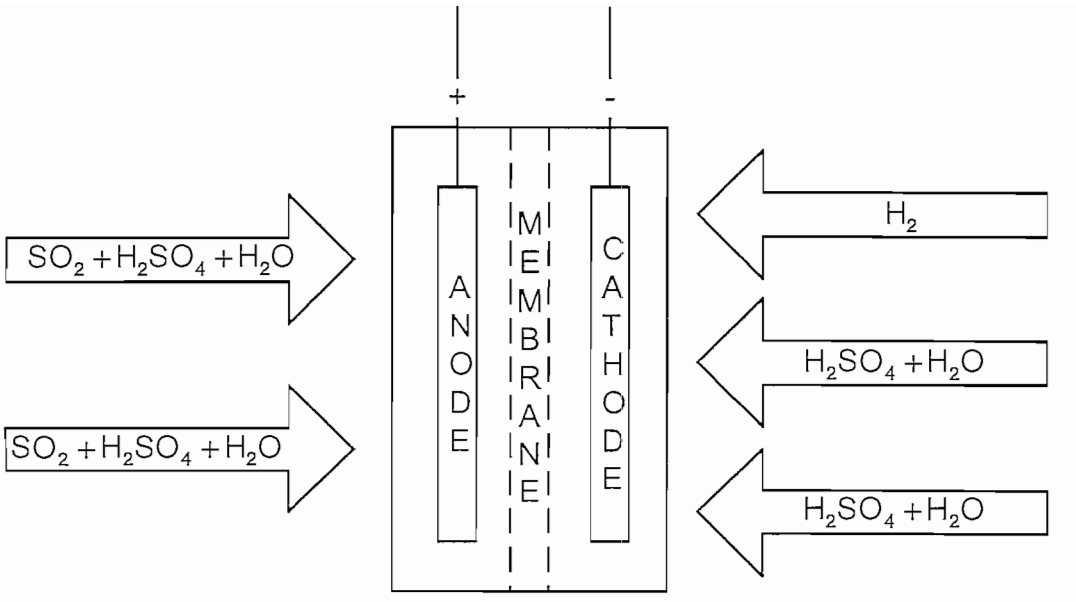


**Figure 2.8: Simplified diagram of the original sulphur dioxide depolariser (Cox, 1978: 50)**

Advances in electrolyser technologies have resulted from fuel cell research and have made new membranes available for use. Membranes should have good ionic conductivity and low permeability to sulphur dioxide (Colón-Mercado & Hobbs, 2007:2650). Current designs by Savannah River National Laboratory (SRNL) in the United States use proton exchange membranes (PEM) like nafion together with gas diffusion carbon membranes (<1mg $Pt/cm^2$) and carbon flow fields in a membrane-electrode-assembly (MEA) construction. The anolyte does not need to contain sulphuric acid although the Tafel plots drawn up by SRNL (Figure 2.10 and Figure 2.11 shows the Tafel plot in question) suggest that the presence of acid would result in higher efficiency. The current PEM cell designs do not require a catholyte and thus it is optional acid flow. Current Westinghouse process design requires the electrolyser to operate at 100-120°C and 20bar at 50-60wt% sulphuric acid conditions (Summers, 2006:9,10). Figure 2.9 shows a simplified diagram of this new design. Figure 2.12 shows how the effect of pressure on the electrolyser – this is the result of $SO_2$ absorption. The same figure shows that the cell current decreases as the anolyte flow rate increases – this is the result of improved mass transfer (Summers, 2006:16).

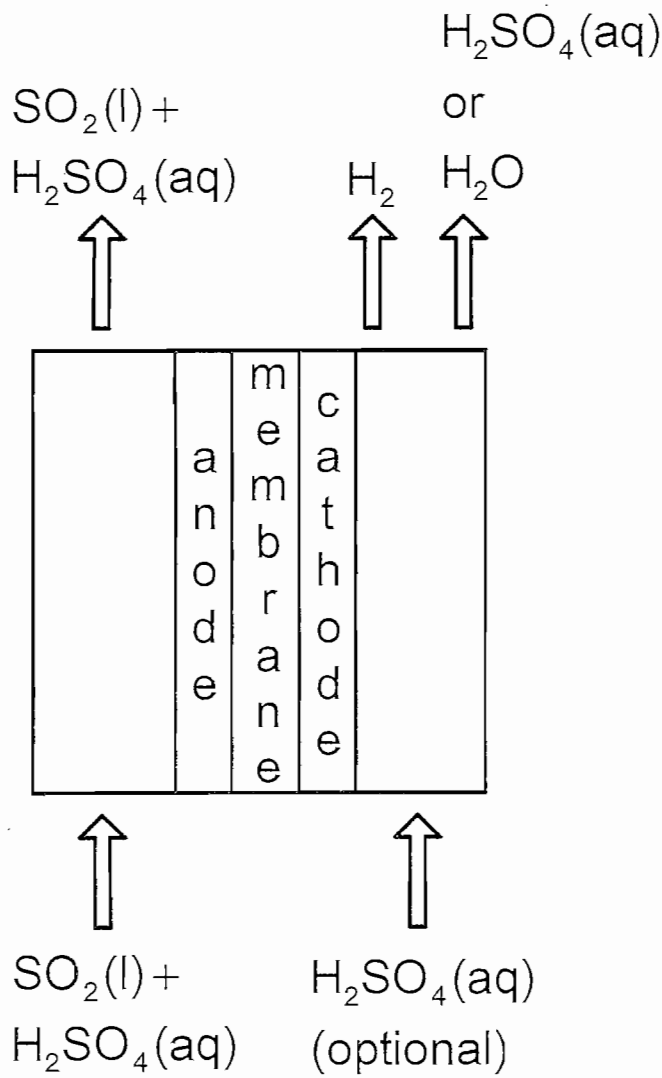


Figure 2.9: Simplified diagram of the new SRNL electrolyser design (Summers, 2006:10)

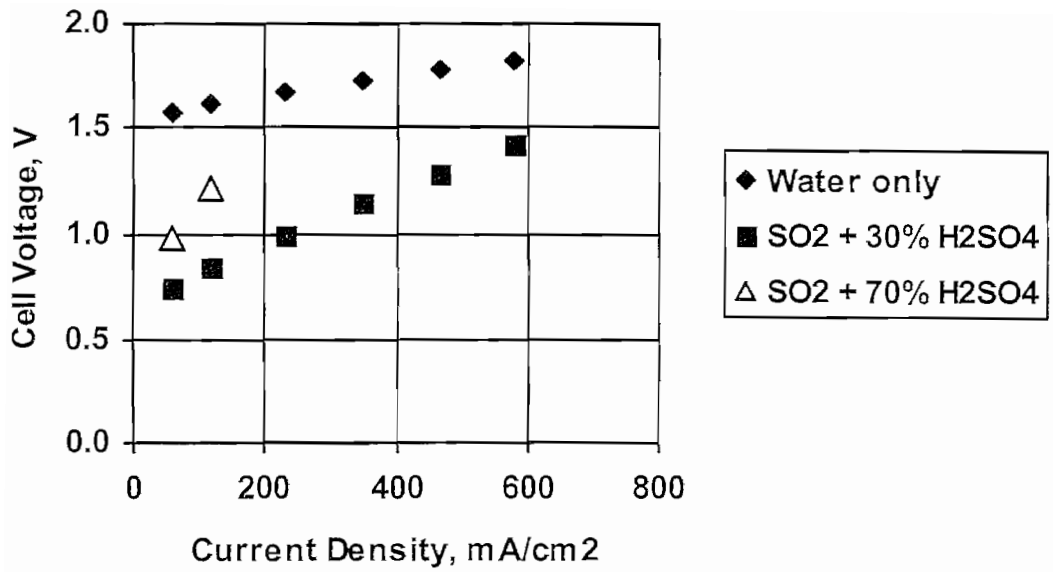


Figure 2.10 Tafel plot for SDE cell at 25°C and atmospheric pressure with different anolyte acid concentrations (Summers, 2006:15)

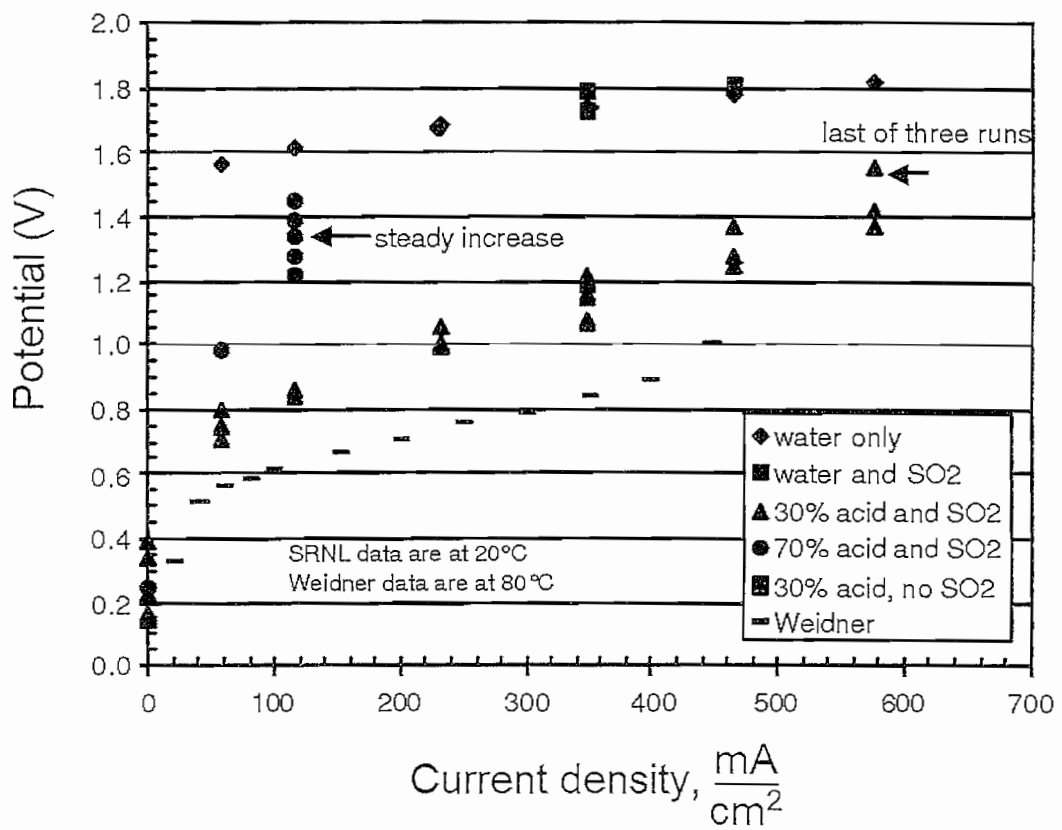


Figure 2.11 Tafel plot for SDE cell (Summers, 2005:11)

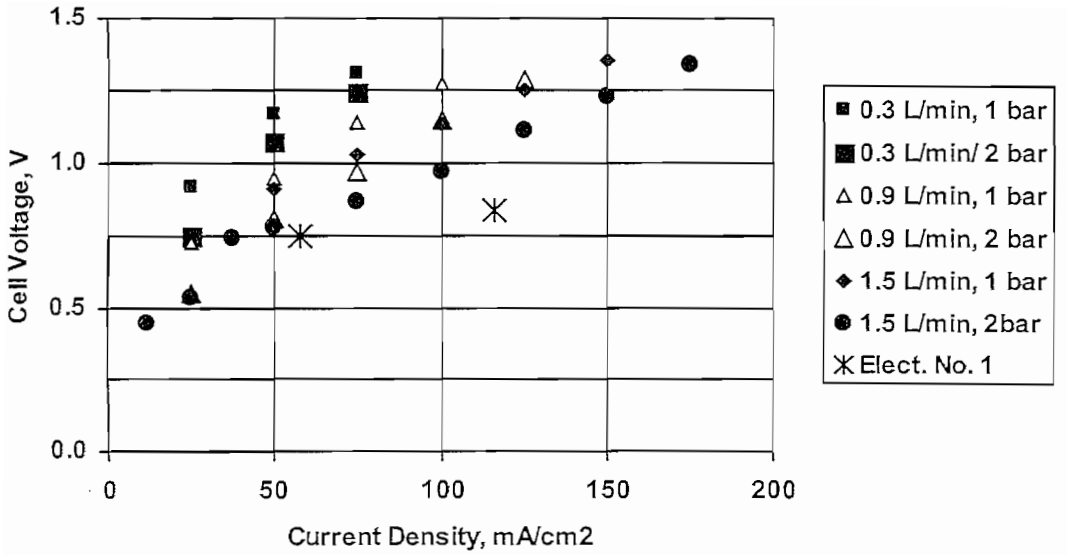


Figure 2.12 Tafel plot for SDE cell at 25°C with different pressures and anolyte flow rates (Summers, 2006: 16)

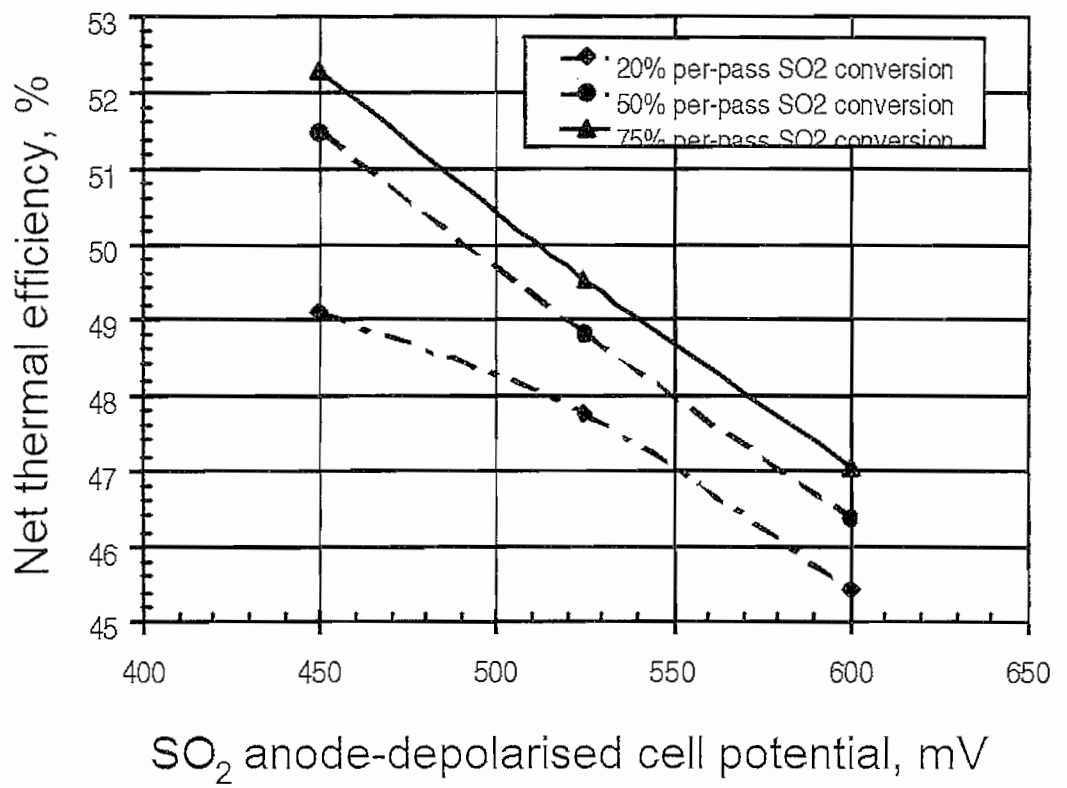


Figure 2.13 Graph showing results of a study conducted using Aspen into the effect of cell conversion of thermal efficiency of the HyS (Summers, 2005:9)

Figure 2.13 shows how the overall HyS thermal efficiency is affected by changes in the $SO_2$ conversion per pass in the electrolyser. Gorensek (2007:5) summarized the electrolyser characteristics of three designs used in past HyS process flow sheets:

**Table 2.1 Electrolyser performance summary and comparison (Gorensek, 2007:5)**

| | 1976 flowsheet | 1983 flowsheet | SRNL flowsheet |
|---|---|---|---|
| Operating pressure (bar) | 25.86 | 20.0 | 20.0 |
| Operating temperature (°C) | 90.0 | 100.5 | 80.0 |
| $H_2SO_4$ concentration (wt%) | 66.3 | 63.0 | 65.0 |
| $SO_2$ concentration (wt%) | 7.7 | 10.8 | 8.95 |
| $SO_2$ conversion (%) | 47.2 | 2.2 | 50.0 |
| Current efficiency (%) | >99.0 | 100 | 99 |
| Cell voltage (mV) | 450 | 607 | 525 |

The electrolyser is the biggest hurdle between the HyS and viable application. Summers (2006:10) concludes that further research is required in order to establish cell operating performance at commercial operating conditions. In addition there are problems with catalysts, to date only large concentrations, of expensive platinum, suspended on graphite were found to be viable (Colón-Mercado & Hobbs, 2007:2653). $SO_2$ crossover over the membranes is still a problem with the Nafion membranes currently used in PEM SDE cells (Summers, 2005:7).

#### *2.2.2.5 Process Alternatives*

The NWU has not yet developed a flowsheet of the HyS. Dries Grundlingh (Grundlingh, 2010) is currently developing one using the Aspen simulation package. His design was not completed before this project was done and as a result could not be used. This provided some difficulty in the completion of this study as there are a number of process alternatives that could be decided on. A brief description of the major process alternatives follows.

##### *2.2.2.5.1 Sulphuric Acid Concentration*

Bilgen *et al.* (1993:13) suggested the use of a series of flashes under vacuum conditions to separate the water out of the sulphuric acid.

Huang and T-Raissi (2007:635,641,644) model the aforementioned design for the sulphuric acid concentration and decomposition section of the SI cycle and suggested two alternative flow sheets both using distillation to separate the acid and water.

Another alternative is to absorb the decomposition reactor's gaseous product stream in the electrolyser's liquid product stream and recycling the resulting liquid product stream from the absorber to the acid decomposition reactor (Cox, 1978:50).

The preferred approach seems to be using a series of flashes followed by an absorption column as described in the previous paragraph. The SRNL flowsheet used by Gorensek (2007:5) and the one proposed by Bilgen *et al.* (1994:13) use this method.

*2.2.2.5.2 Sulphuric Acid Decomposition Section*

The SRNL flowsheet used by Gorensek (2007:5) uses a convectively heated reactor that receives its feed from the bottoms of a high temperature absorption column that absorbs most of the unreacted sulphur trioxide and hydrogen sulphate vapour in the reactor effluent. The reactor effluent is fed to the bottom of the absorption column. This approach seems quite popular and is also used by Bilgen *et al.* (1994:13) and in the Ispra Mark 11-V6 flowsheet (Cox, 1978:50).

Another approach is to use a heated reactor and simply flash the effluent at low temperature (87 °C) into a liquid stream consisting mainly of sulphuric acid and water and a vapour stream consisting of oxygen and sulphur dioxide. The liquid stream is sent to the electrolyser as anolyte. The vapour stream is separated into an oxygen product and a liquid sulphur dioxide stream that is sent to electrolyser as anolyte Jeong (2005:6).

The convectively heated reactors can, of course, be replaced by Coetzee's (2008:5) adiabatic reactor design in any one of these configurations.

*2.2.2.5.3 Separation of Sulphur Dioxide and Oxygen*

Jeong *et al.* (2005:6) suggests using a two stage compression and refrigeration method to separate the sulphur dioxide from the oxygen.

A number of absorber columns – with each column receiving its vapour feed from the previous column – has also been suggested. The resulting sulphur dioxide rich solution can then be fed to the electrolyser (Cox, 1978:50).

*2.2.2.5.4 Electrolyser Section*

Jeong *et al.* (2005:6) use an electrolyser in their proposed flow sheet that receives dilute acid and liquid sulphur dioxide as anolyte and converts all the $SO_2$ in a single pass.

The Ispra Mark 11-V6 flowsheet (Cox, 1978:50) uses a series of absorbers to absorb the sulphur dioxide and all of this sulphur dioxide is converted in a single pass through the electrolyser.

The SRNL HyS flowsheet used by Gorensek (2007:5) in his study of the effect of the electrolyser configuration on the overall thermal efficiency of the HyS used an electrolyser with partial sulphur dioxide conversion in an elaborate flowsheet in which the sulphur dioxide is separated out of a part of the electrolyser effluent and reabsorbed in its feed using a column. The other part of the effluent is directly recycled to the electrolyser feed.

Westinghouse uses a series configuration of absorbers with electrolysers between them and after the last absorber. The vapour feed containing mainly sulphur dioxide and oxygen are fed to the last absorber while the liquid (mostly water) feed is fed to the first absorber. This results in a vapour effluent stream that is almost pure oxygen and a large conversion of sulphur dioxide in a pass of the electrolyser section (Gorensek 2007:9).

## *2.3 Previous Simulations*

### 2.3.1 Introduction

A number of factors need to be taken into account when the reproducibility and correctness of the results of a simulation are considered. Most noteworthy of these are the fluid package used along with the restrictions on its applicability.

### 2.3.2 Simulation Package

The Aspen Plus™ (Aspen) simulation package was chosen for this study for the same reasons that Gorensek (2007:3) considered before using it in his study of the HyS; it is universally accepted, flexible and powerful.

### 2.3.3 Fluid Package

An Oleum data package is available from Aspen Technology, Inc. (AspenTech) that can be used in Aspen. It accurately correlates sulphuric acid properties for any concentration of hydrogen sulphide in water and even up to pure oleum. This package is, however, only accurate up to temperatures of 150°C and pressures of 2 bar (Gorensek, 2007:3). Gorensek (2007:3) further notes that these limitations were removed by Mathias in work commissioned by General Atomics to simulate the SI cycle.

Mathias (2002:7) modelled the SI cycle (which has the sulphuric acid decomposition reaction in common with the HyS). He used the Chen Electrolyte-NRTL (ElecNRTL) physical properties model along with chemistry models to describe the nonideality of the $H_2O/H_2SO_4$ solutions. The components used by Mathias follow.

**Table 2.2 List of components used by Mathias (2002:8-9)**

| Formula | Description |
|---|---|
| $H_2O$ | Water |
| $H_2SO_4$ | Sulphuric acid |
| $SO_2$ | Sulphur dioxide |
| $SO_3$ | Sulphur trioxide |
| $H_2$ | Hydrogen |
| $H_3O^+$ | Hydrated hydronium ion |
| $HSO_4^-$ | Bisulphate ion |
| $SO_4^{-2}$ | Sulphate ion |
| $H_2S_{0.5}O_{2.5}$ | Sulphuric acid-water ion pair |

He defined a number of chemistry models to be used in different process blocks in Aspen. Two of them are applicable and descriptions of them follow.

Mathias (2002:9-10) found that for temperatures below 300°C the following reactions could be used to describe the ionic dissociation of sulphuric acid as well as the molecular dissociation of sulphuric acid to form sulphur trioxide and water:

$$H_2SO_4 + H_2O \leftrightarrow H_3O^+ + HSO_4^-$$

$$HSO_4^- + H_2O \leftrightarrow H_3O^+ + SO_4^{-2}$$

$$H_2O + SO_3 \leftrightarrow H_2SO_4$$

Mathias (2009:10) asserts that sulphuric acid tends to form ion pairs or complexes above 300°C. The chemistry involved at these temperatures follows:

$$H_2O + SO_3 \leftrightarrow H_2SO_4$$

$$H_2O + H_2SO_4 \leftrightarrow 2H_2S_{0.5}O_{2.5}$$

Mathias (2009:42) defined sulphur dioxide, oxygen and hydrogen as Henry components.

Graphical summaries of the fit of thermochemical properties, as predicted by the model developed by Mathias (2002:41-95), to empirically determined values follow.

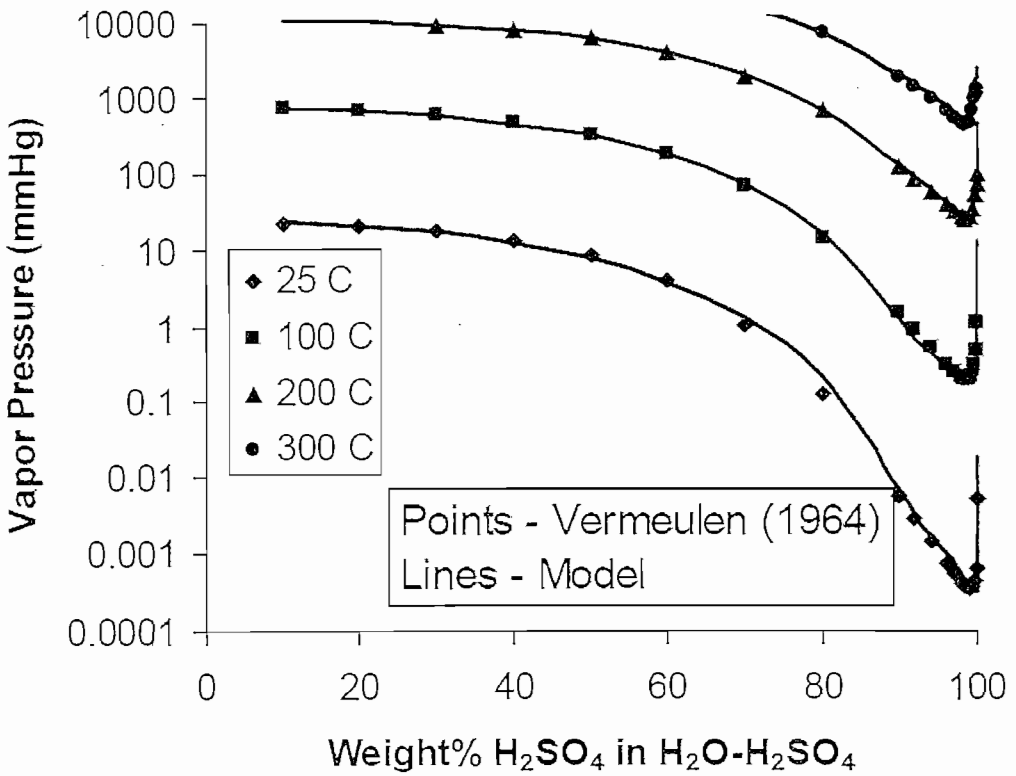


**Figure 2.14: Graph showing vapour pressure of sulphuric acid mixtures (Mathias, 2002:14)**

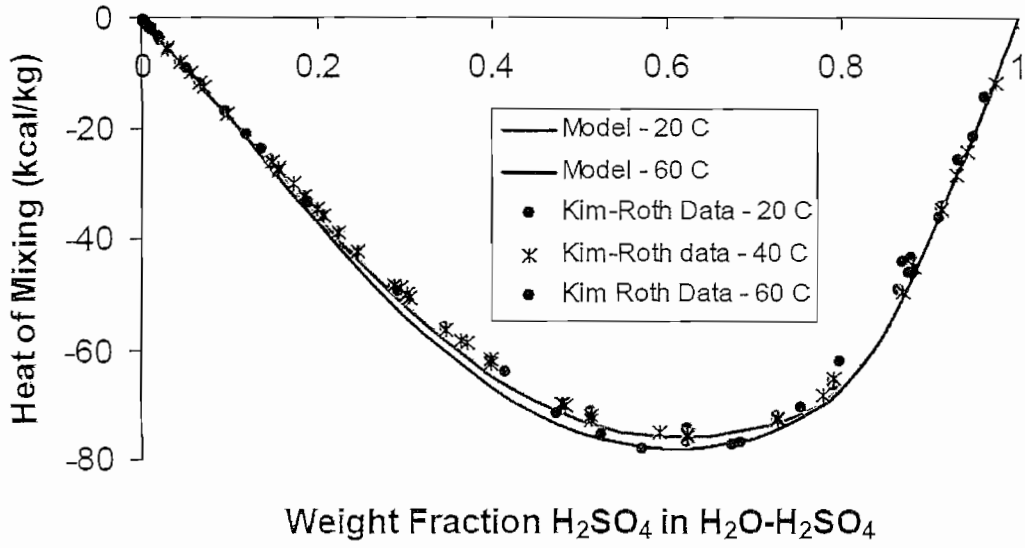


Figure 2.15: Graph showing heat of mixing for aqueous sulphuric acid mixtures (Mathias, 2002:15)

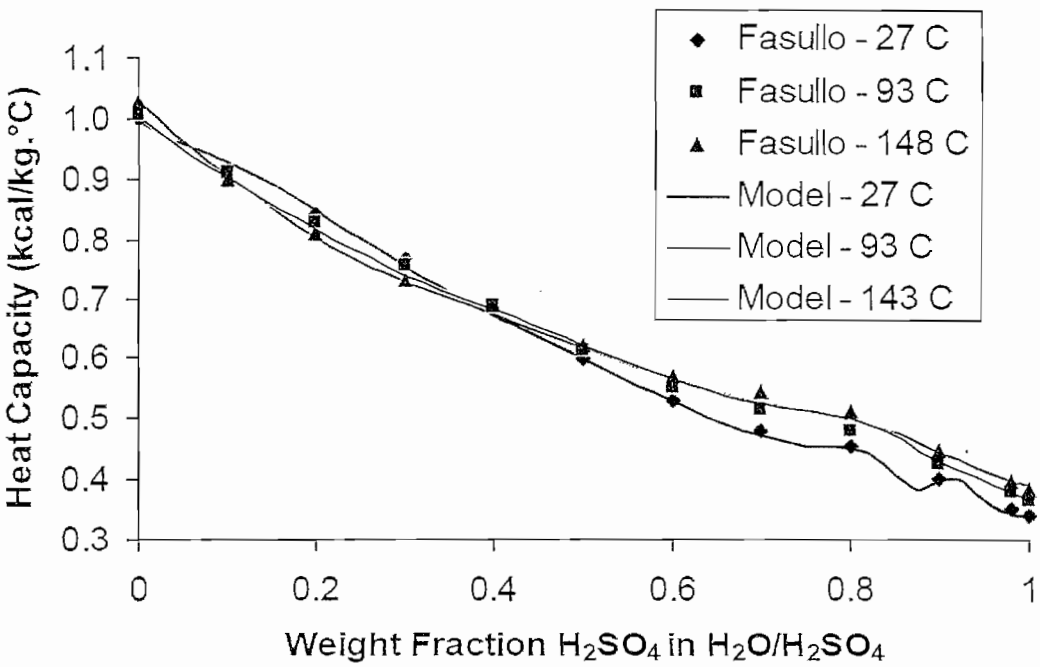


Figure 2.16: Graph showing liquid heat capacity of sulphuric acid mixtures (Mathias, 2002:16)

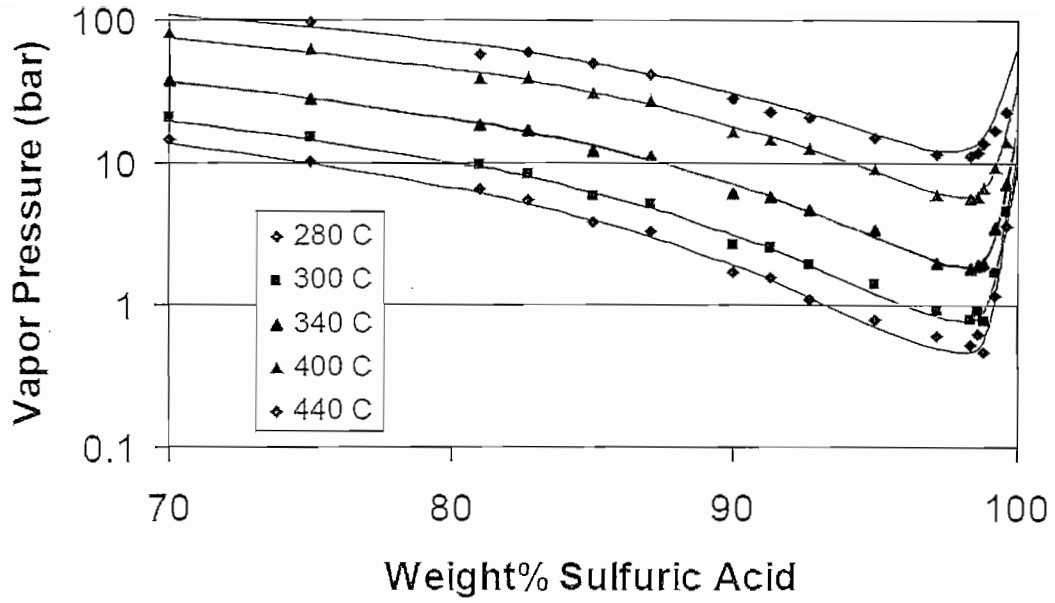


**Figure 2.17: Graph showing vapour pressure of sulphuric acid solutions (Mathias, 2002:16)**

In May 2007 Gorensek (2007:2) finished a report about the effect of different electrolyser configurations on the thermal efficiency of the HyS. He ran simulations in Aspen and used the method suggested by Mathias (as discussed afore). He does assert that it is better to change between the two chemistry models at 270°C rather than 300°C. He reasons that this reduces differences in calculated enthalpies between the models. He also mentions that he made an adjustment to the way in which the solubility of sulphur dioxide in sulphuric acid solutions is calculated. He does not disclose how he did this (Gorensek, 2007:3).

By November 2007 Gorensek and Summers (2007:2) had co-authored a report about a HyS flowsheet using PEM electrolysis and a bayonet decomposition reactor. They use the same method mentioned before that was suggested by Mathias and by Gorensek but mention that the modifications made to the sulphur dioxide solubility consisted of fitting interaction parameters for sulphur dioxide with other aqueous species to the experimental data they had available (Gorensek & Summers, 2007:12). While simulating the rest of the column they abandon this approach because sulphur

dioxide is present as a separate liquid phase and cannot be treated as a Henry (supercritical) component. For this reason, and the convenience of not having to switch between chemistry models based on temperature, they used OLI Systems, Inc.'s Mixed Solvent Electrolyte (MSE) model. The Aspen-OLI interface allows the OLI Engine to be used from within Aspen. The model has only been shown to be accurate to 500°C though (Gorensek & Summers, 2007:20).

Graphical summaries of the fit of thermochemical properties, as predicted by the model developed by Gorensek & Summers (2007:61), to empirically determined values follow.

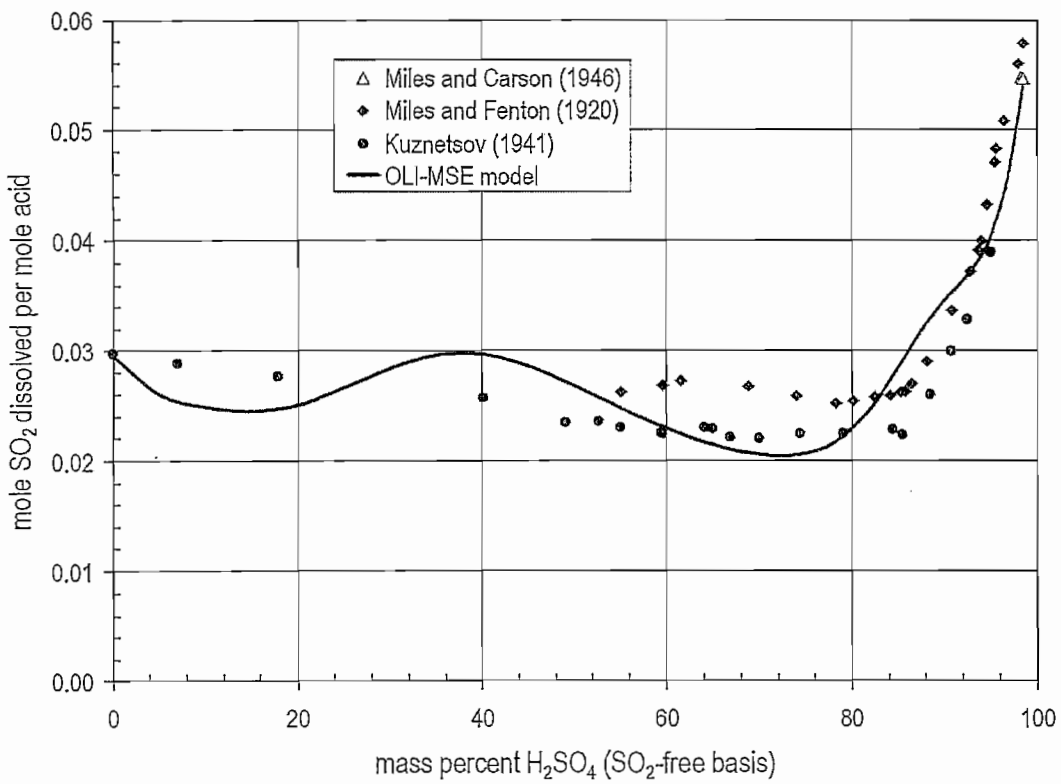


**Figure 2.18: Graph showing the solubility of $SO_2$ in sulfuric acid at 1.013-bar partial pressure (Gorensek & Summers, 2007:61)**

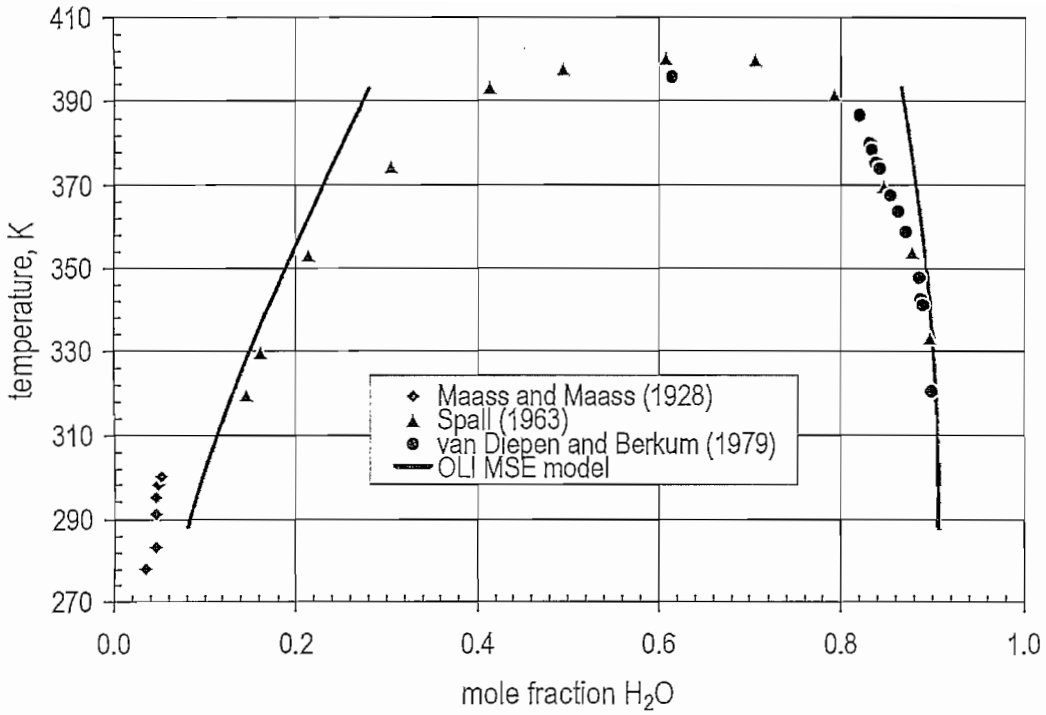


**Figure 2.19: Graph showing liquid-liquid phase equilibrium in the $SO_2$-$H_2O$ system (Gorensek & Summers, 2007:63). (Note that the temperature is the boiling temperature)**

### 2.3.4 Process units

Gorensek (2007:4) asserts that currently insufficient information data is available for the electrolysers to be designed in detail. He made performance projections based on work done at SRNL and Westinghouse and calculated the electric power consumption and the hydrogen generation rate.

## *2.4 Process Control Issues Identified in Literature*

### 2.4.1 Cascaded Units

These are process units connected in series. Each process unit sees only the disturbances from the unit directly upstream from it (Svrcek et. al., 2000:229). In the HyS these are units like the flash drums that could be used in the acid decomposition section.

The absence of recycle streams in certain sections simplifies the simulation of those sections. Control systems can therefore be devised and tested for these sections in a simulation package like Hysys and as long as they can handle feed flow, composition, temperature and pressure fluctuations in the range of what the recycle effects can cause they will be applicable.

### 2.4.2 Material Recycle Streams

At least one recycle stream is inherent in the HyS because it is a cycle; it is the recycle of sulphur compounds between the electrolyser and acid decomposition section. Other recycle streams are required depending on the specific process flow configuration under consideration.

Two problems are associated with the use of recycle streams, namely:

- Time constants in recycle streams
- The snowball effect

Large time constants mean that any change in a recycle process can cause an upset that takes a long time to even back out into a steady state. This together with the positive feedback behaviour that most recycle processes exhibit can cause intermediate vessels to overflow or run empty. This occurs very slowly and therefore cannot easily be detected. In addition it takes very long to return the process to normal operating conditions (Luyben et. al. 1999:22-23).

The snowball effect is a quasi steady-state phenomenon that causes large variations in recycle flows. Often the equipment cannot handle these flows, especially those in the separation section that are particularly sensitive to abnormally high or low flows (Luyben *et al.*, 1999:23).

In the past large tanks were installed in recycle streams to isolate sequences of units and make the conventional cascaded units approach to process control work. The increased chemical inventory has obvious environmental and economic drawbacks (Svrcek et. al., 2000:231). Luyben et. al. (1999: 57-58) suggest the following three part approach:

- A stream somewhere in each recycle loop should be flow controlled in order to prevent the snowball effect.
- A reactant feed stream cannot be flow controlled unless it is in effect converted in one pass.
- If the final product of a plant comes out of the top of a distillation column, then the feed to the column should be liquid and, conversely, if the final product comes out of the bottom of the column, its feed should be vapour. These configurations afford greater product purity stability given feed composition fluctuations.

### 2.4.3 Heat Integration

Heat integration involves the use of process to process heat exchangers in order to improve the thermal efficiency of a plant. They have the disadvantage of making it easier for thermal disturbances to be propagated through the plant (Luyben et. al. 1999:19,139).

Feed-effluent heat exchangers (as used in all alternatives for the acid decomposer section) used in reactor sections can cause multiplicity and open-loop instability (Luyben et. al. 1999:139).

Heat integration should ideally be done with process control in mind and in an iterative fashion together with process dynamics studies. These studies should pick up any multiplicity problems in the acid decomposition section. In addition thermal disturbances can be prevented by the use of small auxiliary utility exchangers (Luyben et. al. 1999:139).

### 2.4.4 Chemical Component Inventories

All the species that are fed to a process leaves somewhere in a product stream or is converted in a reactor. When recycle streams are involved the fraction of a given species can either increase or decrease in an integral fashion (Luyben et. al. 1999:20).

### 2.4.5 Process Units

*2.4.5.1 Acid Decomposition Reactors*

As has been mentioned, Coetzee (2008:5) suggests the use of adiabatic plug flow reactors with inter-stage heating. This arrangement is the preferred way of designing a reactor section if you have control in mind (Luyben et. al., 1999:104).

# 3. SIMULATIONS AND SENSITIVITY ANALYSES

## *3.1 Introduction*

It is important to understand the effect of different conditions on the behaviour of a plant if a control system for it is to be devised. This chapter is a study of the steady state responses of the system which will be accomplished with the help of a sensitivity analysis.

## *3.2 Sensitivity Analysis*

In this sensitivity analysis inventory variables were ignored as a steady state simulation was employed. The energy and material feeds to the plant were taken as manipulated variables (degrees of freedom) while primary and secondary control objectives were taken as response variables. Manipulated variables were varied about the base case values and the responses of the simulation were recorded. Sensitivity diagrams were then drawn up to reveal the extent to which manipulated variables influenced the responses of the plant.

### 3.2.1 The Simplified Excel Simulation of the Process

*3.2.1.1 Introduction*

This simulation was a simple mass balance done in order to obtain a simplified insight into the way the HyS would work under idealised conditions. This provided a feel for the cycle which proved to be helpful for more detailed study. This model was later adapted to solve the water and sulphuric acid recycle rates to the acid decomposition section for entry into the Aspen simulation.

*3.2.1.2 Assumptions*

The first simulation was run in Microsoft Excel and was simplified as far as possible. The simplifications made were:

- The reactor and electrolysis sections were assumed to maintain constant conversion of $H_2SO_4$ and $SO_2$ respectively
- Perfect separation was assumed possible

Consider the assumption that the reactor (sulphuric acid decomposition) section's conversion is constant. The conversion will decrease as the feed flow rate to the reactor section is increased. This will be negligent for sufficient catalyst loadings. Therefore the assumption that the reactor section can maintain constant conversion is valid, because this will be the case if sufficient catalyst loading is used in five consecutive adiabatic packed bed reactors with inter-stage heating to 870°C (See 3.2.3). Similarly the assumption regarding electrolysis section's conversion is valid.

Assuming perfect separation is not valid either. The impact of this assumption is marked and need not be discussed in detail. See 3.2.2 for an idea as to the extent of this assumption's impact.

Even with these assumptions some insight was gained into the behaviour of the HyS cycle. Furthermore, the Aspen simulation would have been very challenging without data and experience gained from this simulation.

*3.2.1.3 Process Flow Description and Diagram*

Figure 3.1 shows a block flow diagram of this simulation. The acid decomposition section uses the stoichiometry discussed in the literature study (repeated below) of this document and a conversion based on sulphuric acid that is entered into the simulation, to calculate the flows of the components in stream S1.

$$H_2SO_4 \rightarrow SO_2 + H_2O + \frac{1}{2}O_2$$

The "flash drum" that follows perfectly separates the gaseous from the liquid components with the former ending up in stream S2 while the latter end up in stream S3. The oxygen/ sulphur dioxide separation unit separates stream S2 into a pure oxygen stream (S4) and a pure sulphur dioxide stream (S5). A water make-up stream (S6) is added to the electrolyser where the following reaction takes place.

$$SO_2 + 2H_2O \rightarrow H_2SO_4 + H_2$$

The extent of this reaction is also determined by a constant conversion of $SO_2$. The pure hydrogen produced leaves the electrolyser via stream S8 while the rest of the products and unused reactants end up in stream S9. Stream S9 enters the sulphuric acid concentration section where the heavy hydrogen sulphate component ends up in stream S10 and is recycled it to the acid decomposition section while the light components are recycled to the electrolyser via stream S7.

Flow values for stream S7 and S10 were specified and recalculated. The Solver add-in was used to find the flow values for these two streams that resulted in the simulation being in mass balance. This could be seen by the specified and calculated variables for streams S7 and S10 being the same.

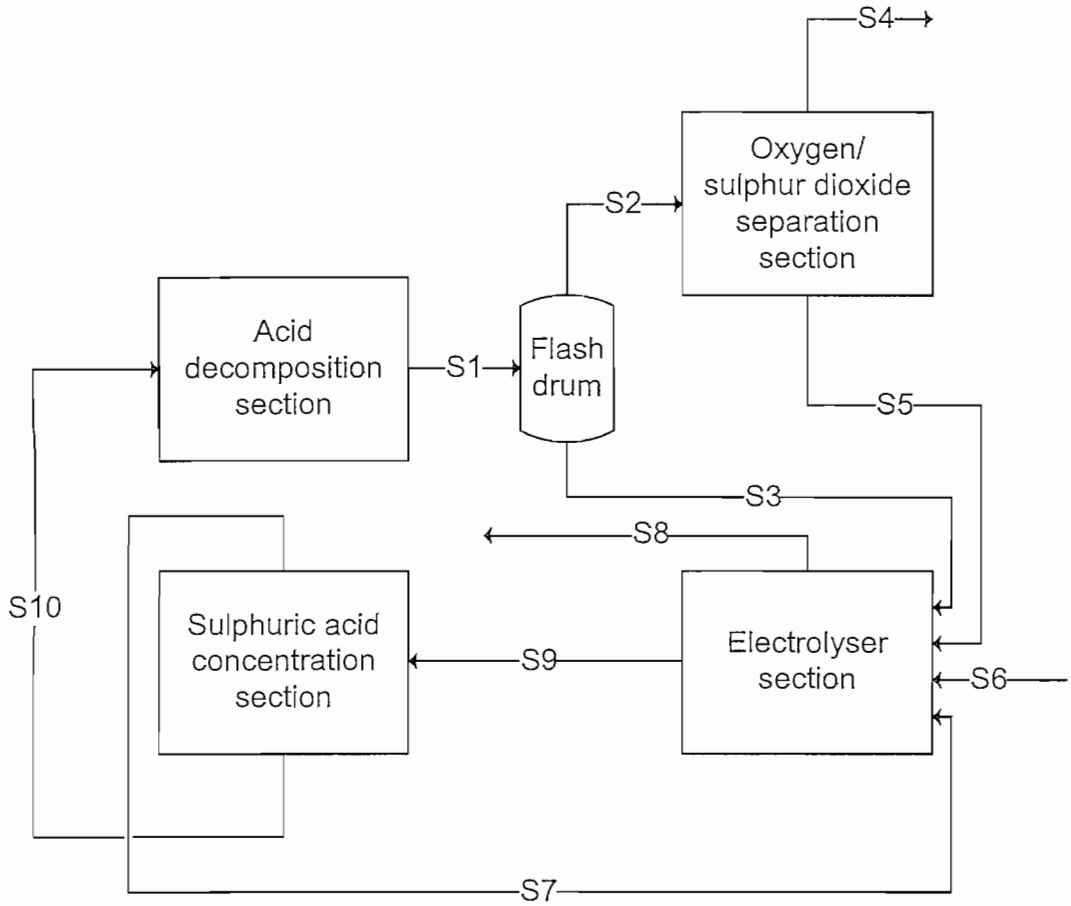


**Figure 3.1: Block flow diagram of the simplified Excel simulation run**

*3.2.1.4 Method*

The following base case for the simulation was chosen

The specified variables:

- Acid decomposition section conversion = 0.72
- Electrolysis section conversion = 0.5
- Water feed flow rate = 1000 kmol/hr

The conversion of the acid decomposition section was based on the extent deemed possible by Coetzee (2008:1). The electrolysis section's conversion is based on values deemed typical for single electrolysers by Gorensek (2007:5). The water feed flow rate was arbitrarily chosen for being wieldy.

This resulted in the following flow values:

**Table 3.1: Base case flow values for simplified Excel simulation**

| | Component flow (kmol/hr) | | | | |
|---|---|---|---|---|---|
| Stream | $H_2O$ | $H_2SO_4$ | $SO_2$ | $O_2$ | $H_2$ |
| S1 | 1000 | 388.89 | 1000 | 500 | 0 |
| S2 | 0 | 0 | 1000 | 500 | 0 |
| S3 | 1000 | 388.89 | 0 | 0 | 0 |
| S4 | 0 | 0 | 0 | 500 | 0 |
| S5 | 0 | 0 | 1000 | 0 | 0 |
| S6 | 1000 | 0 | 0 | 0 | 0 |
| S7 | 1000 | 0 | 1000 | 0 | 0 |
| S8 | 0 | 0 | 0 | 0 | 1000 |
| S9 | 1000 | 1388.9 | 1000 | 0 | 0 |
| S10 | 0 | 1388.9 | 0 | 0 | 0 |

The water flow rate was varied over a range of 15% less than to 15% greater than its base case value. The reactor and electrolyser sections' conversions were dropped incrementally to values 15% smaller than their base case values. The responses of the following variables were noted:

- The flow rate of recycle stream S7
- The flow rate of recycle stream S10
- The hydrogen production rate
- The oxygen production rate

For the base case these values are given in Table 3.2.

**Table 3.2 Response variable values for base case of base case of simplified Excel simulation**

| Response variable | Value | Units |
|---|---|---|
| Recycle stream S7 flow rate | 2000 | kmol/hr |
| Recycle stream S10 flow rate | 1389 | kmol/hr |
| Hydrogen production rate | 1000 | kmol/hr |
| Oxygen production rate | 500 | kmol/hr |

### *3.2.1.5 Results and Discussion*

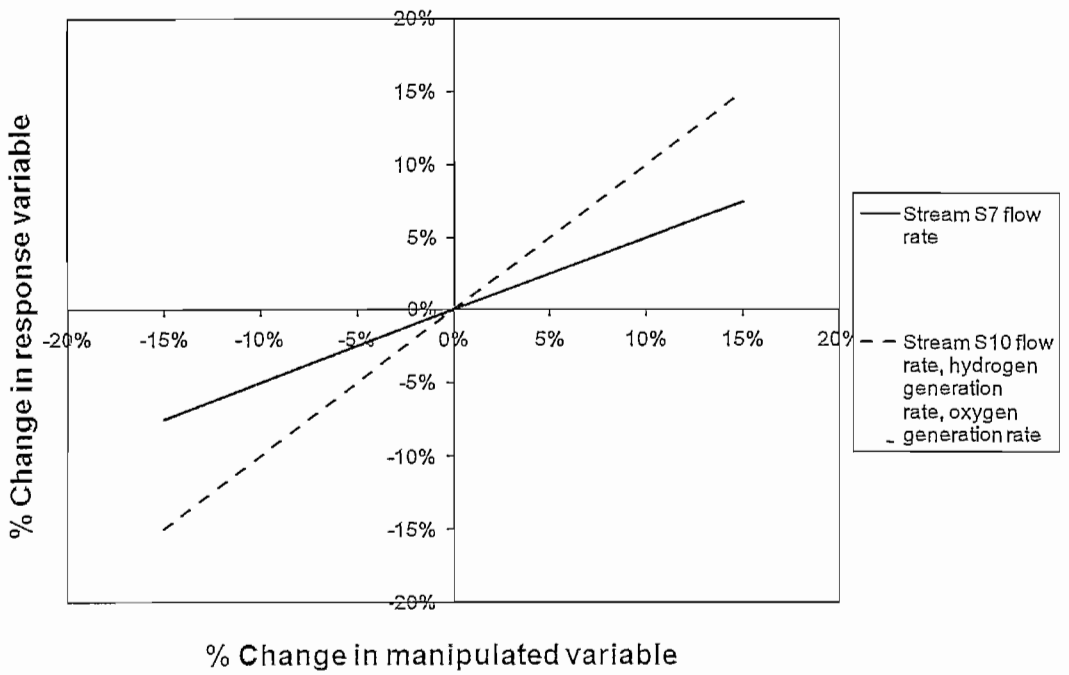


**Figure 3.2: Graph of the effect of changing the water feed flow rate**

Figure 3.2 shows that all the response variables are affected in a proportional manner when the water feed flow rate to the cycle is changed. The reason for this is simple, for the plant to remain in mole balance the mole flow of hydrogen product has to be equal to the mole flow of water feed. Similarly the mole flow of oxygen has to be half that of the feed water. Also, for the plant to remain in mole balance all the water fed to the cycle has to be converted to sulphuric acid and hydrogen in the electrolysis section. This means that the

amount of sulphur dioxide fed to the electrolyser has to increase. This sulphur dioxide is formed in the sulphuric acid decomposition section and so the recycle of sulphuric acid needed to form it (in stream 10) also increases. The electrolyser section does not convert all the sulphur dioxide in one pass and therefore the excess has to be recycled. This recycle of sulphur dioxide is as sensitive to changes in the water feed as the other response variables but stream S7 also recycles water. This water recycle rate does not change throughout the sensitivity analysis and can in fact be set to any arbitrary value. The reason for this is that all the water in the water feed and from the sulphuric acid decomposition section has to be consumed in the electrolyser section in order to maintain mole balance. Therefore no recycle of water is even required. In a non-idealised simulation this will not be the case.

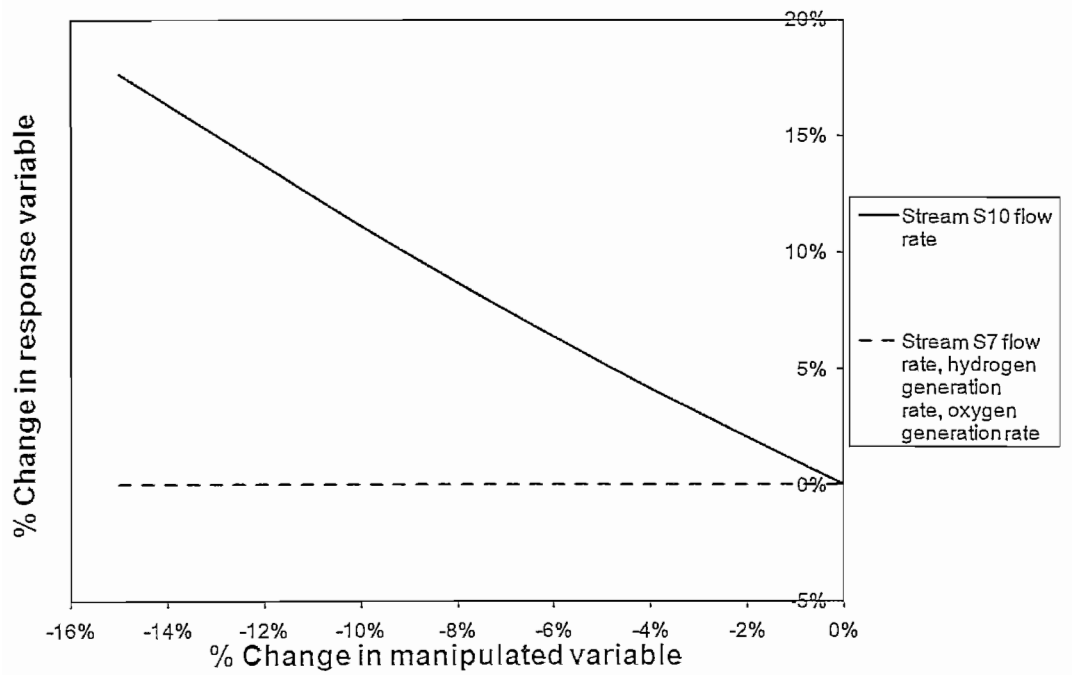


**Figure 3.3: Graph of the effect of decreasing sulphuric acid decomposition section conversion**

Figure 3.3 shows that the acid recycle stream flow rate increases as the sulphuric acid decomposition section conversion decreases. The sulphuric acid recycle stream has to increase as the sulphuric acid decomposition section's conversion decreases because the electrolyser section still requires the same amount of sulphur dioxide to split the water fed to the cycle. This is a problem because if the flow through the reactor increases (*i.e.* the reactor's space velocity increases) the conversion of the reactor will fall. Figure 2.7 shows this concept graphically for the WX-1 catalyst. This cumulative causation could clearly cause problems if the plant's control strategy was not designed with this possibility in mind.

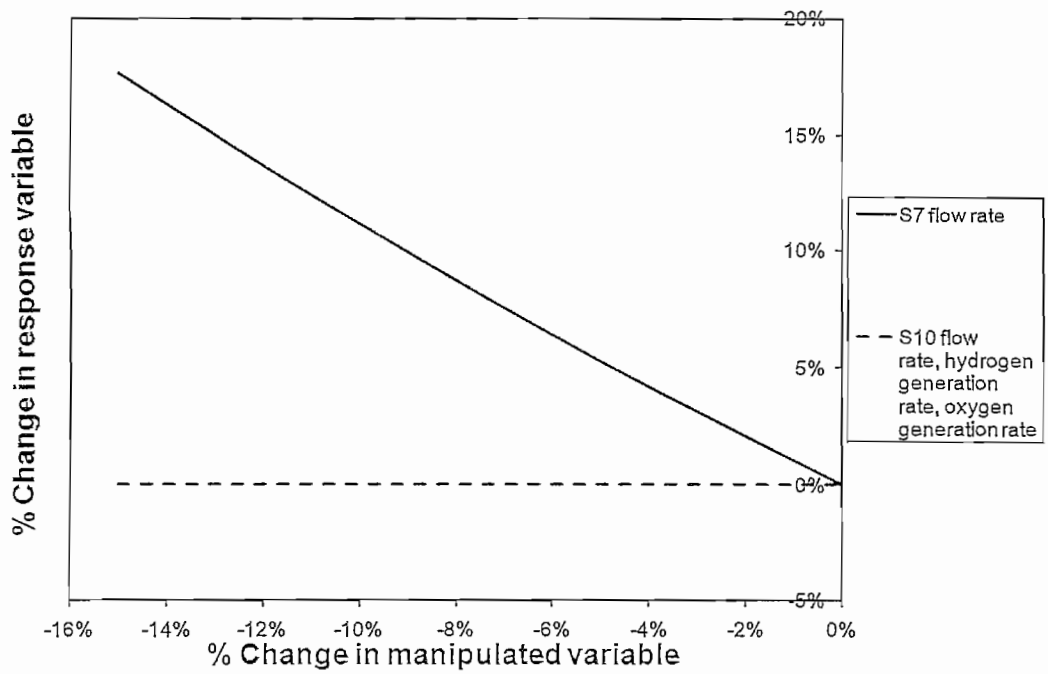


**Figure 3.4: Graph of the effect of decreasing electrolyser section conversion per pass**

Figure 3.4 shows that a decrease in the electrolyser section conversion affects only the flow rate of the recycle stream S7. The reason for this is the perfect separation assumed in the sulphuric acid decomposition section. The entire sulphur dioxide flow that is not consumed in a pass through the electrolyser is simply recycled back to it in stream S7. This recycle stream assumes a value which allows all the water fed to the plant to be reacted in a single pass through the electrolyser section in order for the plant to remain in

a steady state. Intuition warns that a positive feedback situation – similar to the one involving the sulphuric acid recycle and sulphuric acid conversion in the acid decomposition section – is possible here. This may not necessarily be the case as increased flow improves mass transfer in electrolytic cells. Therefore this needs to be studied in detail.

### 3.2.2 Aspen Simulation

*3.2.2.1 Introduction*

This simulation was done in order to obtain a more realistic idea of what the sensitivity of the HyS might be like. The NWU is currently developing a flowsheet for the HyS but have not yet produced a working concept. The flowsheet used in this simulation was developed with simplicity in mind as not to cloud the inherent responses of the HyS.

*3.2.2.2 Assumptions*

Three assumptions were made for the purpose of completing this simulation:

- The property model used to represent the $H_2SO_4$-$H_2O$-$SO_3$-$SO_2$-$O_2$ system is accurate
- The conversion in the acid decomposition section is constant
- The conversion in the electrolyser section is constant

The property model used for this simulation is an extension of the Oleum data package that was developed by Paul M. Mathias. It is discussed in 2.3.3 and its practical use involves, simply, the entering of fitted parameters into the ElecNRTL fluid package in Aspen. This property model sufficiently models the $H_2SO_4$-$H_2O$-$SO_3$ system but is not accurate for high $SO_2$ concentrations dissolved in $H_2O$-$H_2SO_4$ mixtures. For this reason no absorption columns were used in the flowsheet and resultantly the property model should be accurate. Note that little attention has been paid to $O_2$ solubility in any available property model. A more accurate fluid model (than this one, the Aspen Oleum package or the OLI MSE model) should be developed before any further simulations are done at the NWU.

Consider the second assumption. The conversion will decrease as the feed flow rate to the reactor section is increased or the reactant concentration in the feed decreases. The effect of a change in feed flow rate is negligible if each reactor contains sufficient catalyst (See 3.2.3). The reactant concentration has a more marked effect. This is not a problem for all but one of the runs because the reactant concentration was kept constant. In the run carried out to investigate the effect of changing the reactant concentration in the feed to the reactor section the results will be inaccurate. The assumption will therefore be valid for each run except the one investigating changes in the sulphuric acid concentration in stream S1.

No model is available for the SDE so a conversion was chosen that was deemed possible in the light of experiments conducted to date. Gorensek & Summers (2007:34) assumed a constant conversion in their simulation of the HyS using a SDE and a bayonet decomposition reactor. This assumption should be valid for a sufficiently liberal designed SDE but a model should be developed nonetheless.

#### *3.2.2.3 Process Flow Description and Diagram*

Figure 3.5 shows a process flow diagram used for this simulation. It is followed by an equipment list. Operating conditions and flow rates are discussed in 3.2.2.4.

Stream S1 consists of 90 mass percent $H_2SO_4$ with the rest being mainly water. In the Aspen simulation stream S1 was split into streams S1A and S1B that were not connected. Stream S1A's variables were manipulated until all variables for stream S1A and S1B were equal and mass balance was therefore achieved. An adapted version of the simulation in 3.2.1 was used to calculate the $H_2O$ and $H_2SO_4$ flows in this stream but the rest of the component flows were calculated by Aspen. Stream S1 is heated to 870°C in heat exchanger HX-1. Almost all of the $H_2SO_4$ is decomposed to $SO_3$ at this temperature. Stream S2 leaving HX-1 passes to the sulphuric acid decomposition section (REA-1) where 72% of the $SO_3$ is decomposed to $SO_2$ and $O_2$. Stream S3 leaving REA-1 is flashed at 25°C and 3 bar into a tops stream S5 and a bottoms stream S4. Stream S4 flows into stream S10 which feeds the electrolyser (ELC-1).

Stream S5 flows into stream S6 that is flashed in FLS-2 at -85°C and 30bar into tops stream S7 and bottoms S8. Stream S7 is the oxygen product stream. It does contain a noticeable amount of $SO_2$ which might be recovered by a process – perhaps involving membranes. Absorption should be investigated as a possible alternative to this very impractical flash separation step (FLS-2) but the issues involving the modelling of the solubility of $SO_2$ and $O_2$ in $H_2SO_4/H_2O$ mixtures should be resolved first.

Stream S8, along with stream S9 (water makeup) and S22 ($SO_2$ makeup) flow into stream S10. Stream S10 flows over the anode of the electrolyser (ELC-1). 50% of the $SO_2$ in the feed is converted to $H_2SO_4$ and $H_2$ in the electrolyser. The hydrogen that leaves the anode as protons crosses over the membrane in the electrolyser to be reduced at the cathode. Seven moles of water crosses over the membrane with each mole of hydrogen due to electo-osmotic drag (Gorensek, 2007:5). This water and hydrogen leaves the cathode side of the electrolyser in stream S11. The water and hydrogen are separated in flash drum FLS-3 at 25°C and 20bar. The tops stream S12 is the hydrogen product stream while the bottoms stream S13 is recycled to the anode side of the electrolyser by joining stream S10. The anolyte leave the electrolyser in stream S14.

Stream S14 is flashed at 25°C and 20bar in FLS-4. The tops stream S15 is sent to FLS-2 by flowing into stream S6. The bottoms stream of FLS-4 is stream S16 and is flashed in FLS-5 at 269°C and 1bar. The bottoms stream (S17) flows into stream S1 but the tops stream (S18) is flashed in FLS-6 at 237°C and 1 bar. The bottoms stream (S19) flows into stream S1 and the tops stream (S20) is recycled to the electrolyser by flowing into stream S10.

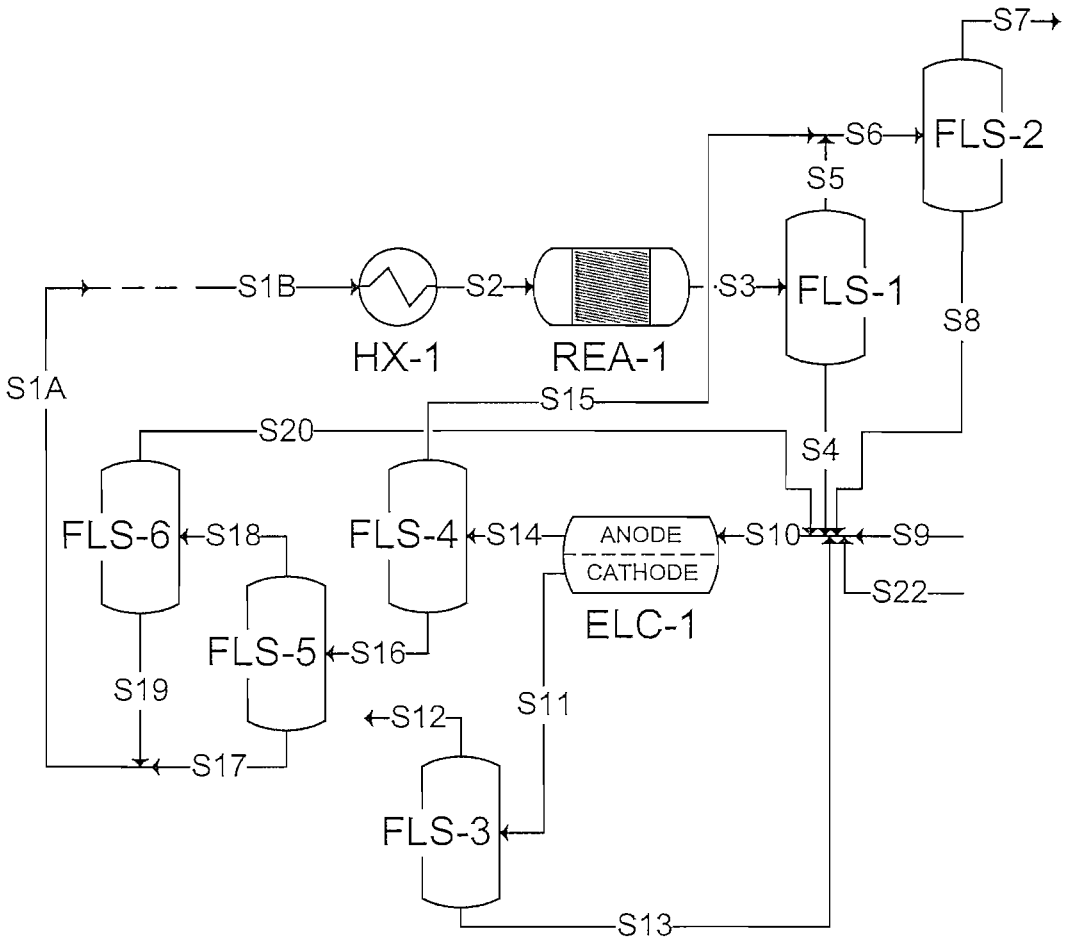


Figure 3.5: Process flow diagram of the process used for the Aspen simulation

**Table 3.3: Equipment list**

| Designation | Description |
|---|---|
| HX-1 | Heat exchanger ($H_2SO_4$ to $SO_3$ decomposition) |
| REA-1 | $SO_3$ decomposition reactor system |
| ELC-1 | Electrolyser |
| FLS-1 | Flash drum |
| FLS-2 | Flash drum ($O_2/SO_2$ separation) |
| FLS-3 | Flash drum ($H_2O/H_2$ separation) |
| FLS-4 | Flash drum |
| FLS-5 | Flash drum ($H_2SO_4/H_2O$ separation) |
| FLS-6 | Flash drum ($H_2SO_4/H_2O$ separation) |

*3.2.2.4 Method*

The following base case for the simulation was chosen

The specified variables:

- Sulphur trioxide decomposer (REA-1) conversion = 0.72
- Electrolysis section (ELC-1) conversion = 0.5
- Water feed (S9) flow rate = 1000kmol/hr
- S1 sulphuric acid mol fraction = 0.9
- Sulphuric acid decomposition (HX-1) temperature = 870°C
- Sulphuric acid decomposition (HX-1) pressure = 3bar
- FLS-1 temperature = 25°C
- FLS-1 pressure = 3bar
- FLS-2 temperature = -85°C
- FLS-2 pressure = 30bar
- FLS-3 temperature = 25°C
- FLS-3 pressure = 20bar
- FLS-4 temperature = 25°C
- FLS-4 pressure = 20bar
- FLS-5 temperature = 269°C
- FLS-5 pressure = 1bar
- FLS-6 temperature = 237°C
- FLS-6 pressure = 1 bar

This resulted in the following flow values:

**Table 3.4: Base case values for stream variables**

| | Apparent component flow (kmol/hr) | | | | | | | |
|---|---|---|---|---|---|---|---|---|
| Stream | H2O | H2SO4 | SO3 | SO2 | H2 | O2 | T (°C) | P (bar) |
| S1 | 154 | 1389 | 0 | 0 | 0 | 0 | 258 | 1 |
| S2 | 1541 | 3 | 1387 | 0 | 0 | 0 | 870 | 3 |
| S3 | 1541 | 3 | 388 | 998 | 0 | 499 | 870 | 3 |
| S4 | 1151 | 391 | 0 | 18 | 0 | 0 | 25 | 3 |
| S5 | 2 | 0 | 0 | 981 | 0 | 499 | 25 | 3 |
| S6 | 2 | 0 | 0 | 1396 | 0 | 512 | 13 | 3 |
| S7 | 0 | 0 | 0 | 40 | 0 | 499 | -85 | 30 |
| S8 | 2 | 0 | 0 | 1356 | 0 | 12 | -85 | 30 |
| S9 | 1000 | 0 | 0 | 0 | 0 | 0 | 25 | 20 |
| S10 | 9807 | 542 | 0 | 1997 | 2 | 13 | 53 | 1 |
| S11 | 7002 | 0 | 0 | 0 | 1000 | 0 | 100 | 20 |
| S12 | 2 | 0 | 0 | 0 | 998 | 0 | 25 | 20 |
| S13 | 7000 | 0 | 0 | 0 | 2 | 0 | 25 | 20 |
| S14 | 808 | 1540 | 0 | 998 | 0 | 13 | 100 | 20 |
| S15 | 0 | 0 | 0 | 415 | 0 | 13 | 25 | 20 |
| S16 | 808 | 1540 | 0 | 583 | 0 | 0 | 25 | 20 |
| S17 | 58 | 932 | 0 | 0 | 0 | 0 | 269 | 1 |
| S18 | 759 | 599 | 9 | 583 | 0 | 0 | 269 | 1 |
| S19 | 96 | 457 | 0 | 0 | 0 | 0 | 237 | 1 |
| S20 | 655 | 150 | 1 | 583 | 0 | 0 | 237 | 1 |
| S22 | 0 | 0 | 0 | 40 | 0 | 0 | 25 | 20 |

The manipulated variables were varied over values ranging from 15% smaller than the base case to 15% greater (unless the change was not physically possible). The responses of the following variables were noted:

- S1 recycle flow rate
- S13 recycle flow rate
- S15 recycle flow rate
- S20 recycle flow rate
- S12 product flow rate
- S7 product flow rate
- S12 product purity (hydrogen mol fraction)
- S7 purity (oxygen mol fraction)
- S20 oxygen recycle rate
- S22 feed flow rate

For the base case these values are given in Table 3.5.

**Table 3.5: Base case values for response variables (second simulation)**

| Response variable | Value | Units |
|---|---|---|
| S1 flow | 1543.6 | kmol/hr |
| S13 flow | 7002.2 | kmol/hr |
| S15 flow | 427.4 | kmol/hr |
| S20 flow | 1389.1 | kmol/hr |
| S12 flow | 1000.0 | kmol/hr |
| S7 flow | 539.0 | kmol/hr |
| S12 hydrogen mol fraction | 0.998 | |
| S7 oxygen mol fraction | 0.926 | |
| S20 oxygen flow | 0.026 | kmol/hr |
| S22 flow | 39.8 | kmol/hr |

*3.2.2.5 Results and Discussion*

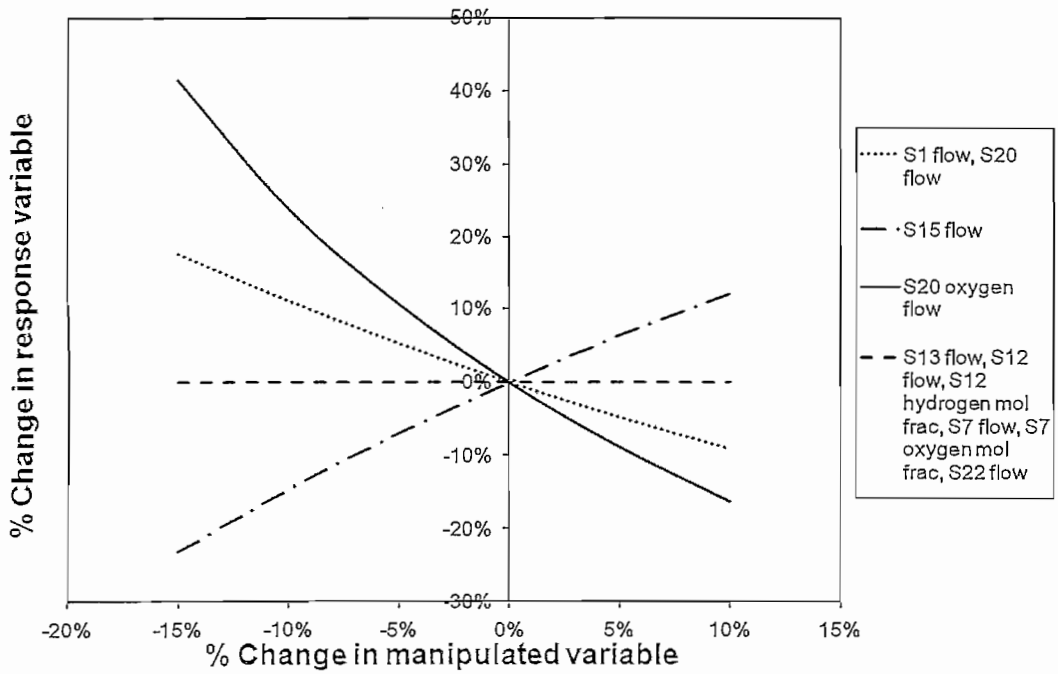


**Figure 3.6: Graph of the effect of changing the conversion of REA-1**

Figure 3.6 shows the response of changing the conversion of the acid decomposition reactor section (REA-1). The product flow rates (S7 and S12) are not changed – resultantly the flow of S13 is also unchanged. The product stream purities remain unchanged as well – therefore the flow of stream S22 remains unchanged too. The flow of stream S22 has to be equal to the sulphur dioxide flow in stream S7 for the system to be in mass balance. The flows of the recycle streams S1 and S20 increase as the conversion of REA-1 decreases. This is because the sulphuric acid recycle rates need to increase in order to maintain the same $SO_2$ evolution rate in REA-1. The flow of oxygen in the recycle stream S20 increases dramatically more than stream S20 itself as the conversion of REA-1 decreases (although the mole fraction is still only $2.256 \times 10^{-5}$ when REA-1's conversion is decreased by 15%). The flow of stream S15 increases as the conversion increases. This is because of the increased liquid recycle volume (stream S16 in particular) in which sulphur dioxide can dissolve.

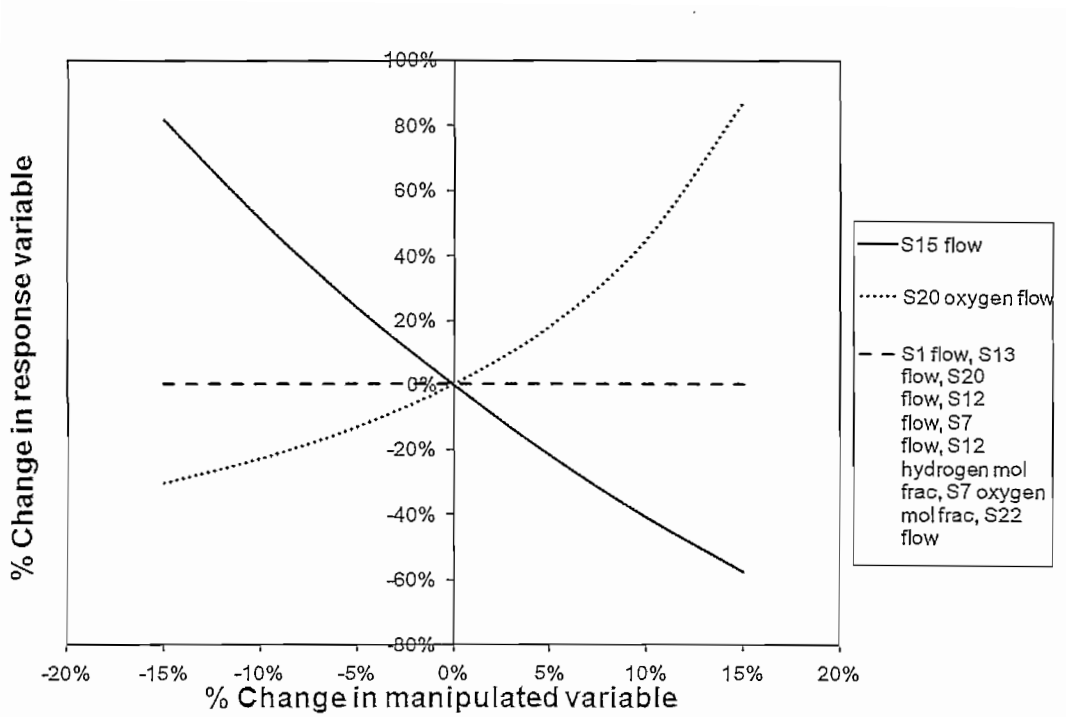


**Figure 3.7: Graph of the effect of changing the conversion of ELC-1**

Figure 3.7 shows that only two variables are affected. The flow of stream S15 is increased drastically as the electrolyser (ELC-1) conversion decreases. This is because the sulphur dioxide recycle to the electrolyser has to be increased so that the overall rate at which the electrochemical reaction takes place remains constant. This is necessary to keep the system in mass balance. Further it can be seen that oxygen accumulates in recycle stream S20 as the conversion of the electrolyser increases. The snowball-like accumulation of oxygen in the anolyte recycle flow of the electrolyser is the reason that FLS-4 and stream S15 are required in the Aspen flow sheet. TNK-2 in the proposed P&ID shown in Figure 4.3 would also serve as a knock-out drum to remove the oxygen (and any other non-condensible buildup) from the recycle stream.

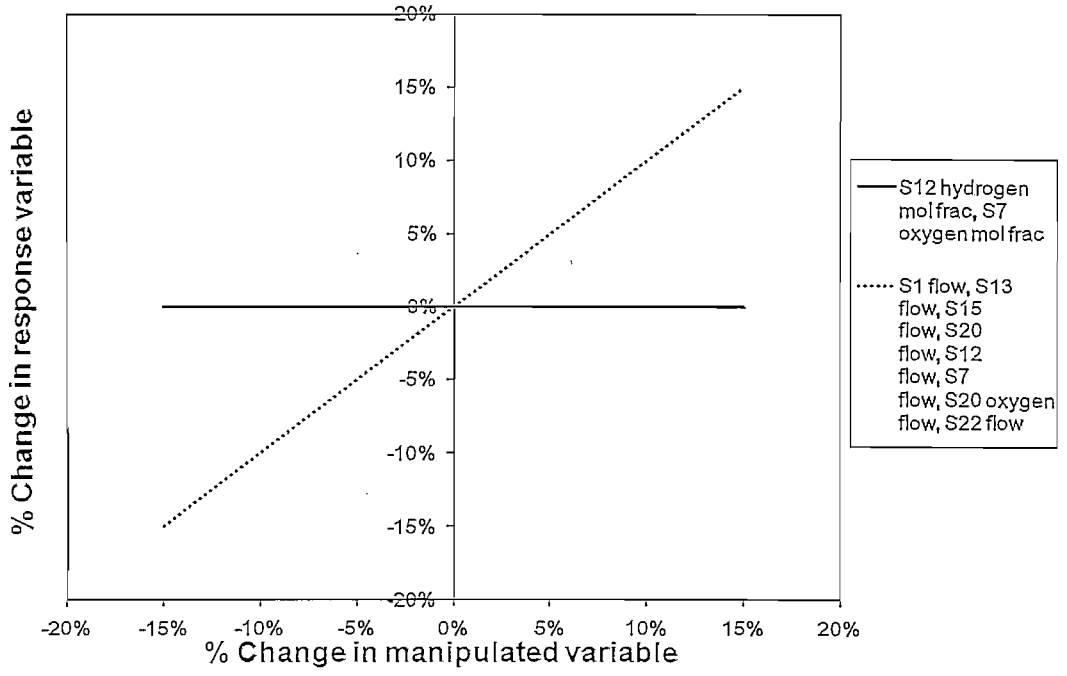


**Figure 3.8: Graph of the effect of changing the flow rate of stream S9**

Figure 3.8 shows the effect of changing the flow rate of the water feed stream (S9). The hydrogen and oxygen product purities remain unchanged but all the stream flow rates change by the same factor the water feed flow rate was changed. This is significant because it means that all the flow rates will need to be adjusted for the production rates to be changed.

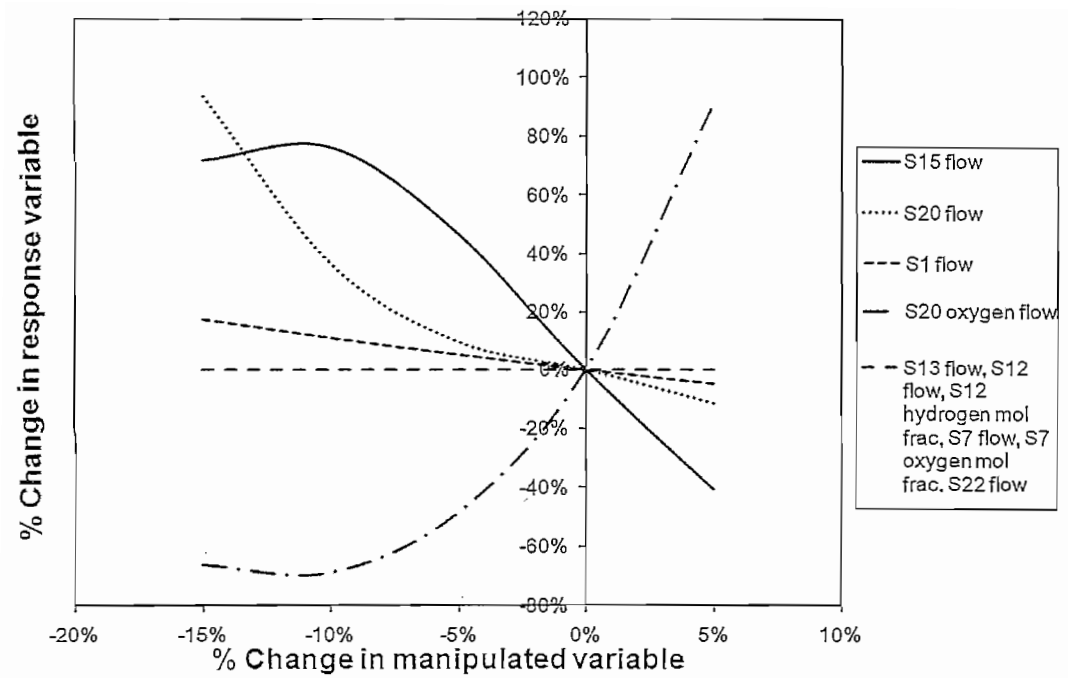


**Figure 3.9: Graph of the effect of changing the sulphuric acid mol fraction in stream S1**

Figure 3.9 shows the effect of changing the sulphuric acid concentration in stream S1. For reasons already discussed the results of this run are not accurate. Another simulation was built in order to get a better idea of the effect of changing this manipulated variable. See section 3.2.4.

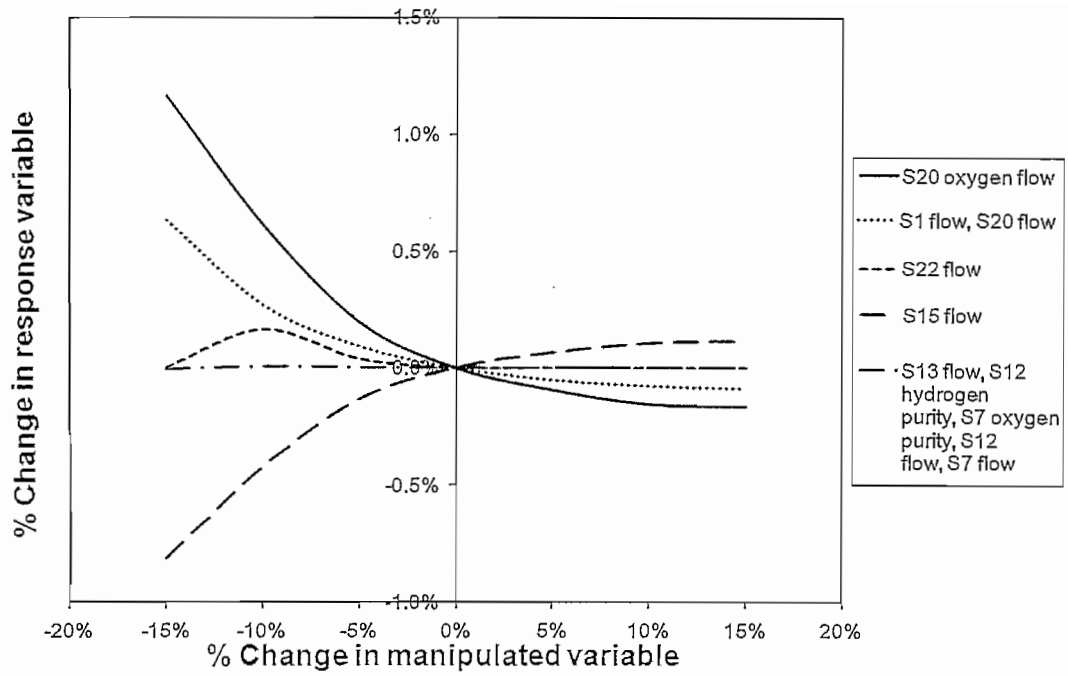


**Figure 3.10: Graph of the effect of changing the temperature of HX-1**

Figure 3.10 shows the effect of changing the temperature of HX-1. Using this simulation it can be seen that only some of the response variables are affected slightly. This is the result of a slight decrease in $H_2SO_4$ decomposition at lower temperatures and increase at higher temperatures. In a real plant even these small changes would not have occurred. The only change that would occur in a real plant would be a change in the helium flow requirement to the reactor section in order to get the reactor temperatures to the required feed temperature (at which the $H_2SO_4$ decomposition reaction would attain the same equilibrium it would have it HX-1's temperature was not changed). The reason this simulation was not able to predict this behaviour is simple. The equilibrium chemistry involved when $H_2SO_4$ decomposes into $SO_3$ and $H_2O$ is part of the fluid package and has to be disabled when the RStoic reactor block is used – as was the case with the reactor section. In summary – changing the temperature of HX-1 should have no effect on the response variables. This run was redone using a more accurate simulation – see section 3.2.4.

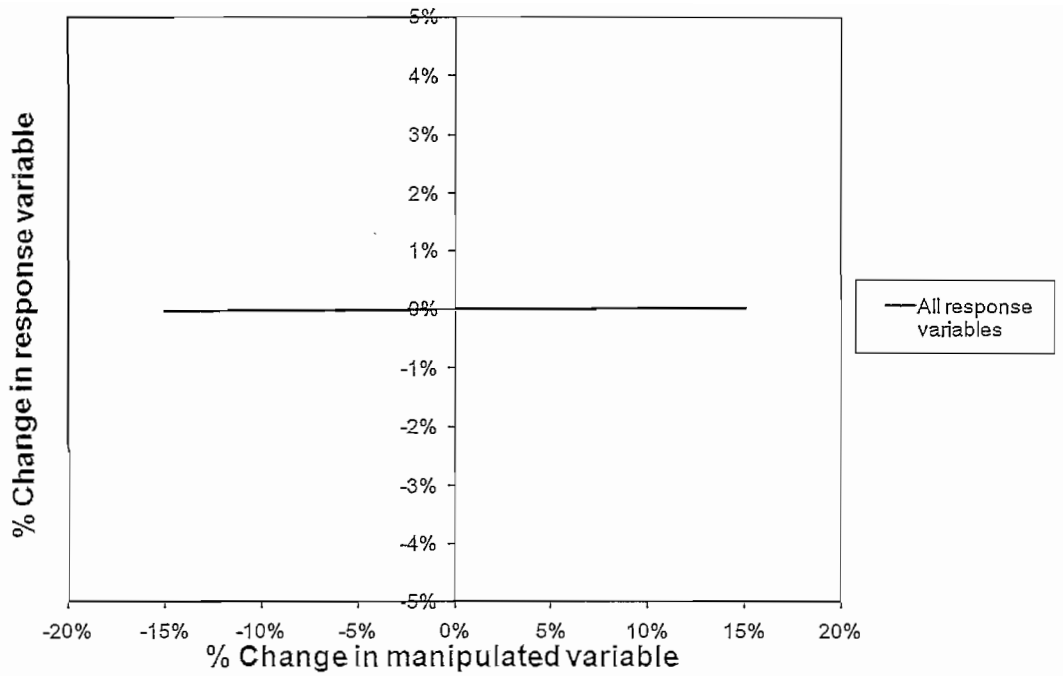


**Figure 3.11: Graph of the effect of changing the pressure of HX-1**

Figure 3.11 shows the effect of changing the pressure of HX-1. It has no effect on any of the response variables.

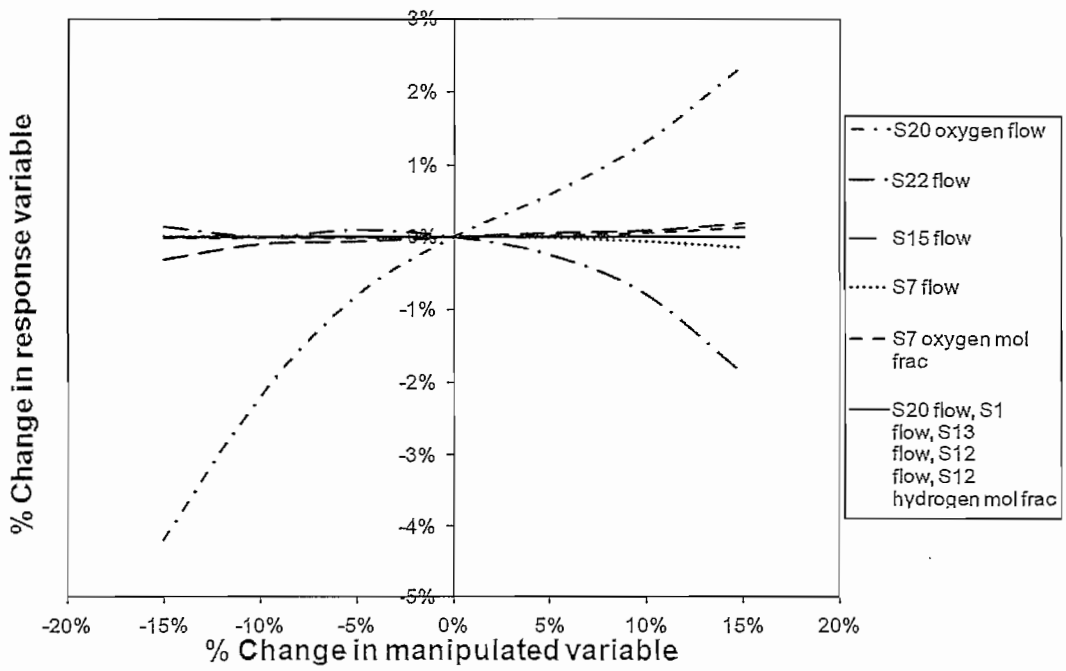


**Figure 3.12: Graph of the effect of changing the temperature of FLS-1**

Figure 3.12 shows the effect of changing the temperature of FLS-1. The oxygen flow in stream S20 shows a slight dependence on the manipulated variable while the sulphur dioxide feed flow rate decreases slightly as the manipulated variable increases but remains almost unchanged as it decreases. The flow of stream S22 decreases slightly as the manipulated variable is increased.

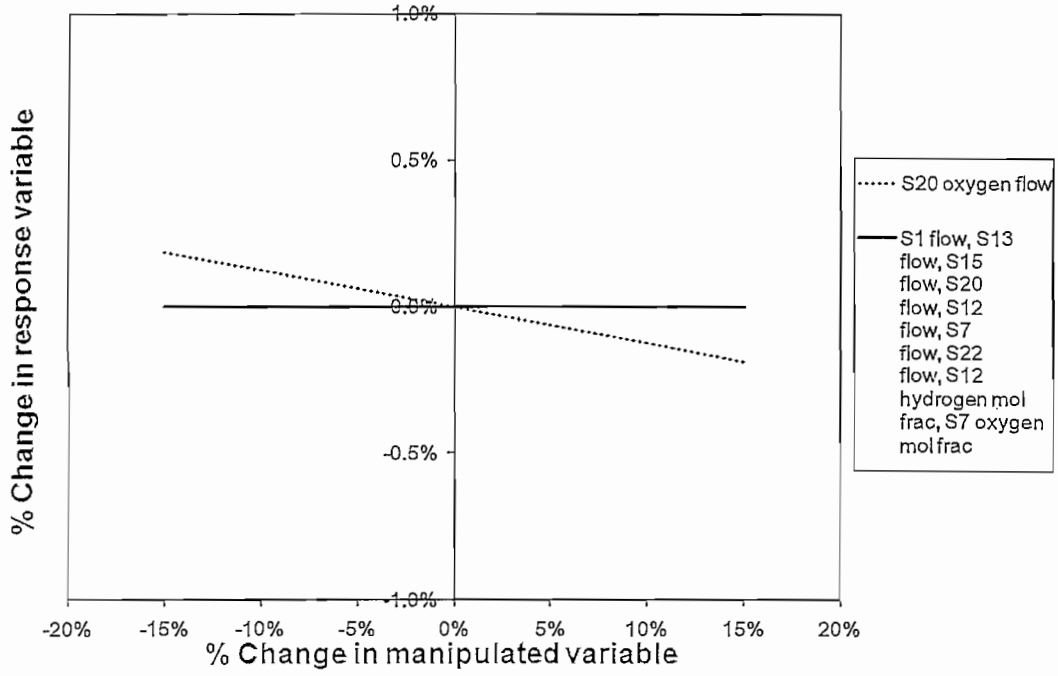


**Figure 3.13: Graph of the effect of changing the pressure of FLS-1**

Figure 3.13 shows that a change in the pressure of FLS-1 has virtually no effect on the response variables. Remember that the base case flow of oxygen in stream S20 accounts for a mole fraction of $1.865 \times 10^{-5}$ of that stream.

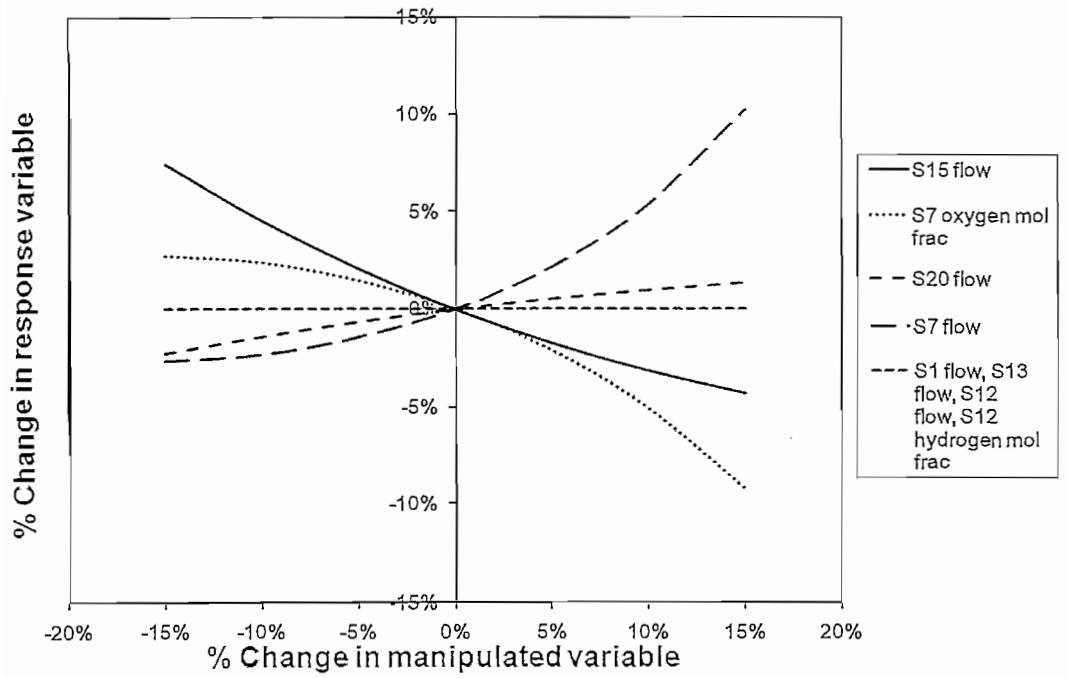


**Figure 3.14: Graph of the effect of changing the temperature of FLS-2**

Figure 3.14 and 3.15 show the effect of changing the temperature of flash drum FLS-2. The flow rate of stream S7 decreases slightly as the flash drum's temperature decreases but increases more as the temperature is increased. The reason for this is that more sulphur dioxide leaves with the oxygen in this product stream. FLS-2 is responsible for the separation of oxygen – a product – from sulphur dioxide that is recycled to the electrolyser. This is made more evident when the oxygen fraction is this stream is considered. As the temperature is decreased, less sulphur dioxide boils up in the flash drum but as it increases more is boiled up. Figure 3.15 shows how the sulphur dioxide make-up stream's flow rate has to compensate in order to keep the system in mass balance – its change is therefore numerically equal to the change in sulphur dioxide flow in stream S7. The oxygen flow in stream S20 is also drastically affected as FLS-2 is also responsible for avoiding accumulation of oxygen in the electrolyser anolyte recycle system. All other sulphur containing streams (S15 and S20) in the anolyte recycle system are also affected slightly.

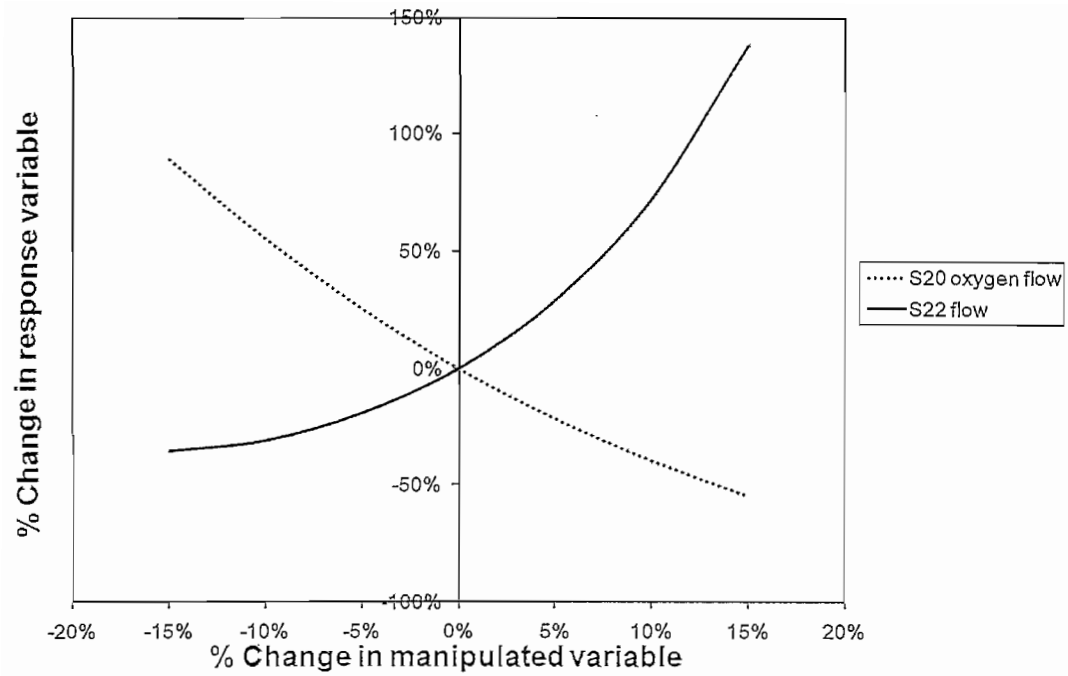


Figure 3.15: Graph of the effect of changing the temperature of FLS-2

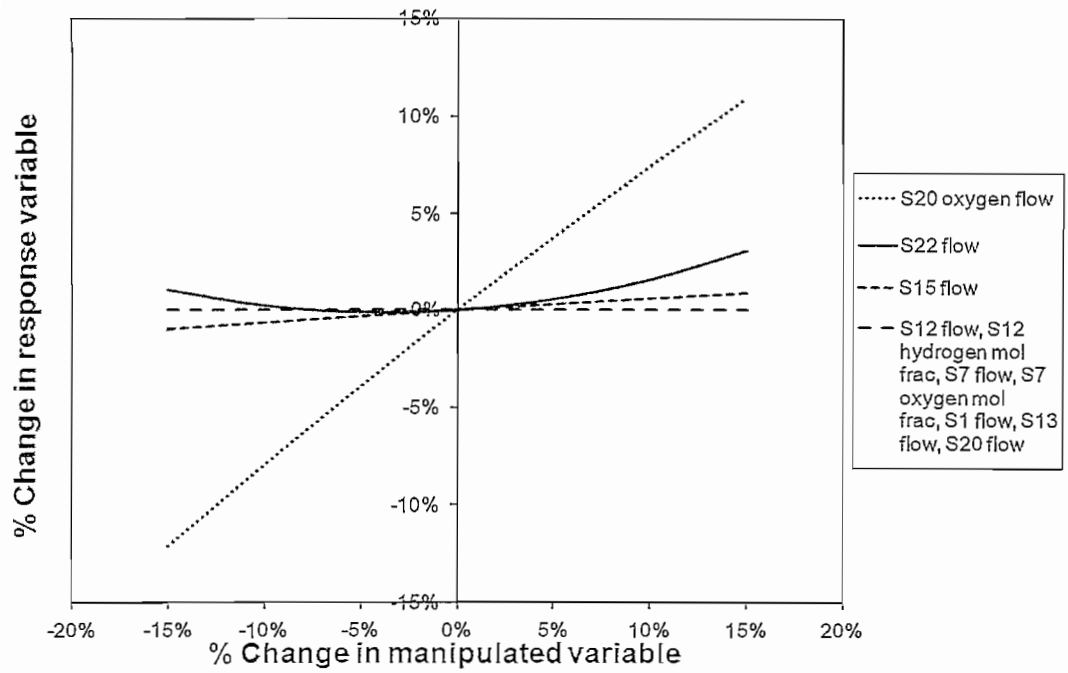


Figure 3.16: Graph of the effect of changing the pressure of FLS-2

Figure 3.16 shows that only the flow rate of oxygen in stream 20 is greatly affected by a change in the pressure of flash drum FLS-2. The reason being a slight increase in the oxygen dissolved in the bottoms stream of the flash drum.

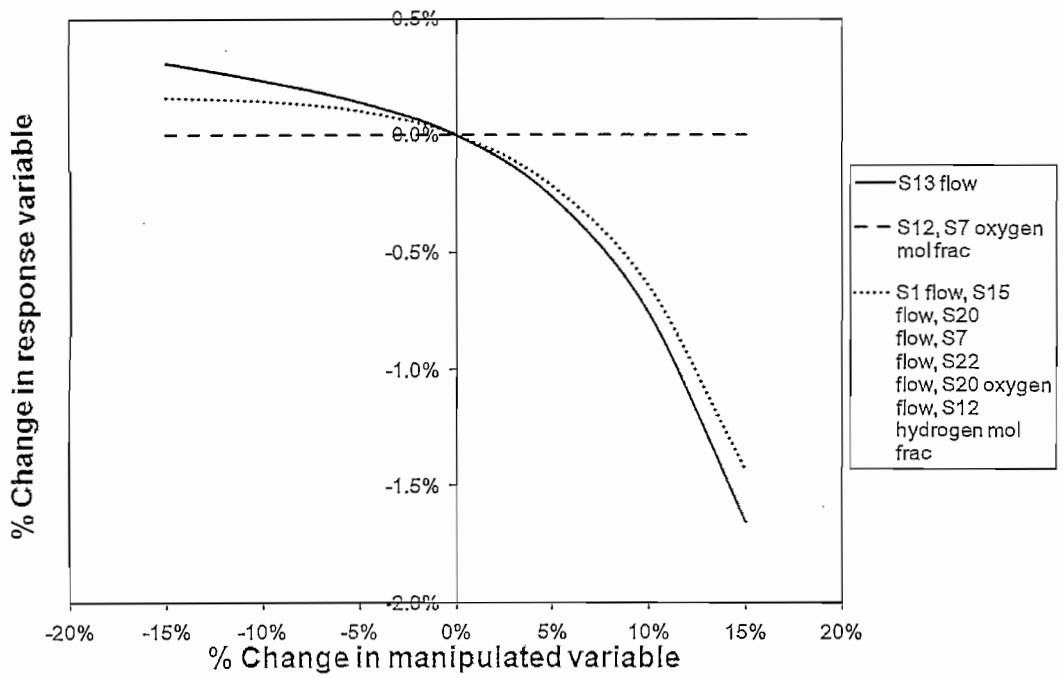


**Figure 3.17: Graph of the effect of changing the temperature of FLS-3**

Figure 3.17 shows the effect of changing the temperature of the flash drum FLS-3. FLS-3 is responsible for separating the product hydrogen from water that crosses over the membrane of the electrolyser with the protons going to the cathode. The flow rate of S13 is changed because it is the bottoms stream leaving the flash. An increase in temperature causes a decrease in the flow rate of stream S13 because more water leaves in stream S12. This water that leaks out causes less hydrogen and oxygen to be formed because the water feed flow rate remains constant. The mol flow rate of stream S12 remains constant because it simply contains less hydrogen as its water content increases. All the other flow rates change as the rate of hydrogen and oxygen production decrease.

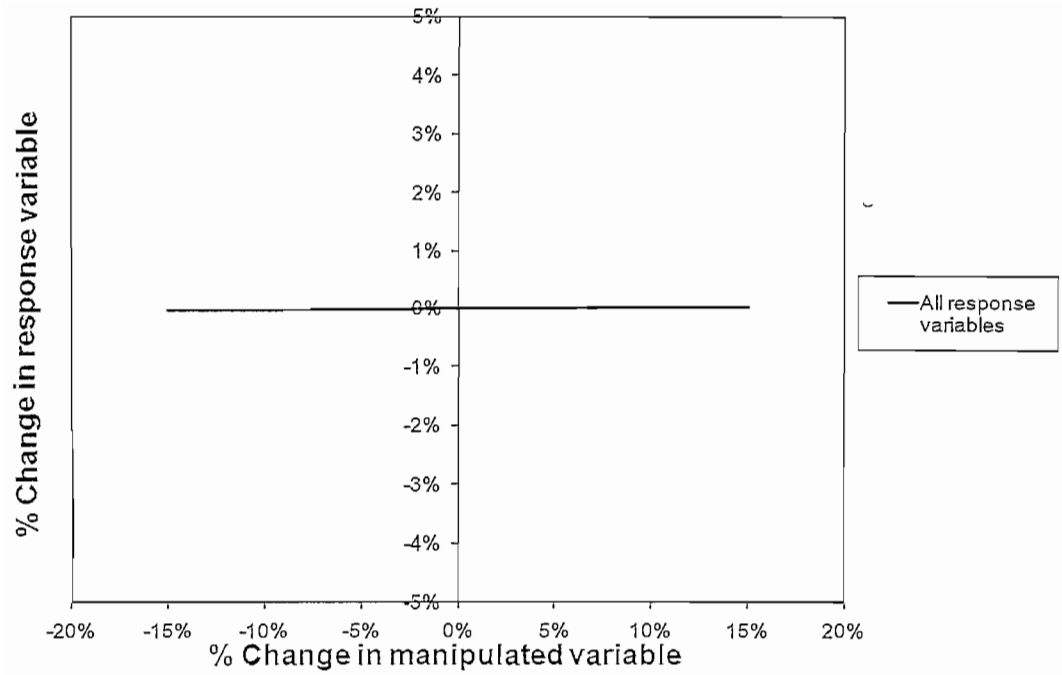


Figure 3.18: Graph of the effect of changing the pressure of FLS-3

Figure 3.18 shows that a 15% increase or decrease in the pressure of flash drum FLS-3 has no significant effect on any of the response variables.

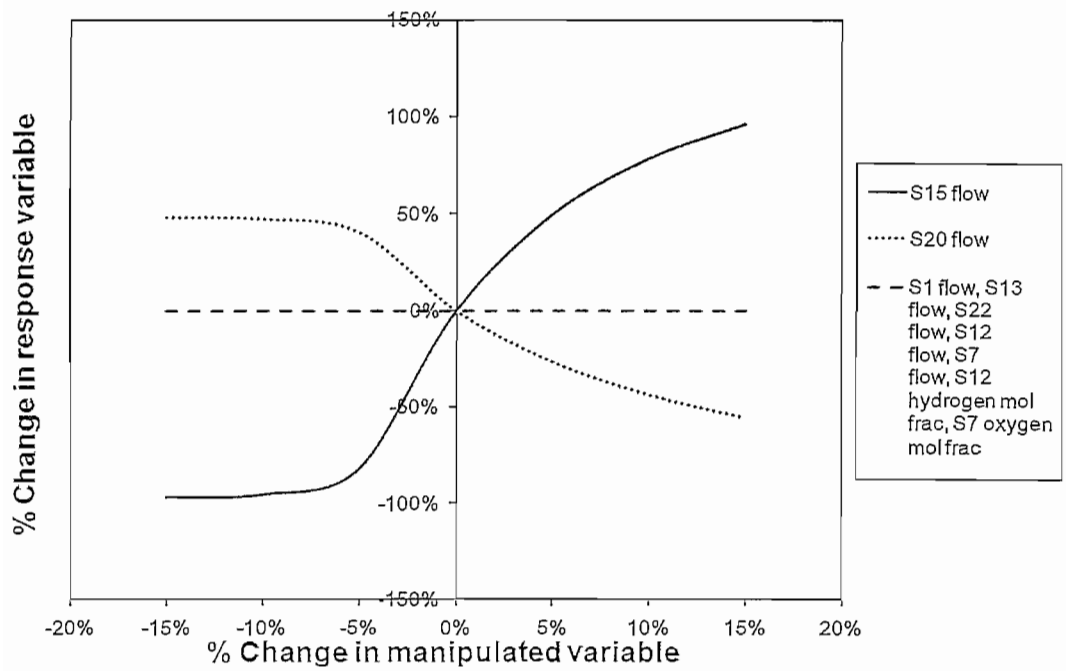


Figure 3.19: Graph of the effect of changing the temperature of FLS-4

Figure 3.19 and 3.20 shows that as the temperature of flash drum FLS-4 is decreased below the base case value the flow rate of stream S15 decreases while the flow rate of stream S20 increases. At temperatures higher than the base case the reverse happens. The temperature of FLS-4 can therefore be used to change the ratio of the streams sent to the sulphur dioxide/oxygen separation system (FLS-2) and the sulphuric acid concentration section (FLS-5 and FLS-6). Figure 3.20 shows that a decrease in the temperature of FLS-4 might not seem to be such a good idea as a 15% decrease in temperature causes a 6500% increase in the oxygen flow rate in stream S20. Even so the mole fraction of oxygen in this stream is still only $8.27 \times 10^{-4}$. Note that FLS-4 is only included in the spreadsheet to prevent the oxygen fraction from snowballing toward 100% in the electrolyser's sulphuric acid recycle loop.

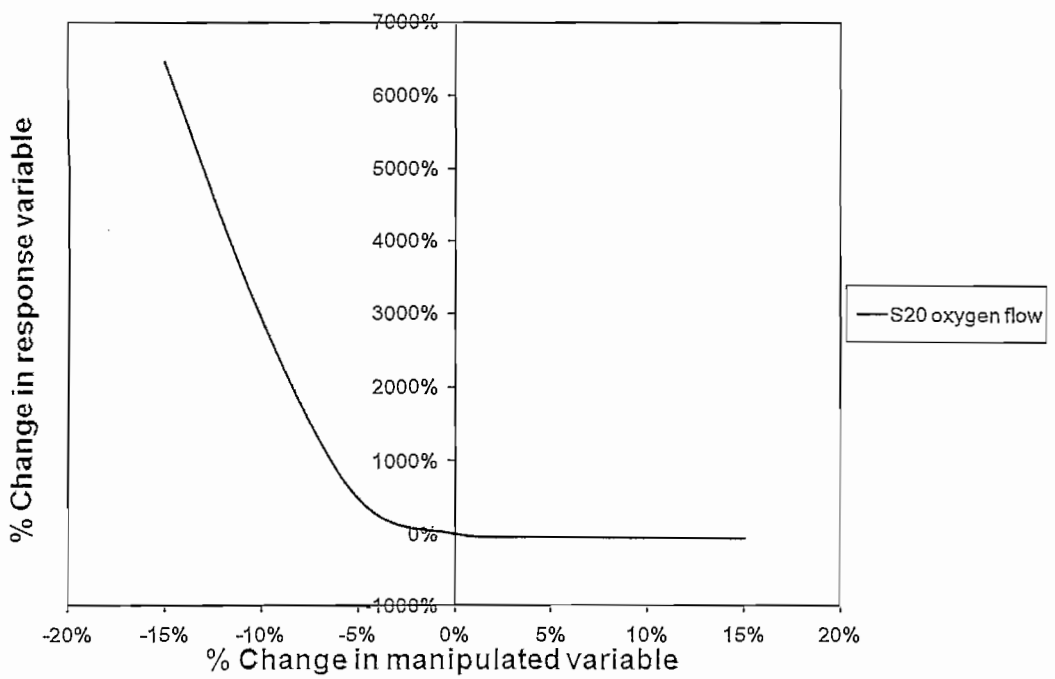


**Figure 3.20: Graph of the effect of changing the temperature of FLS-4**

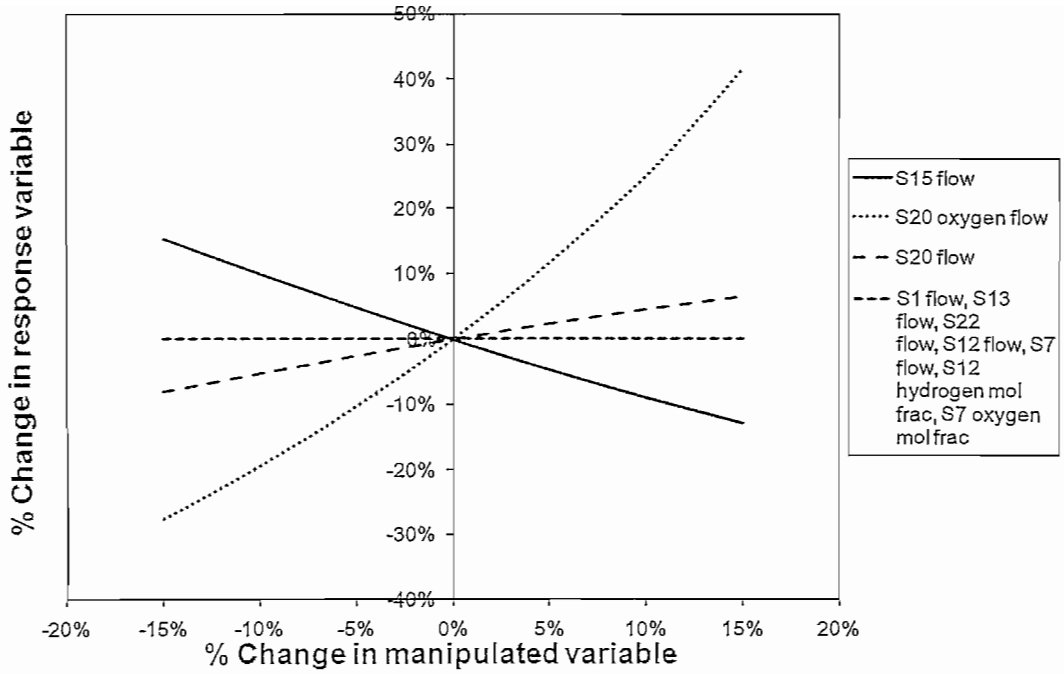


**Figure 3.21: Graph of the effect of changing the pressure of FLS-4**

Figure 3.21 shows the effect of changing the pressure of flash drum FLS-4 on the response variables. Again the split between the sulphuric acid concentration section and the oxygen/sulphur dioxide separation section is affected. As the pressure increases, the flow rate of stream S15 decreases and the flow rate of stream S20 increases. The flow rate of oxygen in stream S20 is affected in the same way but to a greater extent than the overall flow rate of stream S20.

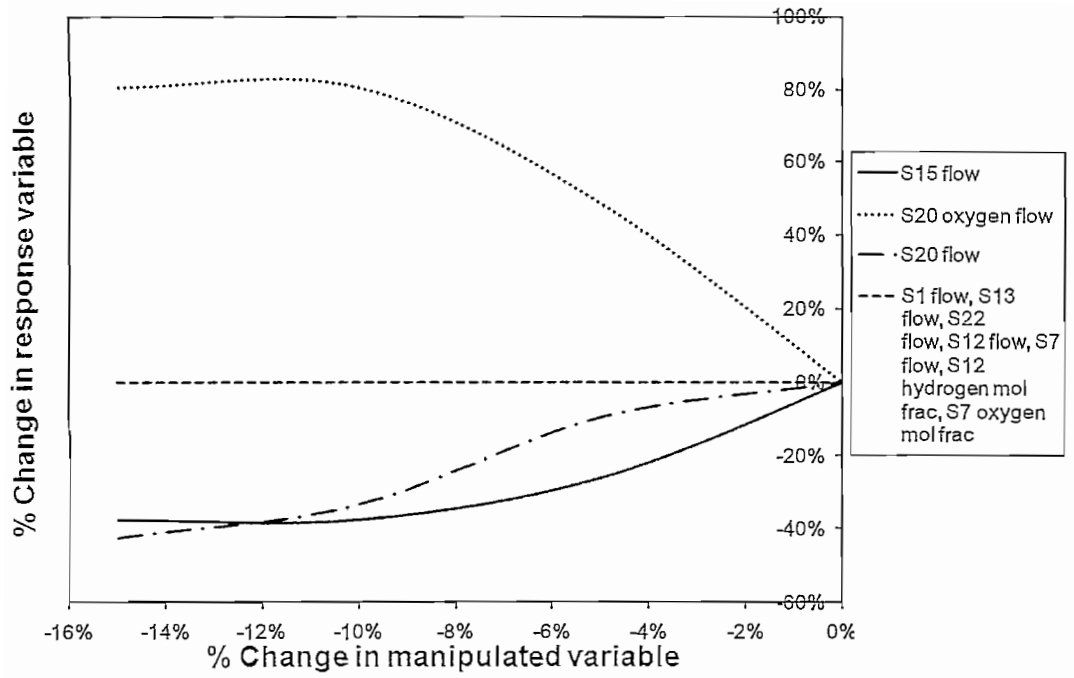


**Figure 3.22: Graph of the effect of changing the temperature of FLS-5**

Figure 3.22 shows the effect of decreasing the temperature of flash drum FLS-5. The temperature cannot even be increased by 5% before Aspen fails to find a solution for which the system is in mass balance. This happens because the flow rate and water content in stream S1B cannot be as high as for S1A given the higher temperature, causing the rest of the cycle to have a higher inflow than outflow. As the temperature decreases, the flow rate of stream S15 and S20 decrease. The flow rate of oxygen in stream S20 increases as the manipulated variable decreases. The other response variables remain unchanged.

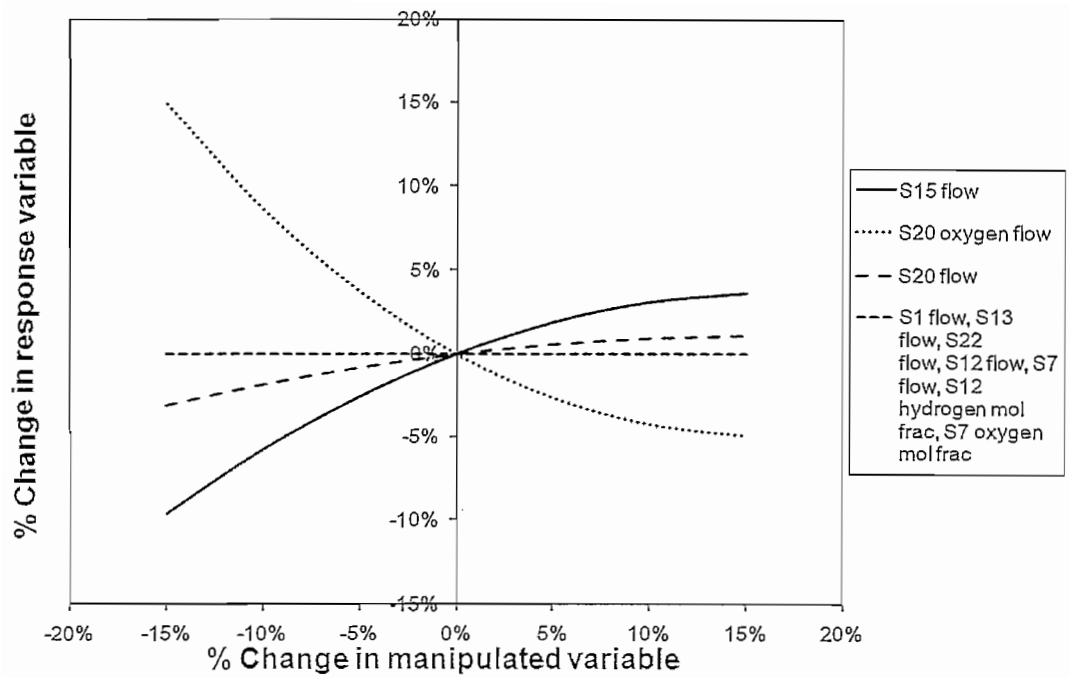


**Figure 3.23: Graph of the effect of changing the pressure of FLS-5**

Figure 3.23 shows the effect of changing the pressure of FLS-5. The flow rate of stream S15 and S20 increase as the pressure increases. The flow rate of oxygen in stream S20 decreases as the pressure increases.

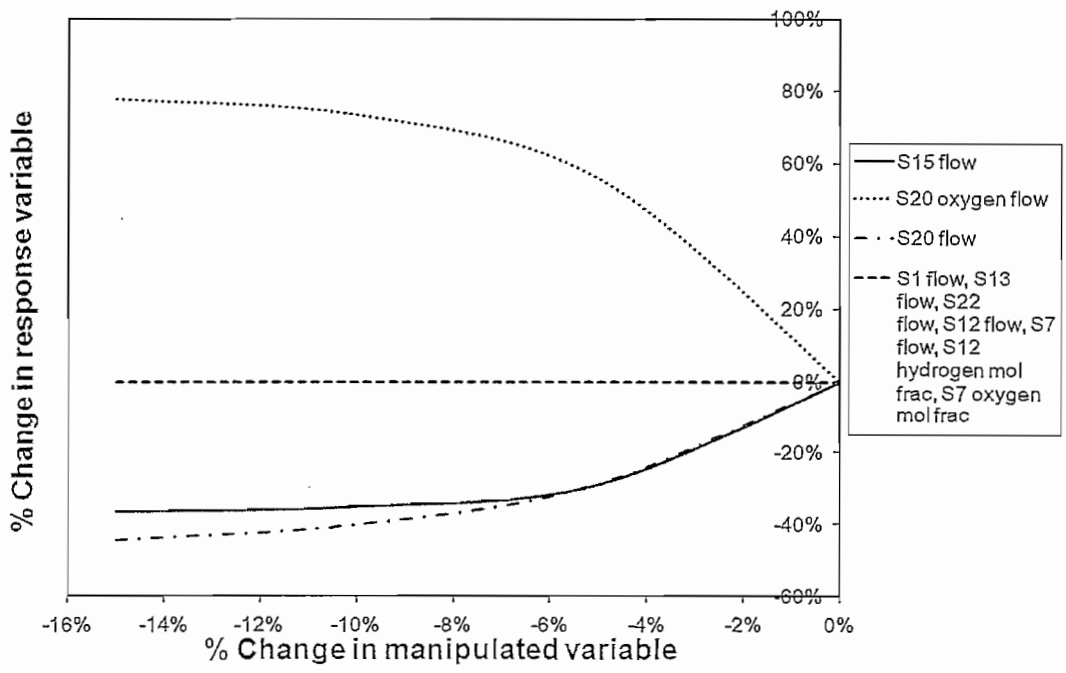


**Figure 3.24: Graph of the effect of changing the temperature of FLS-6**

As in the case of FLS-5, the temperature of FLS-6 cannot be increased by even as much as 5% before there is no way the system can be in mass- and energy balance (for the same reason as for FLS-5). As the temperature decreases, however, the flow rates of stream S20 and S15 decrease while the flow rate of oxygen in stream S20 increases.

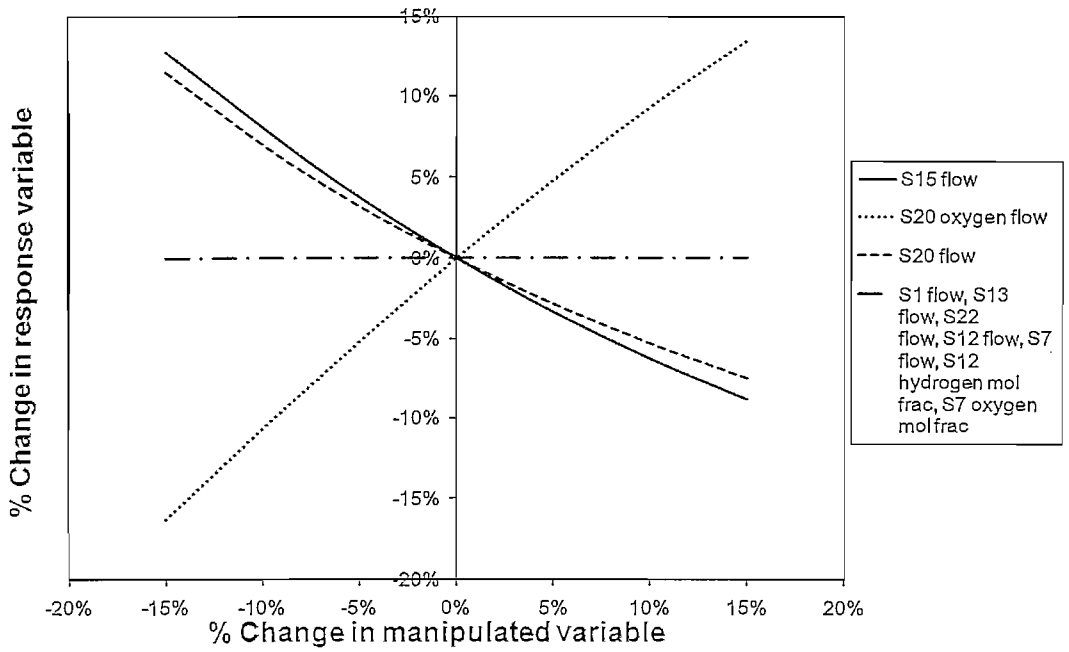


**Figure 3.25: Graph of the effect of changing the pressure of FLS-6**

Figure 3.25 shows the effect of changing the pressure of flash drum FLS-6. As the pressure increases the flow rates of stream S15 and S20 decrease and the flow rate of oxygen in stream S20 increases.

The results of the sensitivity analysis of the system to changing the temperatures and pressures of FLS-5 and FLS-6 make it obvious that optimisation fell outside the scope of this study. Either or both could be operated at a lower temperature – for example – decreasing the anolyte recycle rates required to keep the hydrogen production rate in the electrolyser high enough. This would lead to obvious energy savings.

### 3.2.3 Aspen Simulation of Sulphur Trioxide Decomposition Section

*3.2.3.1 Assumptions*

The following assumptions were made:

- No pressure drop over the plug flow reactors
- $H_2SO_4$ decomposes completely into $SO_3$ and $H_2O$ when heated to the temperatures in the decomposition reactors
- All gases were assumed to be ideal
- Reactors were assumed to be adiabatic

As can be seen in Figure 3.28, a 15% decrease in the system pressure only results in a 1.5% increase in conversion and sulphur dioxide production rate. A pressure drop that gradually occurs over each of the packed beds can therefore safely be assumed to have a negligible effect on the reactor system performance.

The assumption that $H_2SO_4$ decomposes completely to $SO_3$ and $H_2O$ at 870°C and 3bar is safe because the equilibrium conversion is 99.8%.

Assuming ideal gas behaviour is valid because of the very high temperature and relatively low pressure.

Adiabatic operation of the reactors can be very nearly achieved if sufficient insulation is used.

*3.2.3.2 Process Flow Description and Diagram*

Figure 3.26 shows a process flow diagram of the decomposition section simulation. It consists of five heat exchangers and five adiabatic plug flow reactors; arranged alternately. This arrangement was proposed by Coetzee (2008: 3-5) but the reactor sizes were increased for the purposes of this study.

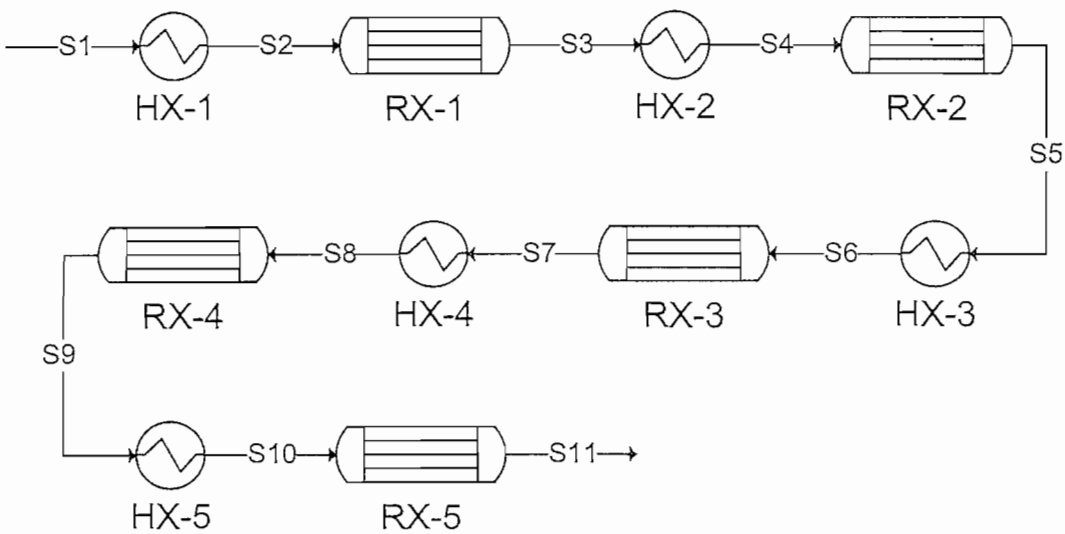


**Figure 3.26: PFD of the acid decomposition section simulation**

**Table 3.6: Equipment list**

| Designation | Description |
|---|---|
| HX-1 | Heat exchanger |
| RX-1 | Adiabatic packed bed reactor |
| HX-2 | Heat exchanger |
| RX-2 | Adiabatic packed bed reactor |
| HX-3 | Heat exchanger |
| RX-3 | Adiabatic packed bed reactor |
| HX-4 | Heat exchanger |
| RX-4 | Adiabatic packed bed reactor |
| HX-5 | Heat exchanger |
| RX-5 | Adiabatic packed bed reactor |

The heat exchangers were taken to simply change the temperature of the stream passing through it. The reactors were modelled using the following two equations (resulting from a mass and energy balance respectively) that were solved numerically (Coetzee, 2009:40,45):

$$\frac{d(X)}{d(V)} = \frac{-r_A}{F_{A0}}$$

$$\frac{d(T)}{d(V)} = \frac{(-r_A)\cdot[-\Delta H_{RX}(T)]}{F_{A0}\cdot\left(\sum\theta_i \cdot C_{p,i} + X\cdot\Delta C_p\right)}$$

Where $X$ is the conversion (of $SO_3$), $-r_A$ is the rate of consumption of $SO_3$, $V$ is the reactor volume, $F_{A0}$ is the molar feed flow rate of $SO_3$, $T$ is the temperature, $\Delta H_{RX}$ is the heat of reaction, $\theta_i$ is the ratio of component $i$'s feed rate to the feed rate of $SO_3$ (the reagent) and $C_p$ is the heat capacity.

The kinetics are first order with regard to the sulphur trioxide concentration and is reversible (Spewock *et al.*, 1976:9A-56). Therefore the rate equation can be written as (Fogler, 1999:77-78):

$$-r_A = -k_1\cdot\left(C_A - \frac{C_C\cdot C_D^{0.5}}{K_C}\right)$$

Where $K_C$ is the equilibrium constant and has units of $(mol/dm^3)^{(1+0.5-1)}$. $C_A$ is the sulphur trioxide concentration, $C_C$ is the sulphur dioxide concentration, $C_D$ is the oxygen concentration and $k_1$ is the reaction rate constant defined by (Coetzee, 2009:44):

$$k_1 = A\cdot\exp\left(\frac{-E_A}{R\cdot T}\right)$$

Where $A$ is the pre-exponential factor, $E_A$ is the activation energy, $R$ is the universal gas constant and $T$ is the temperature. The temperature dependence of the equilibrium constant is given by (Coetzee, 2009:44):

$$K_C(T) = K_C(T_2) \cdot \exp\left[\left(\frac{\Delta H_{RX}(T)}{R}\right) \cdot \left(\frac{1}{T_2} - \frac{1}{T}\right)\right]$$

Where $\Delta H_{RX}$ is the heat of reaction. The reference value for $K_C$ was determined using the RGIBBS block in Aspen for a reference temperature of 1143.15K.

The kinetic constants used were (Coetzee, 2009:44):

$A = 3.75 \text{x} 10^{13}$ h$^{-1}$
$E_A = 196000$ J/mol

The heat of reaction was taken to be (Coetzee, 2009:44):

$\Delta H_{RX} = 98.93$ kJ/mol

Heat capacity values were obtained from Smith *et al.* (2001:657). They are ideal gas heat capacities.

$$\frac{C_P(SO_3)}{R} = 8.06 + 1.056 \cdot 10^{-3} \cdot T - 2.028 \cdot 10^5 \cdot T^{-2}$$

$$\frac{C_P(SO_2)}{R} = 5.699 + 8.01 \cdot 10^{-4} \cdot T - 1.015 \cdot 10^5 \cdot T^{-2}$$

$$\frac{C_P(O_2)}{R} = 3.693 + 5.06 \cdot 10^{-4} \cdot T - 2.27 \cdot 10^4 \cdot T^{-2}$$

$$\frac{C_P(H_2O)}{R} = 3.47 + 1.45 \cdot 10^{-3} \cdot T + 1.21 \cdot 10^4 \cdot T^{-2}$$

A base case simulation was built in Polymath using the aforementioned equations and in Aspen using LHHW (Langmuir-Hinshelwood-Hougen-Watson) kinetics and the RPlug (plug flow reactor) block. The runs for the sensitivity analysis were done using only the Aspen simulation as the Polymath simulation proved very cumbersome to use in this way.

*3.2.3.4 Method*

The following base case for the simulation was chosen.

The specified variables:

- Outlet temperature of all heat exchangers = 870°C
- System pressure = 3bar
- Molar feed flow rate (stream S1) = 10260 kmol/hr
- Fraction $SO_3$ in feed stream (S1) = 0.474

The base case flow values were:

**Table 3.7: Base case flow values for the acid decomposition section**

| | Apparent component flow (kmol/hr) | | | | | |
|---|---|---|---|---|---|---|
| Stream | $H_2O$ | $SO_3$ | $SO_2$ | $O_2$ | T (°C) | P (bar) |
| S1 | 5400 | 4860 | 0 | 0 | 870 | 3 |
| S2 | 5400 | 4860 | 0 | 0 | 870 | 3 |
| S3 | 5400 | 3537 | 1323 | 662 | 653 | 3 |
| S4 | 5400 | 3537 | 1323 | 662 | 870 | 3 |
| S5 | 5400 | 2591 | 2269 | 1134 | 715 | 3 |
| S6 | 5400 | 2591 | 2269 | 1134 | 870 | 3 |
| S7 | 5400 | 1970 | 2890 | 1445 | 768 | 3 |
| S8 | 5400 | 1970 | 2890 | 1445 | 870 | 3 |
| S9 | 5400 | 1574 | 3286 | 1643 | 805 | 3 |
| S10 | 5400 | 1574 | 3286 | 1643 | 870 | 3 |
| S11 | 5400 | 1340 | 3520 | 1760 | 832 | 3 |

The response variable values for the base case were:

**Table 3.8: Base case values for response variables**

| Response variable | Value | Units |
|---|---|---|
| $SO_2$ flow rate in stream S11 | 3520.4 | |
| Total $SO_3$ conversion fraction | 0.7 | |

*3.2.3.5 Results and Discussion*

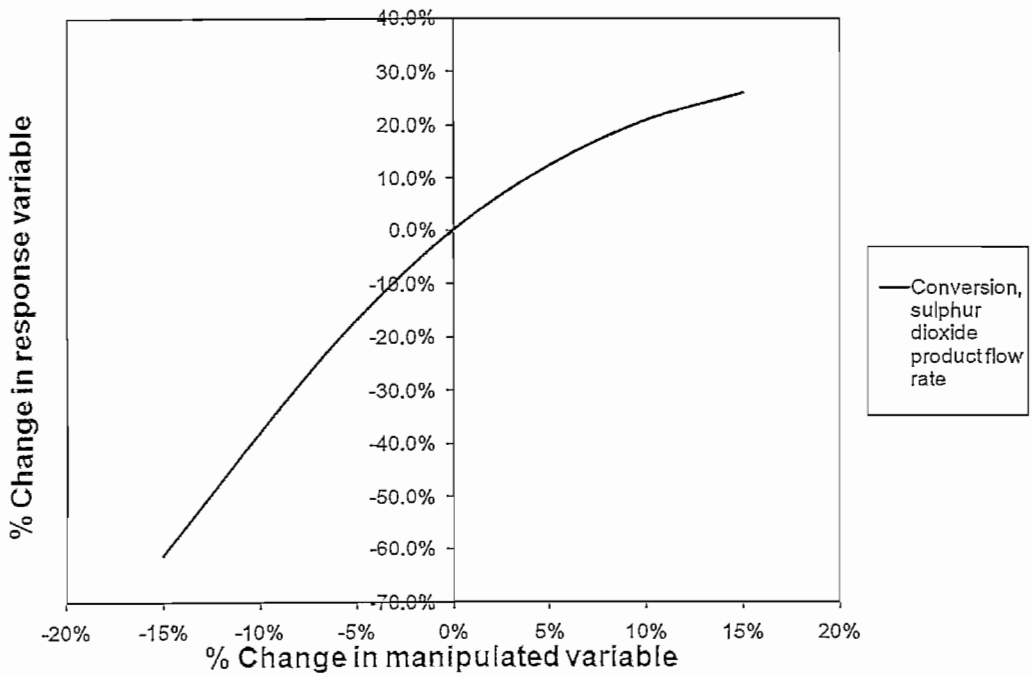


**Figure 3.27: Graph of the effect of changing the feed temperature to all reactors**

Figure 3.27 shows the result of changing the temperature of the streams leaving the heat exchangers. This is likely to occur if the PBMR core temperature is altered or the flow rate of the flower transferring the heat to the HyS cycle is reduced. The change in conversion (and therefore $SO_2$ product rate) is a result of the temperature dependence of the reaction rate and the equilibrium conversion.

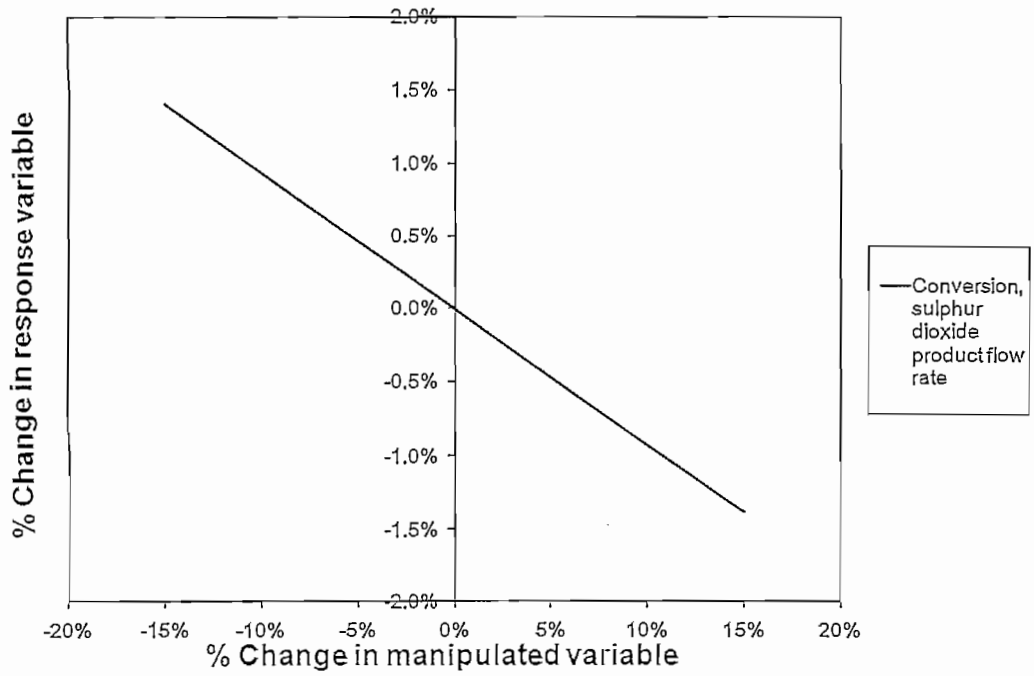


Figure 3.28: Graph of the effect of changing the pressure in all reactors

Figure 3.28 shows the result of changing the pressure of the reacting gas passing through the reactor chain. The degree of change in conversion is much less pronounced than is the case corresponding to a change in temperature.

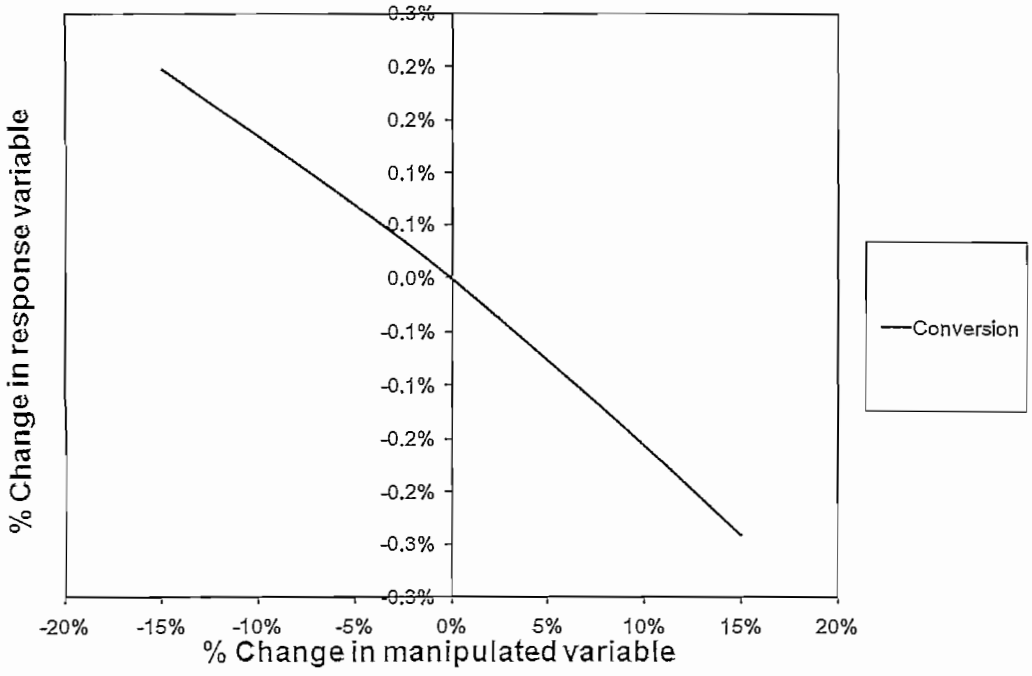


**Figure 3.29: Graph of the effect of changing the molar feed flow rate**

Figure 3.29 and Figure 3.30 show the result of changing the feed flow rate to the reactor chain. An increase in flow causes a slight decrease in the conversion of the reactor system but a pronounced increase in the $SO_2$ product rate. For a less conservatively sized reactor system these two lines would be less linear.

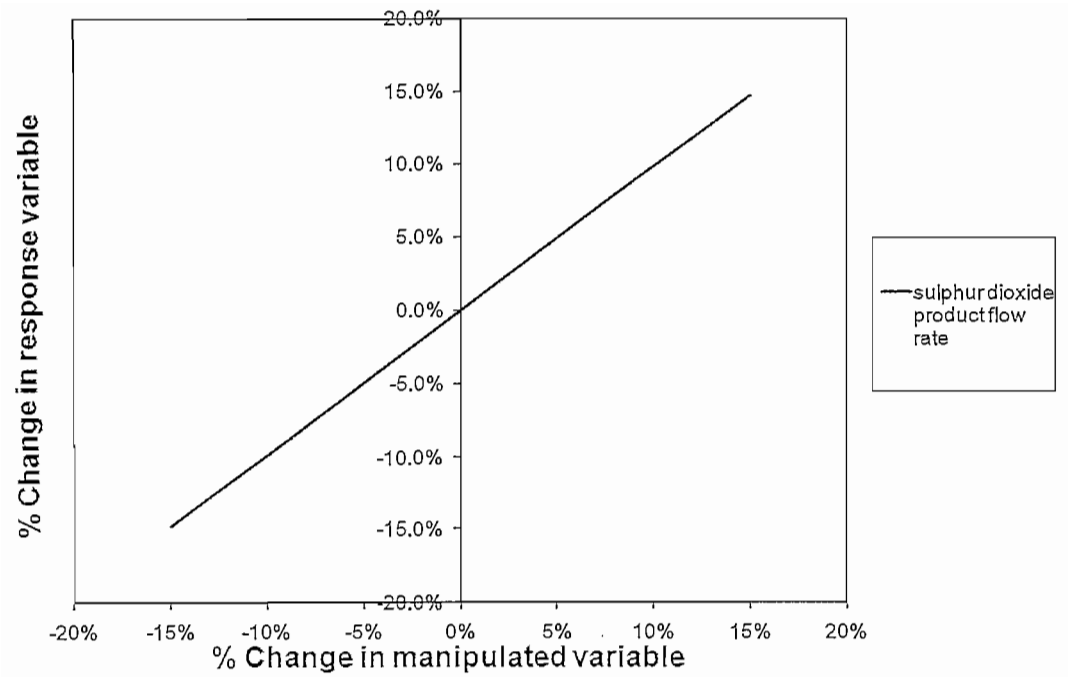


Figure 3.30: Graph of the effect of changing the molar feed flow rate

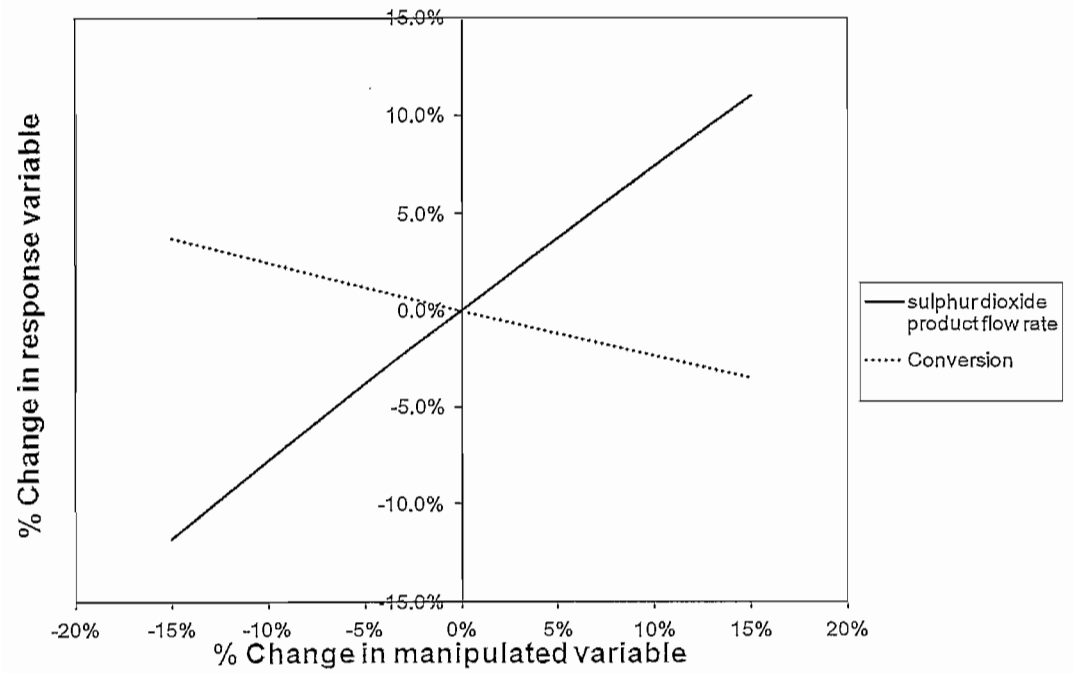


Figure 3.31: Graph of the effect of changing the mole fraction of sulphur trioxide in the feed

Figure 3.31 shows the result of changing the mole fraction of $SO_3$ in stream S1. An increase in the $SO_3$ fraction causes an increase in the $SO_2$ production rate but causes a decrease in conversion. Inert water carries heat that can be used to convert $SO_3$ to $SO_2$ without being involved in the calculation of the conversion fraction. So the temperature at the exit of each reactor is higher if more water is present as there is a smaller fraction of endothermically reacting $SO_3$ present to "consume" heat.

### 3.2.4 Aspen simulation of the cycle including detailed reactor

*3.2.4.1 Introduction*

This simulation was done in order to get accurate results for two of the runs done under 3.2.2.

*3.2.4.2 Assumptions*

The assumptions for this simulation are the same as for the Aspen simulation discussed in 3.2.2 (see 3.2.2.2 for a discussion of the assumptions). There is one difference in the assumptions made. The reactor section was simulated in more detail.

Assumptions made for the reactor section are that there is no pressure drop across the reactors and that the reactors operate adiabatically. Both of these assumptions are discussed in 3.2.3.1.

*3.2.4.3 Process flow description and diagram*

This process is identical to the one discussed in 3.2.2 except that the reactor section as laid out in 3.2.3 has replaced the equilibrium reactor block used in 3.2.2. Figure 3.32 shows the PFD of this process; note that the unit and stream names are the same as in 3.2.2 but the names of the units and streams within the sulphuric acid decomposition section have been altered. Table 3.9 is an equipment list for this process. Stream S1 was split as was done in 3.2.2 but it is not indicated on this drawing.

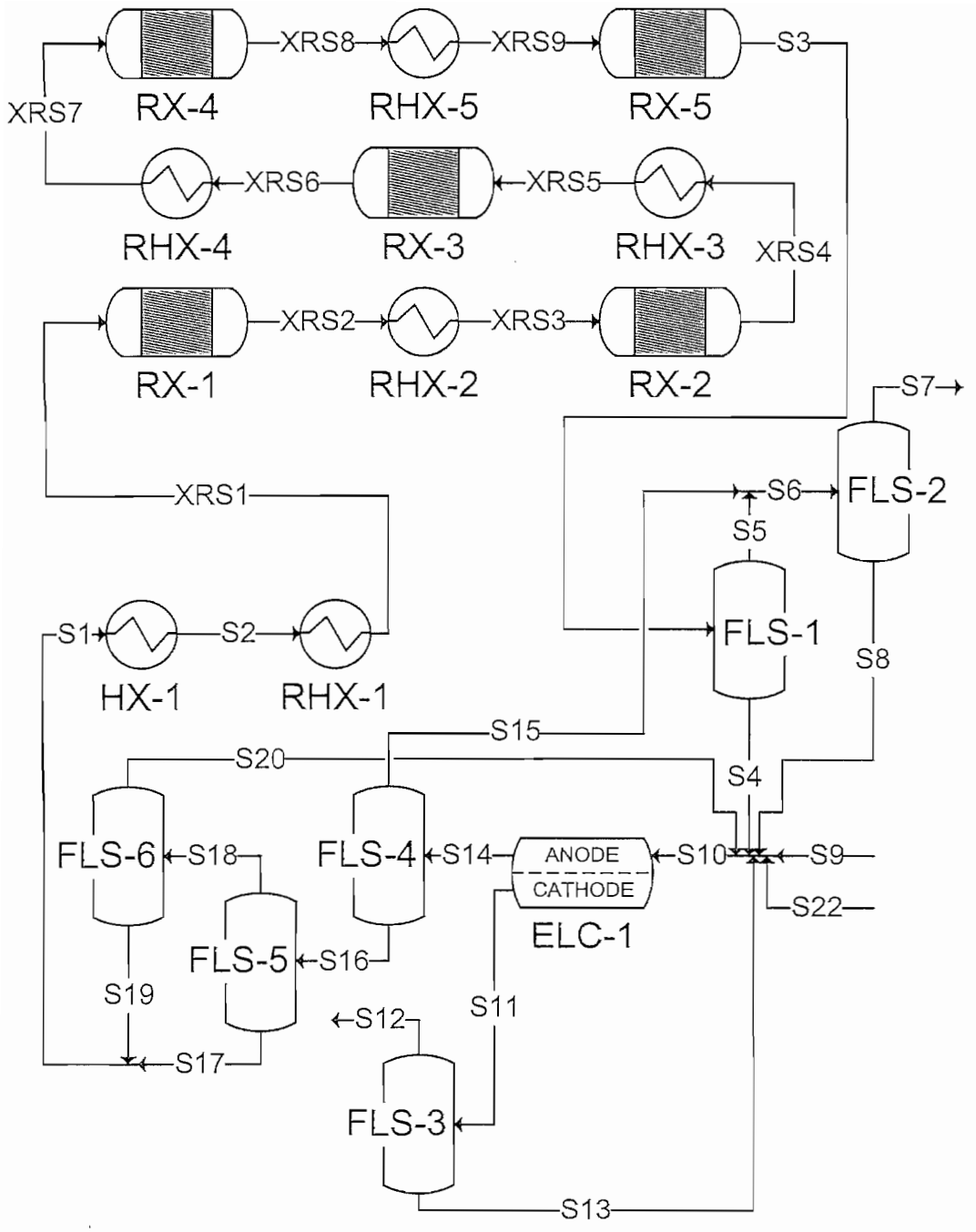


Figure 3.32: Process flow diagram of the final Aspen simulation

**Table 3.9: Equipment list**

| Designation | Description |
|---|---|
| HX-1 | Heat exchanger |
| ELC-1 | Electrolyser |
| FLS-1 | Flash drum |
| FLS-2 | Flash drum |
| FLS-3 | Flash drum |
| FLS-4 | Flash drum |
| FLS-5 | Flash drum |
| FLS-6 | Flash drum |
| RX-1 | Packed bed reactor |
| RX-2 | Packed bed reactor |
| RX-3 | Packed bed reactor |
| RX-4 | Packed bed reactor |
| RX-5 | Packed bed reactor |
| RHX-1 | Heat exchanger |
| RHX-2 | Heat exchanger |
| RHX-3 | Heat exchanger |
| RHX-4 | Heat exchanger |
| RHX-5 | Heat exchanger |

*3.2.4.4 Method*

Only two manipulated variables were considered in this simulation. These were done in order to get more accurate data for the sensitivity analysis done on the same variables in 3.2.2. The following base case for the simulation was chosen

The specified variables:

- S1 sulphuric acid mol fraction = 0.9
- Sulphuric acid decomposition (HX-1) temperature = 870 °C

This resulted in the following flow values:

Table 2.3: Stream variable values

| | Apparent component flow (kmol/hr) | | | | | | | |
|---|---|---|---|---|---|---|---|---|
| Stream | H2O | H2SO4 | SO3 | SO2 | H2 | O2 | T (°C) | P (bar) |
| S1 | 541 | 4869 | 0 | 0 | 0 | 0 | 258 | 1 |
| S2 | 5401 | 9 | 4860 | 0 | 0 | 0 | 870 | 3 |
| S3 | 5401 | 9 | 1292 | 3568 | 0 | 1784 | 837 | 3 |
| S4 | 4102 | 1302 | 0 | 69 | 0 | 0 | 25 | 3 |
| S5 | 7 | 0 | 0 | 3499 | 0 | 1784 | 25 | 3 |
| S6 | 7 | 0 | 0 | 5021 | 0 | 1829 | 13 | 3 |
| S7 | 0 | 0 | 0 | 142 | 0 | 1784 | -85 | 30 |
| S8 | 7 | 0 | 0 | 4879 | 0 | 45 | -85 | 30 |
| S9 | 3574 | 0 | 0 | 0 | 0 | 0 | 25 | 20 |
| S10 | 34994 | 1831 | 0 | 7136 | 7 | 45 | 51 | 1 |
| S11 | 25024 | 0 | 0 | 0 | 3575 | 0 | 100 | 20 |
| S12 | 6 | 0 | 0 | 0 | 3568 | 0 | 25 | 20 |
| S13 | 25018 | 0 | 0 | 0 | 7 | 0 | 25 | 20 |
| S14 | 2834 | 5399 | 0 | 3568 | 0 | 45 | 100 | 20 |
| S15 | 0 | 0 | 0 | 1522 | 0 | 45 | 25 | 20 |
| S16 | 2834 | 5399 | 0 | 2046 | 0 | 0 | 25 | 20 |
| S17 | 203 | 3265 | 0 | 0 | 0 | 0 | 269 | 1 |
| S18 | 2663 | 2102 | 32 | 2046 | 0 | 0 | 269 | 1 |
| S19 | 338 | 1604 | 0 | 0 | 0 | 0 | 237 | 1 |
| S20 | 2295 | 528 | 2 | 2046 | 0 | 0 | 237 | 1 |
| S22 | 0 | 0 | 0 | 142 | 0 | 0 | 25 | 20 |
| XRS1 | 5401 | 9 | 4860 | 0 | 0 | 0 | 870 | 3 |
| XRS2 | 5401 | 9 | 3454 | 1406 | 0 | 703 | 658 | 3 |
| XRS3 | 5401 | 9 | 3454 | 1406 | 0 | 703 | 870 | 3 |
| XRS4 | 5401 | 9 | 2488 | 2373 | 0 | 1186 | 723 | 3 |
| XRS5 | 5401 | 9 | 2488 | 2373 | 0 | 1186 | 870 | 3 |
| XRS6 | 5401 | 9 | 1876 | 2985 | 0 | 1492 | 776 | 3 |
| XRS7 | 5401 | 9 | 1876 | 2985 | 0 | 1492 | 870 | 3 |
| XRS8 | 5401 | 9 | 1503 | 3357 | 0 | 1678 | 813 | 3 |
| XRS9 | 5401 | 9 | 1503 | 3357 | 0 | 1678 | 870 | 3 |

*3.2.4.5 Results and discussion*

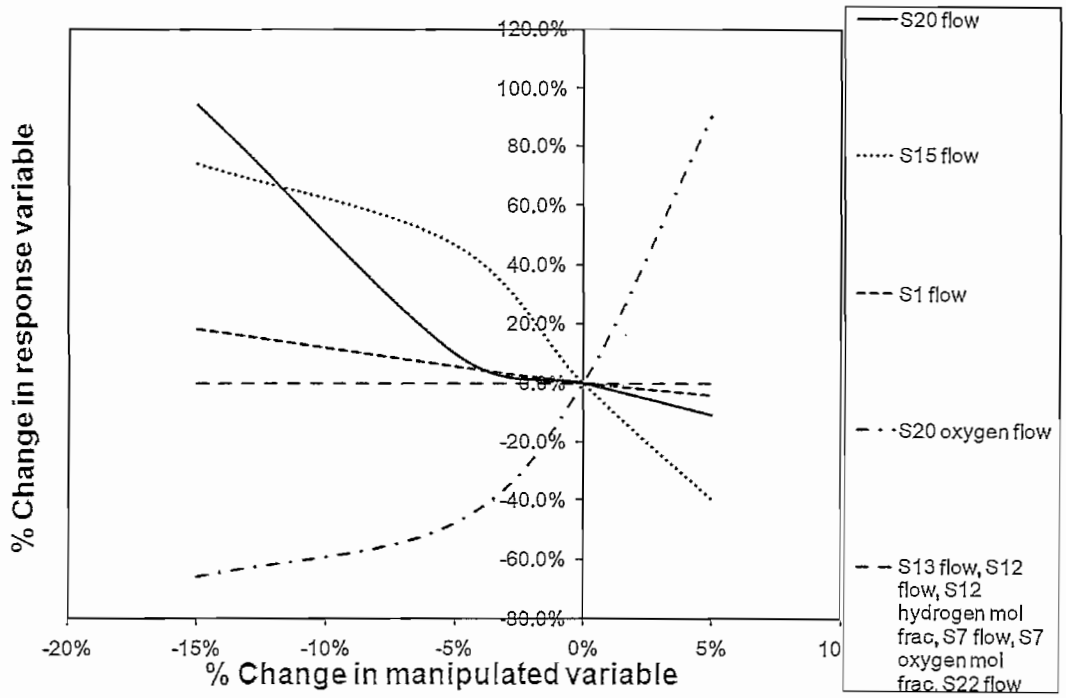


**Figure 3.33: Graph of the effect of changing the $H_2SO_4$ mole fraction in stream S1**

Figure 3.33 shows the effect of changing the concentration of $H_2SO_4$ in stream S1. Figure 3.9 shows a very similar result obtained using a simpler model for the rector system. See section 3.2.2.5 for a discussion of the factors at play.

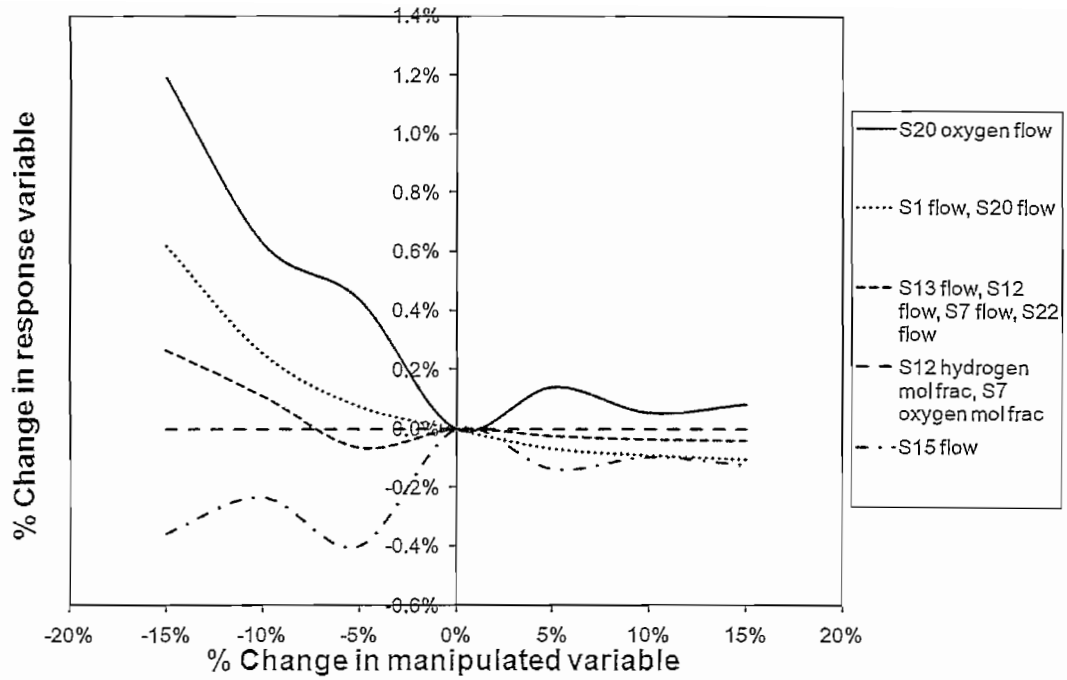


**Figure 3.34: Graph of the effect of changing the temperature of HX-1**

Figure 3.34 shows the result of changing the temperature at which the process stream leaves HX-1. The results show how the slight change in $H_2SO_4$ conversion to $SO_3$ and $H_2O$ affects the response variables. Note the similarity between Figure 3.34 and Figure 3.10.

# 4. PROPOSED PROCESS CONTROL

## *4.1 Introduction*

This chapter contains an outline of a process control strategy devised using only the knowledge obtained from sensitivity analysis using steady state simulations. It is therefore not clear if this control strategy will provide stable control and should not be viewed as a practicable solution to the question of process control but rather as a summary of the lessons learned thus far.

Sensitivity analysis results would suggest that the cycle should be stable consequent to most foreseeable process condition fluctuations. Therefore heavy use is made of operator input to control the process (especially where flow control is concerned). Operator input can be substituted by applicable advanced process control strategies.

The process is discussed under four headings corresponding to the four main process sections that the cycle has been broken up into. Some control strategies transcend this artificial compartmentalisation and are discussed under the heading encompassing the condition to be controlled.

Stream tables for the P&IDs are not provided as the stream information is the same as the similarly named streams in section 3.2.4.

## *4.2 Sulphuric acid decomposition section*

Figure 4.1 shows a process and instrumentation diagram (P&ID) of the sulphuric acid decomposition section. The sulphuric acid decomposition section contains tank TNK-1 to isolate the sulphuric acid decomposition section from upstream process noise. Streams S17B and S19B from the sulphuric acid concentration section flow into TNK-1. TNK-1 is open to the atmosphere and its level is controlled by either increasing the flow rate of stream S1B (using control loop 1) when the level is too high or by manually opening the ball valve on stream S21. The pressure of stream S1A leaving TNK-1 is increased to slightly higher than 3 bar. The higher pressure stream S1B is throttled by control loop 1 to control the flow rate of sulphuric acid entering the reactor train. This flow rate set point is manipulated to control the sulphur dioxide production rate in the sulphuric acid decomposition section. Its use as level control of TNK-1 will be discussed in more detail in section 4.3.

The sulphuric acid is heated and vaporised (with the accompanying decomposition into sulphur trioxide and water) in heat exchanger RHX-1. The helium feed to the shell of heat exchanger RHX-1 is throttled in order to control the temperature of process stream XRS-1 to a setpoint of 870°C. XRS-1 passes through adiabatic plug flow reactor RX-1 where sulphur trioxide is decomposed into sulphur dioxide and oxygen. The following four reactor stages are controlled in an identical fashion to the first.

Process stream S3A leaves the fifth reactor stage and is throttled (by control loop 7) to control the pressure in the reactor train. Stream S3A flows to the sulphur dioxide/ oxygen separation section.

The helium that has passed through the heat exchangers in the reactor train returns to the intermediate heat exchanger that links it to a HTR or other high temperature heat source.

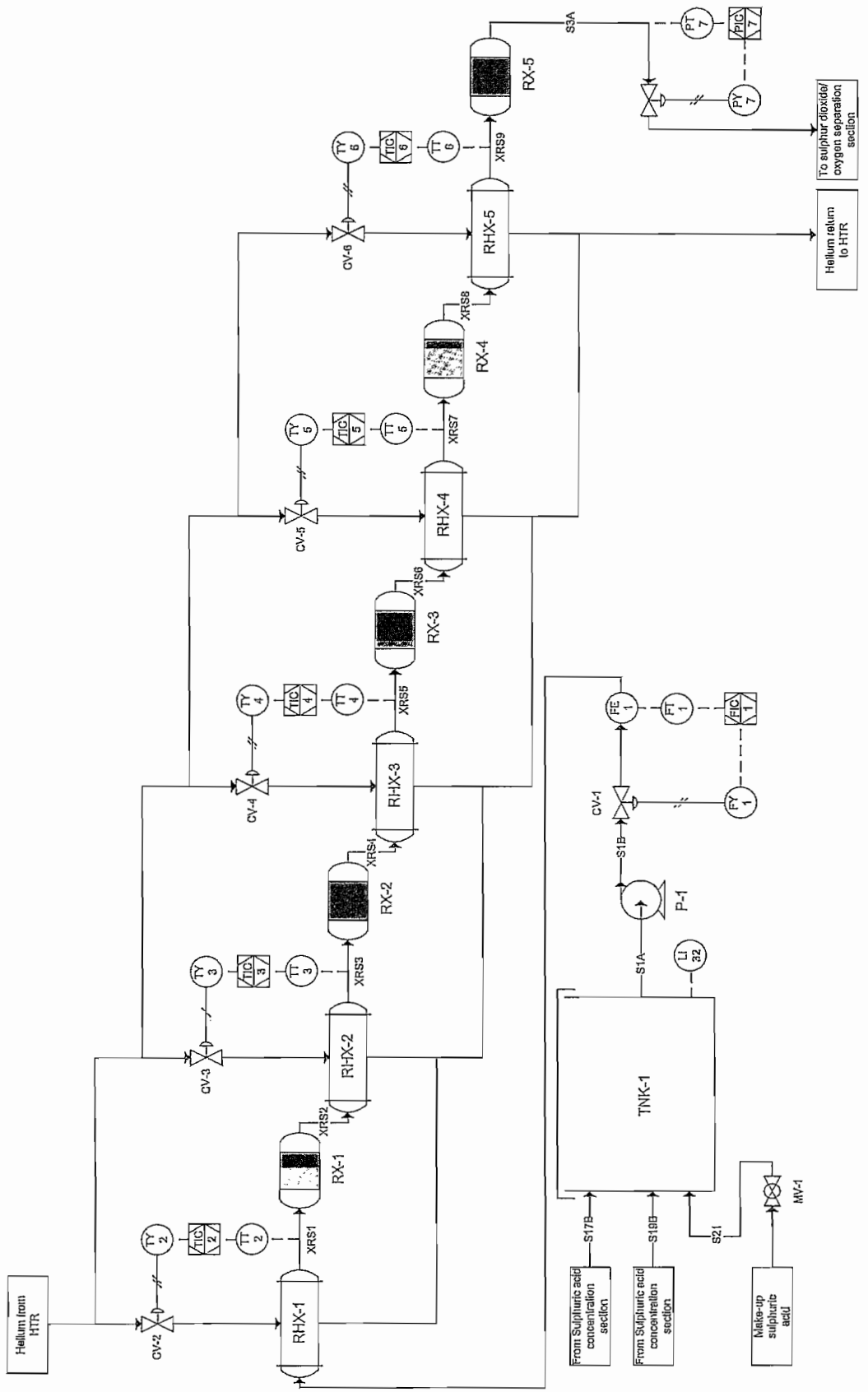


Figure 4.1: P&ID of the sulphuric acid decomposition section

**Table 4.1: Equipment list for sulphuric acid decomposition section**

| Designation | Description |
|---|---|
| P-1 | Pump |
| RHX-1 | Heat exchanger |
| RHX-2 | Heat exchanger |
| RHX-3 | Heat exchanger |
| RHX-4 | Heat exchanger |
| RHX-5 | Heat exchanger |
| RX-1 | Adiabatic plug flow reactor |
| RX-2 | Adiabatic plug flow reactor |
| RX-3 | Adiabatic plug flow reactor |
| RX-4 | Adiabatic plug flow reactor |
| RX-5 | Adiabatic plug flow reactor |
| TNK-1 | Sulphuric acid tank |

## 4.3 Oxygen/ sulphur dioxide separation section

Figure 4.2 shows a P&ID of the oxygen/ sulphur dioxide separation section. Stream S3A from the sulphuric acid decomposition section flows through heat exchanger HX-1 where it is cooled down by cooling water. The cooled down process stream S3B flows into drum FLS-1. The cooling water flow is throttled in order to control the temperature of separator drum FLS-1. Stream S23B also flows into flash drum FLS-1 from the electrolyser section.

The bottoms stream of separator drum FLS-1 (S4A) is pumped to the electrolyser section by pump P-1. This stream is throttled (by control loop 8) in order to control the level in FLS-1. The tops stream leaving FLS-1 (S5A) is throttled in order to control the pressure in FLS-1 by control loop 10.

Stream S5A is compressed by CMP-1. The compressed stream is called S5B and is refrigerated in HX-8. Stream S15A from the electrolyser section is similarly compressed by CMP-2 before being refrigerated in HX-8. Refrigerated stream S6 flows to separator drum FLS-2. The refrigerant flow rate to HX-8 is throttled by control loop 12 in order to control the temperature in FLS-2.

The bottoms of FLS-2 (S8) is throttled by control loop 13 to control the level in FLS-2 before flowing to the electrolyser section. The tops of FLS-2 (S7) is throttled by control loop 11 in order to control the pressure in FLS-2. Stream S7 is the oxygen product stream. It does contain a significant amount of sulphur dioxide that can be recovered by, for example, the use of membranes. The recovered sulphur dioxide can be used as a source for stream S22 in the electrolyser section.

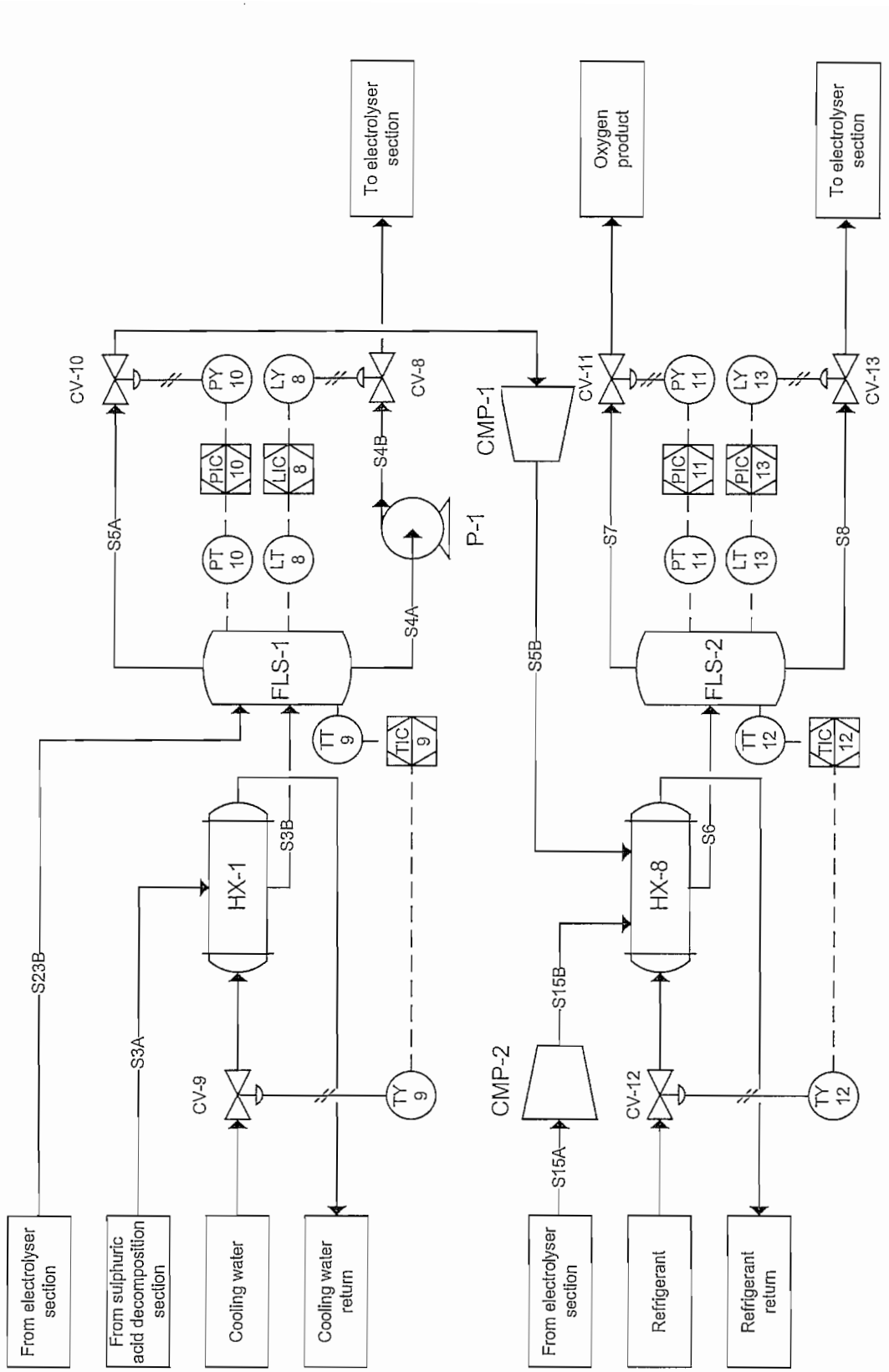


**Figure 4.2: P&ID of the oxygen/ sulphur dioxide separation section**

**Table 4.2: Equipment list for the oxygen/ sulphur dioxide separation section**

| Designation | Description |
|---|---|
| CMP-1 | Compressor |
| CMP-2 | Compressor |
| FLS-1 | Separation drum |
| FLS-2 | Separation drum |
| HX-1 | Heat exchanger |
| HX-8 | Heat exchanger |
| P-1 | Pump |

## 4.3 Electrolyser section

Figure 4.3 is a P&ID of the electrolyser section. Water feed stream S9 is flow controlled by loop 14 according to the desired hydrogen production rate. Stream S9 flows into tank TNK-2. TNK-2 serves a similar role to tank TNK-1.

Sulphur dioxide makeup stream S22 is flow controlled by loop 15 before flowing into TNK-2. The flow setpoint for stream S22 is adjusted in order to keep the sulphur dioxide concentration in TNK-2 at a pre-determined level. The sulphur dioxide concentration can periodically be determined by means of sampling and lab analysis. To return to the level control of TNK-1 in the sulphuric acid decomposition section, if the flow rate of S1A is increased then the concentration of SO2 in TNK-2 will increase and the flow rate of S22 will have to be decreased. This will result in a greater outflow than inflow of sulphuric acid from TNK-1.

Streams S4B and S8 both flow into TNK-2 from the sulphur dioxide/ oxygen separation section. Stream S20B flows into TNK-2 from the sulphuric acid concentration section.

Liquid stream S10A is pumped to heat exchanger HX-2 by P-3. S10B is throttled in order to control the level in TNK-2. Stream S10B is heated in HX-2 and leaves as S10C. The low pressure utility steam flow to HX-2 is throttled by control loop 17 in order to control the temperature of stream S10C.

Stream S10C flows to the anode side of electrolyser ELC-1. Sulphuric acid is formed at the anode side of the electrolyser while protons cross over the membrane to the cathode side. A significant amount of water also crosses the membrane as a result of electro-osmotic drag.

The cathode side product stream S11A consists of water and hydrogen gas. S11A is cooled in HX-4 using cooling water. The cooling water flow is throttled

by control loop 18 in order to control the temperature of stream S11B. S11B passes to separator drum FLS-3.

The bottoms stream of FLS-3 (S13A) is pumped back to TNK-2 by P-4 but is throttled by control loop 20 in order to control the level in FLS-3. The tops of FLS-3 (S12) is throttled by control loop 19 in order to control the pressure in FLS-3. S12 is the hydrogen product stream consisting of hydrogen of high purity.

The anode side product stream of electrolyser ELC-1(S14B) is cooled by HX-3 before flowing into separation drum FLS-4. The cooling water flow to HX-3 is throttled by control loop 23 in order to control the temperature in FLS-4.

The bottoms stream of FLS-4 (S16) is throttled by control loop 21 in order to control the level in FLS-4. S16 flows to the sulphuric acid decomposition section. The tops stream of FLS-4 (S15A) is throttled by control loop 22 in order to control the pressure in FLS-4 before flowing to the oxygen/ sulphur dioxide separation section.

Pressure control in TNK-2 is achieved by adding a vapour product stream (S23A) that is cooled (by HX-7) and throttled by control loop 24. The cooling water to HX-7 is throttled by control loop 25 in order to control the temperature in stream S23B. S23B flows to the oxygen/ sulphur dioxide separation section.

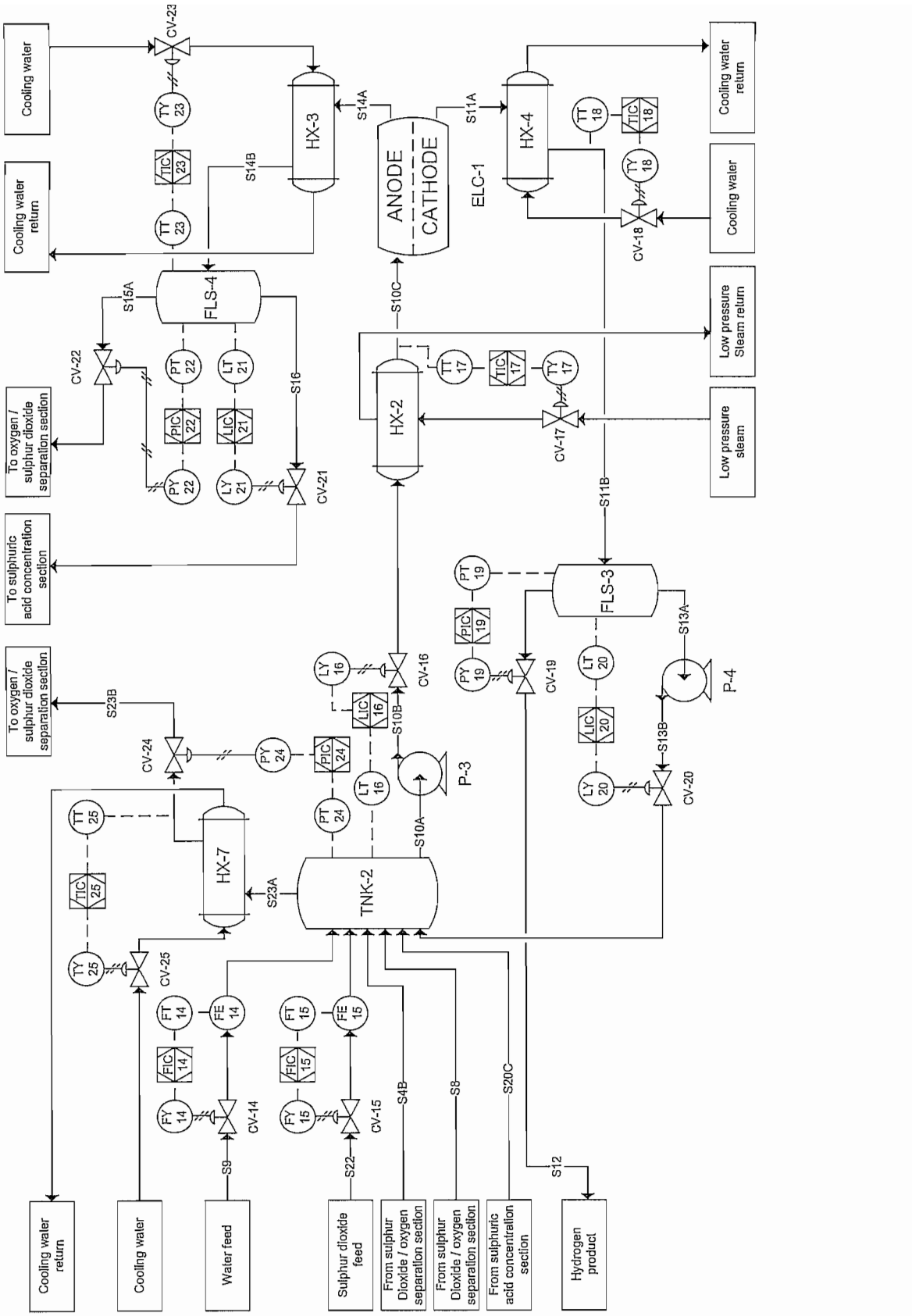


Figure 4.3: P&ID of the electrolyzer section

Table 4.3: Equipment diagram for the electrolyser section

| Designation | Description |
|---|---|
| ELC-1 | Electrolyser |
| FLS-3 | Separation drum |
| FLS-4 | Separation drum |
| HX-2 | Heat exchanger |
| HX-3 | Heat exchanger |
| HX-4 | Heat exchanger |
| HX-7 | Heat exchanger |
| P-3 | Pump |
| P-4 | Pump |
| TNK-2 | Tank |

## *4.5 Sulphuric acid concentration section*

Figure 4.4 shows a process and instrumentation diagram for the sulphuric acid concentration section. Stream S16A is heated in HX-8 by a helium stream. This helium stream is throttled in order to control the temperature in the downstream flash drum FLS-5. The pressure in flash from FLS-5 is controlled by throttling the feed stream S16B. FLS-5's bottoms stream (S17A) is pumped to the sulphuric acid decomposition section by P-5 and is throttled in order to control the level in FLS-5.

FLS-5's tops stream (S18A) is cooled by air-cooled heat exchanger HX-6 before passing into separation drum FLS-6. The temperature in FLS-6 is controlled by varying the speed of the drive on HX-6's fan. FLS-6's bottoms stream (S19A) is pumped to the sulphuric acid decomposition section by P-6 and is throttled by control loop 30 to control the level in FLS-6.

Stream S20A is throttled to control the pressure in FLS-6 before being compressed by CMP-3. The compressed stream (S20B) is cooled in HX-9. The cooling water feed to HX-9 is throttled in order to control the temperature of stream S20C. Stream S20C passes to the electrolyser section.

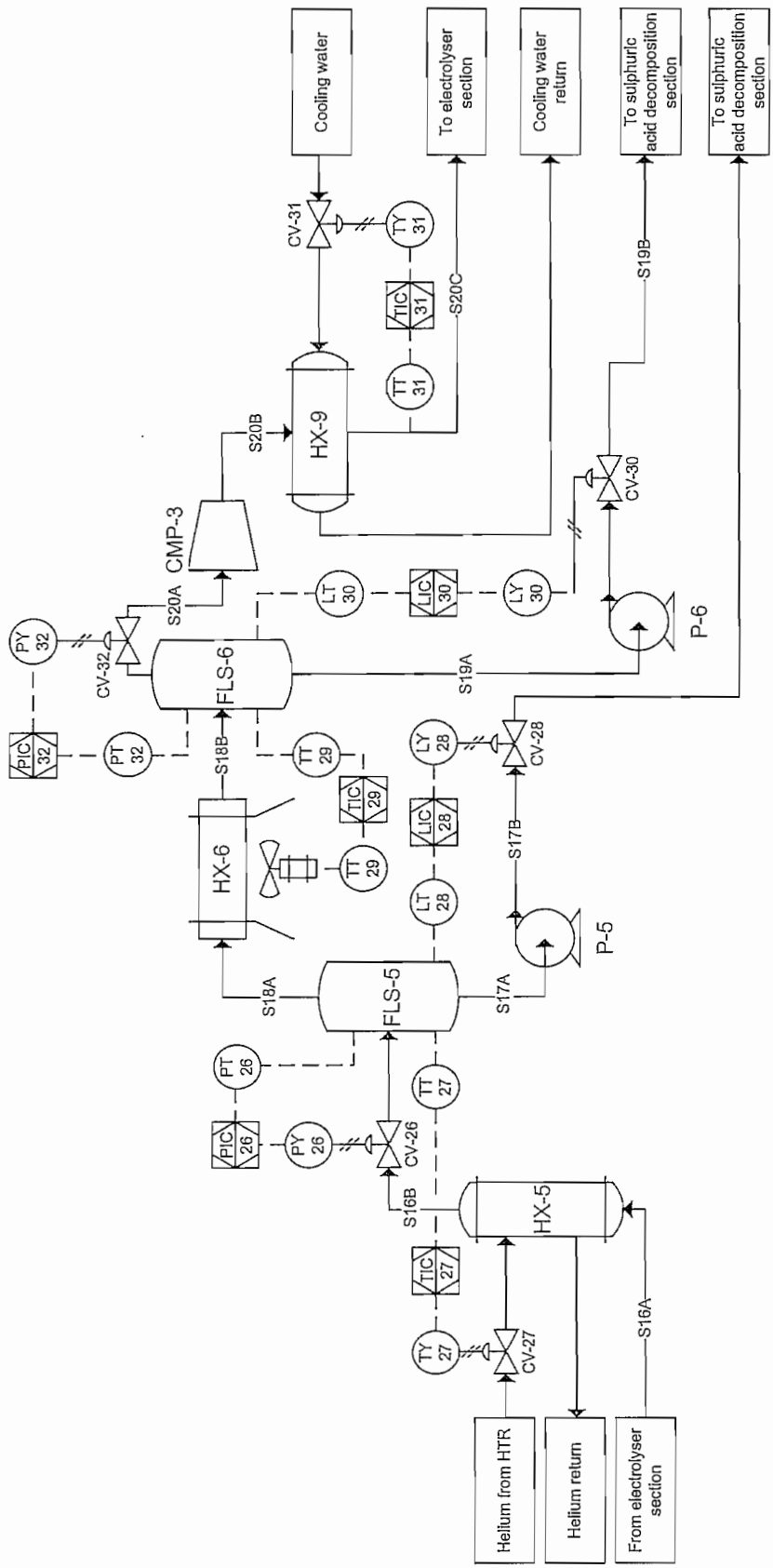


Figure 4.4: Sulphuric acid concentration section

**Table 4.4: Equipment list for the sulphuric acid concentration section**

| Designation | Description |
|---|---|
| CMP-3 | Compressor |
| FLS-5 | Flash drum |
| FLS-6 | Separation drum |
| HX-5 | Heat exchanger |
| HX-6 | Heat exchanger |
| HX-9 | Heat exchanger |
| P-5 | Pump |
| P-6 | Pump |

# 5. CONCLUSIONS AND RECOMMENDATIONS

A flowsheet for the HyS was developed based on examples found in literature as well as the, to date incomplete, work of Dries Grundlingh (Grundlingh, 2010). The reactor section's design was copied almost verbatim from the work of Coetzee (2009:39-49). Some process layout lessons were learned by trial and error. For example, oxygen levels in the electrolyser's sulphuric acid recycle loop can snowball unless this oxygen is somehow removed; for this reason FLS-4 was introduced into the flowsheet (note that TNK-2 as shown in Figure 4.3 would also fulfil this task but was not included in the Aspen simulation). Another lesson learned was that a single flash drum might work to separate oxygen from sulphur dioxide, but a minimum of two are needed to concentrate sulphuric acid if both the desired flow rate and concentration are to be achieved. The flowsheet used in this study is not at all optimised or heat integrated; it was developed to be simple. Before even a pilot plant is built other process alternatives should be investigated and the most promising one optimised and heat integrated.

A number of possible snowball effects were concerned. The first was the accumulation of oxygen in the sulphuric acid concentration section (as already mentioned in this chapter). This steady state instability was completely nullified by the addition of FLS-4 to the flowsheet (as can be seen in the sensitivity plots of chapter 3).

Snowballing of the levels of the two tanks (TNK-1 and TNK-2) suggested in chapter 4 can occur if the rates of sulphur dioxide production in the sulphuric acid decomposition section is not equal to the rate of sulphur dioxide conversion in the electrolyser section; or if the rate of sulphuric acid production in the electrolyser section is not equal to the rate of sulphuric acid conversion in the sulphuric acid decomposition section.

As for challenges faced while trying to simulate the hybrid sulphur cycle, the literature survey made it quite clear that the thermodynamics is an issue that has not been satisfactorily resolved. Furthermore the OLI MSE fluid package was not available for use in this study.

A preliminary control structure is suggested in chapter 4. This control structure is based on the literature study, personal experience and steady state analysis alone. It is not suggested that it will work in real life; it is merely a summary of lessons learned thus far. It is recommended that at least some optimisation and dynamic simulation is done, before a final control structure is compiled.

In summary of the recommendations toward the development of a design for a hybrid sulphur cycle demonstration plant, the following work needs to be done:

- The $H_2SO_4$, $SO_3$, $SO_2$, $O_2$, $H_2$, $H_2O$ system thermodynamics should be studied to the point that predictions can be made over the entire temperature and pressure range of the HyS as well as for any composition of the vapour-liquid-liquid system $H_2O$/ $H_2SO_4$/ $SO_2$
- Experimental work needs to be done on the electrolyser in order to be sure of the scale-up and mathematical modelling of such electrolysers
- All the process alternatives (including absorption) should be investigated and an optimal flowsheet devised for the HyS
- Dynamic simulations should be built for this optimised flowsheet in order to characterise the dynamic behaviour of the HyS and develop a realistic control strategy

From the content of this chapter, and this work as a whole, it should be clear that the realisation of the HyS cycle as part of a hydrogen economy is some way off in the future. The ability to build a demonstration pilot plant at the NWU is much closer on the temporal scale but requires some further research.

# REFERENCES

BANERJEE, A.M., PAI, M.R., BHATTACHARYA, K., TRIPATHI, A.K., KAMBLE, V.S., BHARADWAJ, S.R., KULSHRESHTHA, S.K. 2007. Catalytic Decomposition of Sulfuric Acid on Mixed Cr/Fe oxide samples and its Application in Sulfur-Iodine cycle for Hydrogen Production. *Hydrogen Energy*, Jul. 9.

BARBAROSSA, V., BRUTTI, S., DIAMANTI, M., SAU, S., DE MARIA, G. 2006. Catalytic Thermal Decomposition of Sulphuric Acid in Sulphur-Iodine Cycle for Hydrogen Production. *Hydrogen Energy*, 31 (2006): 883-890.

BROWN, L.C., BESENBRUCH?, G.E., LENTSCH, R.D., SCHULTZ, K.R., FUNK, J.F., PICKARD, P.S., MARSHALL, A.C., SHOWALTER, S.K. 2002. High Efficiency Generation of Hydrogen Fuels Using Nuclear Power. Lexington: University of Kentucky (Technical Report) 78p.

BROWN, L.C., FUNK, J.F., SHOWALTER, S.K. 2000. High Efficiency Generation of Hydrogen Fuels Using Nuclear Power. Lexington: University of Kentucky (Technical Report) 73p.

COETZEE, M.D. 2008. Proposed Concept Design for the High Temperature Sulphuric Acid Decomposition Reactor Applicable to the Hybrid Sulphur (HyS) Process. (Proceedings of the 4th International Topical Meeting on High Temperature Reactor Technology. Washington)

COETZEE, M.D. 2009. The Chemical Reactor for the Decornposition of Sulphuric Acid for the Hybrid Sulphur Process. Potchefstroom: NWU. (Dissertation – M.Eng.) 172p.

COLÓN-MERCADO, R.H., HOBBS, D.T. 2007. Catalyst Evaluation for a Sulfur Dioxide-Depolarized electrolyzer. *Electrochemistry Communications*, 9 (2007) 2649-2653.

COX, K. 1978. Thermochemical Production of Hydrogen from Water, a Critical Review. Los Alamos: University of California (Technical Report) 55p.

DOCTOR, R.D. 2006. Evaluation of a Continuous Calcium-Bromine Thermochemical Cycle. Chicago: Argonne National Laboratory (Slideshow) 27 slides.

FOGLER, H.S., 1999. Elements of Chemical Reaction Engineering. New Jearsey: Prentice-Hall. 967p.

FORSBERG, C., BISCHOFF, B., MANSUR, L.K., TROWBRIDGE, L., TORTORELLI, P. 2003. A Lower-Temperature Iodine-Westinghouse-Ispra Sulfur Process for Thermochemical Production of Hydrogen. Oak Ridge: Oak Ridge National Laboratory (Report) 15p.

GELBARD, F., ANDAZOLA, J.C., NARANJO, G.E., VELASQUEZ, C.E., REAY, A.R. 2005. High Pressure Sulfuric Acid Decomposition Experiments for the Sulfur-Iodine Thermochemical Cycle. Albuquerque: Sandia National Laboratories (Report) 66p.

GINOSAR, D.M., PETKOVIC, L.M., GLENN, A.W., BURCH, K.C. 2006. Stability of Supported Platinum Sulfuric Acid Decomposition Catalysts for use in Thermochemical Water Splitting Cycles. *Hydrogen Energy*, 32 (2007) 482-488.

GORENSEK, M.B. 2007. Effec of Electrolyzer Configuration and Performance on Hybrid Sulfur Process Net Thermal Efficiency. Aiken: Savannah River National Laboratory (Report) 11p.

GORENSEK, M.B., SUMMERS, W.A. 2007. Hybrid Sulfur flowsheets using PEM electrolysis and a bayonet decomposition reactor. Aiken: Savannah River National Laboratory (Report) 41p.

GRUNDLINGH, D. 2010. Personal communication with the author. Telephonic.

HUANG, C., T-RIASSI, A. 2005. Analysis of Sulfur-Iodine Thermochemical Cycle for Solar Hydrogen Production. Part I: Decomposition of Sulfuric Acid. *Solar Energy*, 78 (2005) 632-646.

JEONG, Y.H., KAZIMI, M.S., HOHNHOLT, K.J., YILDIZ, B. 2005. Optimization of the Hybrid Sulfur Cycle for Hydrogen Generation. Cambridge: MIT (Report) 60p.

KIM, T., GONG, G., LEE, B.G., LEE, K., JEON, H., SHIN, C., KIM, H., JUNG, K. 2006. Catalytic Decomposition of Sulfur Trioxide on the binary metal oxide catalysts of Fe/Al and Fe/Ti. *Applied Catalysis*, 305 (2006) 39-45.

KUGELER, K. 2007. HTR Technology (NUCI 878). Potchefstroom: NWU. 261p. (Study notes)

LE DUIGOU, A., BORGARD, J.M., LAROUSSE, B., DOIZI, D., ALLEN, R., EWAN, B.C., PRIESTMAN, G.H., ELDER, R., DEVONSHIRE, R., RAMOS, V., CERRI, G., SALVINI, C., GIOVANNELLI, A., GIOVANNI, D.M., CORGNALE, C., BRUTTI, S., ROEB, M., NOGLIK, A., RIETBROCK, P.M., MOHR, S., DE OLIVEIRA, L., MONNERIE, N., SCHMITZ, M., SATTLER, C., MARTINEZ, A.O., MANZANO, D.L., ROJAS, J.C., DECHELOTTE, S., BAUDOUIN, O. 2007. HYTEC: An EC Funded search for a long term massive hydrogen production route using solar and nuclear technologies. *International Journal of Hydrogen Energy*, 32 (2007) 1516-1529

LE DUIGOU, A., BORGARD, J.M., LAROUSSE, B., DOIZI, D., WERKOFF, F. 2006. HYTEC: Aims and First Assessments of an EC Funded Project on

Massive Scale Hydrogen Production via Thermochemical Cycles. Lyon: HYTEC (Report) 11p.

LUYBEN, W.L., TYRÉUS, B.D., LUYBEN, M.L. 1999. Plantwide Process Control. New York: McGraw-Hill. 395p.

MARSHALL, A.C. 2002. An Assessment of Reactor Types for Thermochemical Hydrogen Production. Albuquerque: Sandia National Laboratories (Report) 51p.

MATHIAS, P.M. 2002. Modeling the Sulfur-Iodine Cycle. Albuquerque: Sandia National Laboratories (Report) 99p.

ÖZTÜRK, I.T., 1993. An Improved Process for $H_2SO_4$ Decomposition Step of the Sulfur-Iodine Cycle. *Energy Convers.*, 36 (1995) 11-21.

PBMR (Pty) Limited. 2008. Fuel Element Design for PBMR. [Web:] http://www.pbmr.com/contenthtml/files/Image/HowFuelLarge.jpg [Date of use: 13 October 2008]

PBMR (Pty) Limited. 2008. Process Heat Applications. [Web:] http://www.pbmr.com/index.asp?Content=226 [Date of use: 13 October 2008]

PBMR (Pty) Limited. 2008. Main Power System Layout. [Web:] http://www.pbmr.com/contenthtml/files/Image/MPSLablesLarge.jpg [Date of use: 13 October 2008]

PBMR (Pty) Limited. 2008. Main Power System Layout. [Web:] http://www.pbmr.com/contenthtml/files/Image/ProcessHeatLarge.jpg [Date of use: 13 October 2008]

PBMR (Pty) Limited. 2008. What is PBMR?. [Web:] http://www.pbmr.com/index.asp?Content=216 [Date of use: 13 October 2008]

PENFIELD, S.R., CORREIRA, M., ALLEN, D.T., 2006. Development Requirements for Process Energy Applications of the PBMR. Johannesburg: 3rd International Topical Meeting on High Temperature Reactor Technology (Conference proceedings) 6p.

SMITH, J.M., VAN HESS, H.C., ABBOTT, M.M. 2001. Chemical Engineering Thermodynamics. Boston: Mc Graw-Hill. 789p.

SPEWOCK, S., BRECHER, L.E., TALKO, F. 1976. The Thermal Catalytic Decomposition of Sulfur Trioxide to Sulfur Dioxide and Oxygen. Pittsburg: Westinghouse Research Laboratories (Report) 16p.

SUMMERS, W.A. 2006. Hybrid Sulfur Thermochemical Process Development. Aiken: Savannah River National Laboratory (Slideshow) 26 slides.

SUMMERS, W.A. & BUCKNER, M.R., 2005. Hybrid Sulfur Thermochemical Process Development. Aiken: Savannah River National Laboratory (Report) 11p.

SUMMERS, W.A., GORENSEK, M.B., BUCKNER, M.R. 2005. The Hybrid Sulfur Cycle for Nuclear Hydrogen Production. Aiken: Savannah River National Laboratory (Report) 7p.

SUMMERS, W.A. & STEIMKE, J.L. 2006. Development of the Hybrid Sulfur Thermochemical Cycle. Aiken: Savannah River National Laboratory (Report) 11p.

SVRCEK, W.Y., MAHONEY, D.P., YOUNG, B.R. 2000. A Real-Time Approach to Process Control. Chichester: Wiley. 307p.

UHRIG, R.E. 2005. Producing Hydrogen using Nuclear Heat. Knoxville: University of Tennessee (Report) 12p.

YILDIZ, B., CONZELMANN, G., PETRI, M.C., FORSBERG, C. 2005. Configuration and Technology Implications of Potential Nuclear Hydrogen System Applications. Chicago: Argonne National Laboratory (Report) 120p.

# APPENDICES

# A. THE NUCLEAR HEAT SOURCE

## *A.1 Introduction*

In this section the reactor types that could conceivably be used to supply the HyS with process heat and electricity are considered. The best reactor type is pointed out along with the reasoning behind its selection. The reactor type, and the specific reactor design to be used as heat source for this project, is then described in detail. Finally the integration of the HyS with a nuclear heat source is shown and explained.

## *A.2 Possible Reactor Types*

Marshall (2002:15) did a study entitled "An Assessment of Reactor Types for Thermochemical Hydrogen Production". In this study nine reactor types were considered as potential heat sources for the sulphur-iodine thermochemical cycle. The sulphur-iodine cycle, of course, has the same high-temperature endothermic reaction as the hybrid-sulphur cycle, namely:

$$H_2SO_4 \rightarrow SO_2 + H_2O + \frac{1}{2}O_2$$

The nine reactor types considered by Marshall (2002:15) were:

1. Pressurised water reactors (PWRs)
    - Pressurised water reactors (light and heavy water)
    - Supercritical-phase pressurised water reactors
2. Boiling water reactors (BWRs)
    - Boiling water reactors (light and heavy water)
    - Boiling water reactors with superheat
3. Organic-cooled reactors
    - Diphenyl
    - Other organic coolants
4. Alkali liquid metal-cooled reactors
    - Lithium-cooled
    - Other (Na, K, NaK)
5. Heavy liquid metal-cooled reactors
    - Lead-bismuth
    - Other (Pb, Bi, Sn, Hg)
6. gas-cooled reactors
    - Noble gases (He, Ar)
    - Other gases ($CO_2$, $H_2$, $N_2$, Air, Ar, Steam)
7. Molten salt-cooled reactors
    - 2LiF-$BeF_2$
    - Other salts
8. Liquid-core reactors
    - Molten salt-core
    - Liquid metal-core
    - Aqeous-core
9. Gas-core reactors
    - $UF_6$
    - Other gas/fuel ($UF_4$, U-plasma)

The chosen reactor had to comply with 5 basic requirements and 5 other important criteria were also taken into account. The basic requirements are (Marshall, 2002:16):

1. Chemical compatibility
2. Coolant stability
3. Pressure requirements
4. Nuclear requirements
5. Feasibility

And the other important criteria are (Marshall, 2002:6):

1. Safety
2. Operational issues
3. Capital cost
4. Intermediate loop compatibility
5. Other merits and issues

Each of the requirements and criteria were weighted with a value from 0 to 4 with a higher value denoting better compliance. The reactor that met all the requirements and had the highest mean score was to be selected. The following table summarises their findings and makes it clear that gas-cooled reactors are the best choice of reactor to provide process heat for the sulphuric acid decomposition step of the HyS process.

**Table A.1: Assessment of reactor concepts to provide heat for sulphuric acid decomposition (Marshall, 2002:35)**

| Coolant | Gas | Salt | Heavy metal | Liquid core | Alkali metal | PWR | BWR | Organic | Gas core |
|---|---|---|---|---|---|---|---|---|---|
| 1. Materials compatibility | 4 | 3 | 3 | 3 | 2 | - | 0 | - | - |
| 2. Coolant stability | 4 | 3 | 4 | 3 | 4 | - | - | 0 | - |
| 3. Operating pressure | 4 | 4 | 4 | 4 | 4 | 0 | - | - | - |
| 4. Nuclear issues | 4 | 4 | 4 | 3 | 3 | - | - | - | - |
| 5. Feasibility | 4 | 3 | 2 | 3 | 2 | - | - | - | 0 |
| 1. Safety | 3 | 4 | 3 | 3 | 2 | - | - | - | - |
| 2. Operations | 3 | 3 | 3 | 2 | 3 | - | - | - | |
| 3. Capital cost | 2 | 3 | 3 | 1 | 1 | | | | |
| 4. Intermediate loop compatibility | 4 | 3 | 3 | 3 | 3 | - | - | - | - |
| 5. Other merits and issues | 3 | 3 | 3 | 3 | 3 | - | - | - | - |
| Unweighted mean score | 3.5 | 3.3 | 3.2 | 2.8 | 2.7 | N/A | N/A | N/A | N/A |

The PWR, BWR, organic-cooled reactors and gas core reactors do not meet the basic requirements as defined by Marshall (2002:36,44). The pressure in a PWR would be too high at the required temperature of 900°C, the superheated steam created in a BWR would be too corrosive, the thermal and radiation dissociation of organic coolants would cause a reactor to clog with carbonaceous deposits, and gas-core reactors require too much developmental work to be feasible.

## *A.3 The High Temperature Gas Cooled Reactor*

The HTRs are the most advanced gas cooled reactors to have been built. They have evolved from the Magnox and later the Advanced Gas-Cooled Reactor (Kugeler, 2007:1.1). A number of high temperature reactors (HTRs) have been operated successfully in the past. They are listed in Table A.2 and are followed by a discussion of the characteristics common to all HTRs.

**Table A.2: Overview of HTR plants that have been built and operated (Kugeler, 2007:10.2)**

| Plant | Thermal power | Electrical power | Fuel element | Site | Operation |
|---|---|---|---|---|---|
| AVR | 46 MW | 15 MW | pebble shaped fuel elements | Jülich, Germany | 1965 - 1988 |
| DRAGON | 20 MW | - | tubular fuel elements | Winfrith, Great Britain | 1966 - 1975 |
| Peach Bottom | 115 MW | 40 MW | tubular fuel elements | Susquehanna, USA | 1965 - 1988 |
| THTR | 750 MW | 308 MW | pebble shaped fuel elements | Schmehausen, Germany | 1985 - 1988 |
| Fort St. Vrain | 852 MW | 342 MW | block shaped fuel elements | Platteville, USA | 1976 - 1989 |

The HTR concept is based on six characteristics, namely (Kugeler, 2007:1.6):

- The reactor should consist of only fissile and fertile material along with a weakly absorbing moderator in order to ensure the best possible neutron economy
- Helium should be used as coolant because it is chemically inert and does not affect the neutron economy
- The core should consist of only ceramic materials so it can be operated at very high temperatures
- Coolant outlet temperatures should be high enough to be suited to closed cycle gas turbine power plants
- The fuel should be distributed uniformly in the core in order to ensure a large heat transfer surface and a high power density in the fuel
- Use the good neutron economy to exploit the U-235-, Th-232-, U-233-fuel cycle.

In addition to these all HTRs have the following safety characteristics (Kugeler, 2007:1.7):

- Ceramic fuel elements cannot melt, not even in the most extreme accidents
- Coated particles contain fission products very effectively and allow very high operating temperatures
- Helium is an excellent coolant as it is chemically inert, does not influence the neutron balance and allows high operating temperatures that translate into high generating efficiency
- Ceramic (graphite) core structures allow high temperatures and robust design
- Reactors have low power density, are robust and have a high heat capacity so they have large thermal inertia in all operational and control procedures
- Core designs that can tolerate loss of coolant and active decay heat removal. Self acting decay heat removal keeps fuel temperatures below critical values so that fission products are retained and the fuel doesn't melt
- Very strong negative temperature coefficients of reactivity limit nuclear power and fuel temperature to allowable limits even in the case of a hypothetical reactivity excursion. Additionally PBMRs have no excess reactivity
- Efficient retention of fission products by the coated particles in normal operation means that the helium circuits are very clean and therefore low release of radioactivity and dose values to operational staff
- The efficient retention of fission products in coated particles during extreme accidents prevents catastrophic release of radioactivity to the environment

From all this it is obvious that the HTR is a safe, proven technology. South Africa is currently developing a pebble bed modular reactor (PBMR) to be used in conjunction with a Brayton power conversion cycle to generate electricity. Its robust design makes it the ideal reactor to be used as heat source for the HyS process and has been chosen as the heat source of choice in this study. Figure A.1 shows the layout of the PBMR and power conversion unit as currently planned.

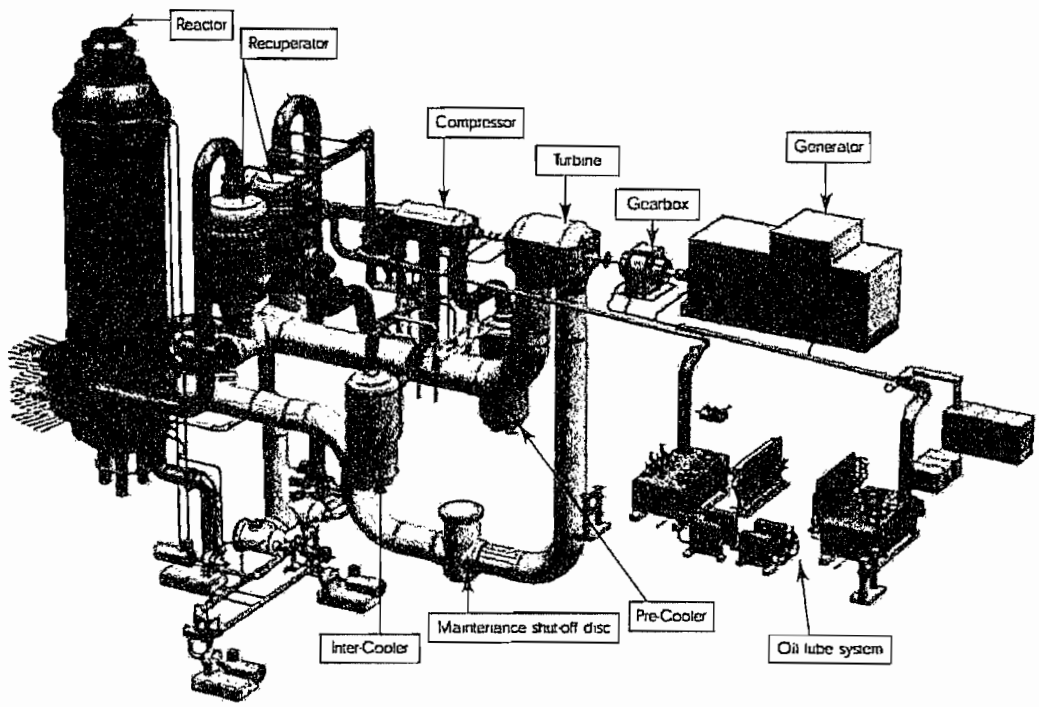


**Figure A.1: Isometric view of the planned PBMR power plant with Brayton power conversion cycle (PBMR, 2008)**

The PBMR is a helium cooled, graphite moderated HTR. The helium enters the top of the reactor at 500 °C and is heated up to 900 °C by the time it leaves the bottom of the RPV. Its reactor pressure vessel (RPV) has an inside diameter of 6.2m and stands 27m tall. The RPV contains the core barrel that holds the ceramic core structures in place. These core structures include the outer graphite reflector, the 450 000 fuel spheres and a central graphite reflector (PBMR, 2008).

The fuel consists of enriched uranium dioxide kernels that are coated with pyrolytic carbon and silicon carbide layers. These particles are dispersed in 60mm diameter pyrolytic carbon spheres to form fuel elements. Figure A.2 shows the structure of these fuel spheres. The shape of the fuel elements allows for online refuelling with spheres continually being added at the top of the reactor and withdrawn from the bottom. This results in a very high availability (PBMR, 2008).

The PBMR has two diverse control systems. The one involves 24 control rods that are located in the outer reflector while the other system consists of absorber spheres that can be dropped into 8 borings in the central reflector. (PBMR, 2008).

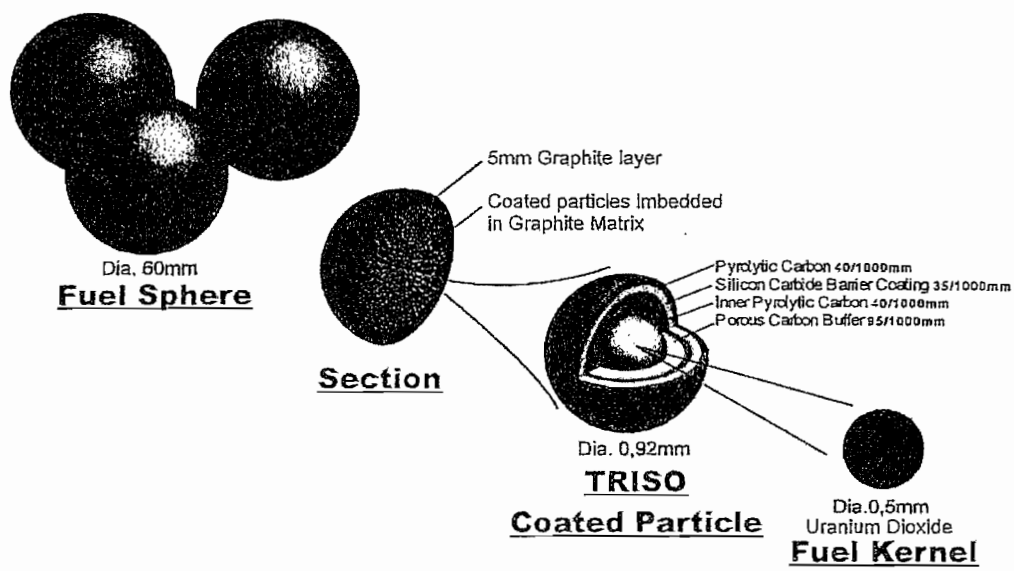


**Figure A.2: Diagram showing the structure of the PBMR fuel elements (PBMR, 2008)**

## *A.4 Integration of the PBMR with the HyS*

Figure A.3 shows the process flow diagram of a way in which a PBMR plant can be coupled to the HyS process. The helium leaves the PBMR at a temperature of around 900°C and passes through the intermediate heat exchanger (IHX) where it heats up the gas used in the intermediate loop. This intermediate loop is used to isolate the coolant used in the nuclear reactor core from the chemical plant lest the product hydrogen and oxygen become contaminated with radioactive material. The fluid in this intermediate loop is then used to provide process heat to the sulphuric acid decomposition section of the HyS plant. The helium leaving the IHX passes through a steam generator (SG) before returning to the PBMR. The steam generated in the SG is used to generate electricity with a Rankine power conversion unit (PCU). The electricity generated is used in the electrolysis section of the HyS plant and the excess electricity can be exported to the local grid. The Rankine PCU makes use of a high pressure steam turbine (HPST) and intermediate pressure steam turbine (IPST) and a low pressure steam turbine (LPST) (Penfield et. al., 2006:5,6).

Figure A.4 shows the current PBMR design configured to supply process heat. Two configurations are currently under development. The first provides intermediate temperature helium (at around 750°C) for high pressure steam production with electricity cogeneration. The second (which is of more interest here) is to provide high temperature helium (950°C reactor outlet temperature) for the purposes of steam methane reforming, high temperature steam electrolysis and thermochemical processes for hydrogen production (PBMR, 2008).

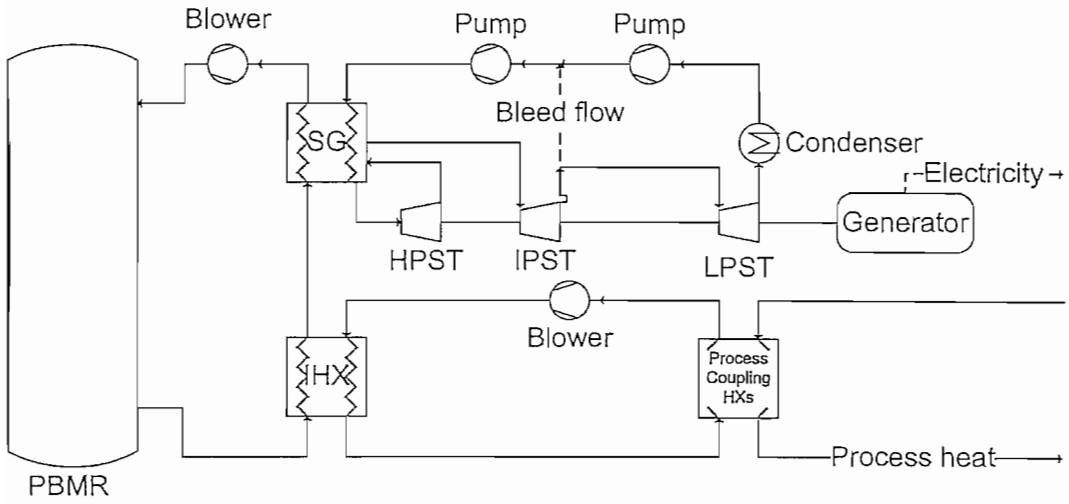


**Figure A.3: Process flow diagram of a process heat plant (PHP) option for the HyS process (Penfield et. al., 2006:5)**

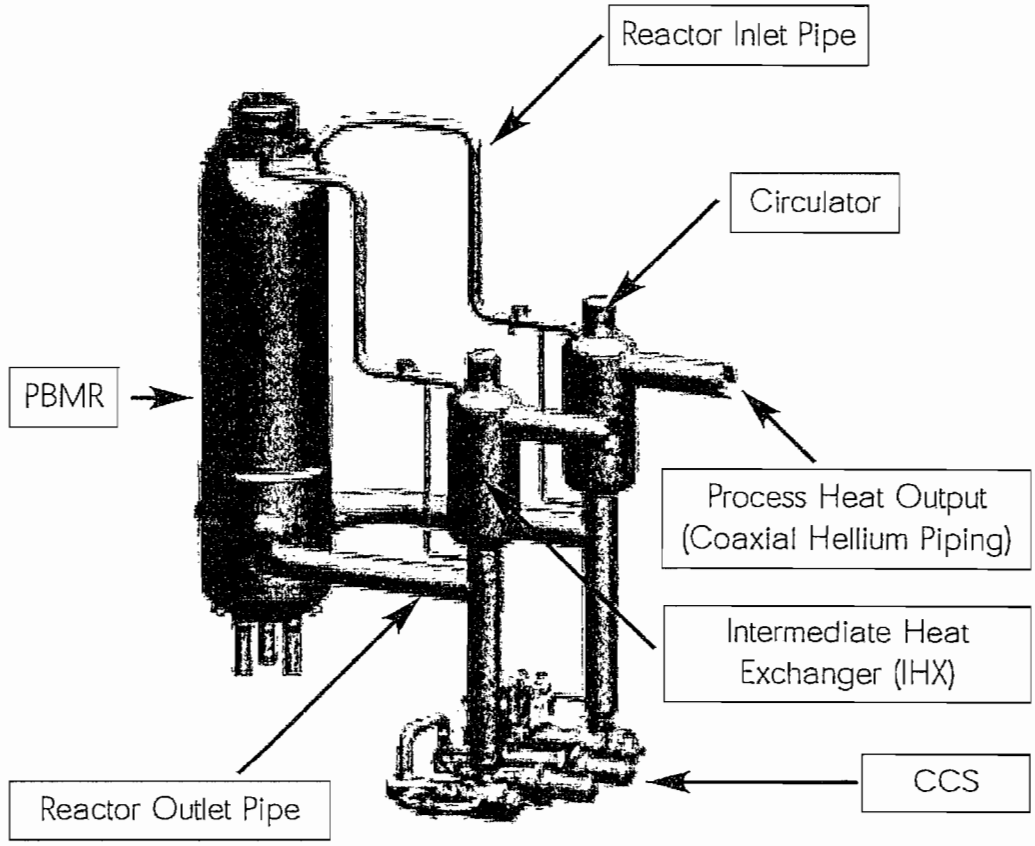


**Figure A.4: Diagram showing a PBMR configured to supply process heat (PBMR, 2008)**